Fouling and its control in membrane distillation – A review

Leonard D. Tijing[a], Yun Chul Woo[a], June-Seok Choi[b], Sangho Lee[c], Seung-Hyun Kim[d], Ho Kyong Shon[a,*]

[a] Centre for Technology in Water and Wastewater (CTWW), School of Civil and Environmental Engineering, University of Technology, Sydney (UTS), P.O. Box 123, Broadway, NSW 2007, Australia

[b] Construction Environment Research Division, Korea Institute of Construction Technology (KICT), 283, Goyangdae-Ro, Ilsanseo-Gu, Goyang-Si, Kyeonggi-Do, 411-712, Republic of Korea

[c] School of Civil and Environmental Engineering, Kookmin University, Seongbuk-gu, Seoul, 136-702, Republic of Korea

[d] Civil Engineering Department, Kyungnam University, Wolyoung-dong, Changwon, 631-701, Republic of Korea

*Corresponding author: H.K. Shon, e-mail: hokyong.shon-1@uts.edu.au, fax: +61 2 9514 2633

Abstract

Membrane distillation (MD) is an emerging thermally-driven technology that poses a lot of promise in desalination, and water and wastewater treatment. Developments in membrane design and the use of alternative energy sources have provided much improvement in the viability of MD for different applications. However, fouling of membranes is still one of the major issues that hounds the long-term stability performance of MD. Membrane fouling is the accumulation of unwanted materials on the surface or inside the pores of a membrane that results to a detrimental effect on the overall performance of MD. If not addressed appropriately, it could lead to membrane damage, early membrane replacement or even shutdown of operation. Similar with other membrane separation processes, fouling of MD is still an unresolved problem. Due to differences in membrane structure and design, and operational conditions, the fouling formation mechanism in MD may be different from those of pressure-driven membrane processes. In order to properly address the problem of fouling, there is a need to understand the fouling formation and mechanism happening specifically for MD. This review details the different foulants and fouling mechanisms in the MD process, their possible mitigation and control techniques, and characterization strategies that can be of help in understanding and minimizing the fouling problem.

Keywords: Membrane distillation, fouling, scaling, mitigation, porous membrane, desalination

Contents

Abbreviations
1. Introduction
2. Overview of MD
    2.1. Membrane wetting
    2.2. Theoretical background
        2.2.1. Mass transfer
        2.2.2. Heat transfer
        2.2.3. Temperature polarization coefficient
3. MD fouling
    3.1. Inorganic fouling
        3.1.1. Effect of membrane dry-out on fouling
    3.2. Organic fouling
    3.3. Biological fouling
4. MD fouling control and cleaning
    4.1. Pretreatment
    4.2. Membrane flushing
    4.3. Gas bubbling
    4.4. Temperature and flow reversal
    4.5. Surface modification for anti-fouling membrane
    4.6. Effect of magnetic field and microwave irradiation
    4.7. Use of antiscalants
    4.8. Chemical cleaning
5. Fouling monitoring and characterization techniques
    5.1. Physical characterization
    5.2. Chemical characterization
    5.3. Biological characterization
6. Future perspectives and concluding remarks
Acknowledgements
References

Abbreviations

AFM	atomic force microscopy
APS	Accelerated precipitation softening
AGMD	air gap membrane distillation

BSA	bovine serum albumin
CA	contact angle
$CaCl_2$	calcium chloride
$CaCO_3$	calcium carbonate
$CaSO_4$	calcium sulphate
CFU	colony forming unit
CLSM	confocal laser scanning microscopy
COD	chemical oxygen demand
DCMD	direct contact membrane distillation
DLVO	Derjaguin-Landau-Verwey-Overbeek
EDS	energy dispersive X-ray spectroscopy
EPS	extracellular polymeric substances
$FeCl_3$	ferric chloride
FlFFF	flow field-flow fractionation
FTIR	fourier-transform infrared spectroscopy
HA	humic acid
HCl	hydrochloric acid
HPSEC	high pressure size exclusion chromatography
LC-OCD	liquid chromatography-organic carbon detection
LEP	liquid entry pressure
LGMD	liquid gap membrane distillation
LSI	Langelier saturation index
MB	methylene blue
MD	membrane distillation
MDBR	membrane distillation bioreactor
MEF	multi-effect distillation
MEMD	multi-effect membrane distillation
MF	microfiltration
MGMD	material gap membrane distillation
MMBF	macromolecular or biofouling
MSF	multistage flash
MWT	magnetic water treatment
NaCl	sodium chloride
NaOH	sodium hydroxide
Na_2SO_4	sodium sulfate
NF	nanofiltration
NOM	natural organic matters

OMW	olive mill wastewater
PACl	poly-aluminum chloride
PAM	polypropylene acid ammonium
PP	polypropylene
PSD	pore size distribution
PTFE	polytetrafluoroethylene
PVDF	polyvinylidene fluoride
RCW	recirculating cooling water
RO	reverse osmosis
SEM	scanning electron microscopy
SGMD	sweeping gas membrane distillation
SI	saturation index
TCM	traditional Chinese medicine
TDS	total dissolved solids
TEM	transmission electron microscopy
TOC	total organic carbon
TPC	temperature polarization coefficient
UF	ultrafiltration
UTDR	ultrasonic time-domain reflectometry
VMD	vacuum membrane distillation
V-MEMD	vacuum multi-effect membrane distillation
XRD	X-ray diffraction

Nomenclature

A	constant in Antoine equation (dimensionless)
B	constant in Antoine equation (dimensionless)
B_g	pore geometric factor (dimensionless)
C	constant in Antoine equation (dimensionless)
C_m	overall mass transfer coefficient for water vapor through the membrane (kg/m^2 s Pa)
D_{AB}	diffusivity of water vapor in air (m^2/s)
d	pore diameter (m)
J	mass flux (kg/m^{2}h)
J_{vd}	mass flux considering the effect of vapor pressure depression (kg/m^{2}s)
k_m	effective thermal conductivity of the microporous membrane (W/m K)
k_2	thermal conductivity of the biofouling layer (W/m K)
h_1	convective heat transfer coefficient at the feed side (W/m^{2}k)

h_4 convective heat transfer coefficient at the permeate side (W/m^{2}k)

M_A molecular weight (kg/kmol)

p total pressure for the transport of volatile component (Pa)

p_{fm} partial vapor pressure at the membrane surface of the feed side (Pa)

p'_{fm} reduced partial vapor pressure due to vapor pressure depression (Pa)

p_{pm} partial vapor pressure at the membrane surface of the permeate side (Pa)

R universal gas constant (J/mol K)

R_1 convective heat transfer resistance at the hot feed (K m^2/W)

R_{12} effective resistance of the resistances R_1 and R_2 in series (K m^2/W)

R_{124} effective resistance of the resistances R_1, R_2, and R_4 in series (K m^2/W)

R_2 conductive heat transfer resistance associated with the fouling layer (K m^2/W)

R_3 effective heat transfer resistance associated with the resistances (R_m, R_v) in the membrane (m^{2}K/W)

R_4 convective heat transfer resistance at the cold permeate (K m^2/W)

R_m conductive heat transfer resistance associated with the porous membrane (K m^2/W)

R_t total heat transfer resistance (K m^2/W)

R_v pseudo heat transfer resistance associated with the vaporization of water (K m^2/W)

t_f bulk temperature at the feed side (K)

t_{fl} temperature at the fouling layer/feed side water interface (K)

t_{fm} temperature at the membrane surface of the feed side (K)

t_p bulk temperature at the permeate side (K)

t_{pm} temperature at the membrane surface of the permeate side (K)

T Kelvin temperature (K)

T_m mean temperature within the membrane (K)

V_w molar volume of liquid water (m^3/mol)

Greek symbols

β small parameter that characterizes the Kelvin effect (dimensionless)

δ_m membrane thickness (m)

δ_2 thickness of the biofouling layer (m)

ΔT_K effective temperature difference across the membrane in the presence of a fouling layer (K)

ε membrane porosity

θ contact angle of the membrane surface (deg)

λ heat of vaporization of water (W s/kg)

σ surface tension of the solution (N/m or kg/s^2)

τ membrane tortuosity

1. Introduction

The shortage of fresh water is one of the biggest challenges in the modern era [1, 2]. As water is a major need for survival, there is a necessity for new technologies to help provide fresh water supply [3]. Desalination is considered as one of the major key solutions that is sustainable and effective technology to the problem of fresh water scarcity [4, 5]. As the population balloons to more than 7 billion people, demand for fresh water has been increasing steadily. In the Arabian Peninsula, the demand for fresh water is reported to increase at a rate of at least 3% annually [6]. Thus, environmental and safety regulations are becoming more stringent to ensure sustainable solutions, and more efforts have been focused on improving the current membrane-based desalination technologies such as RO. Among the promising techniques is by MD.

MD is one of the emerging desalination technologies for the production of fresh water. MD is a thermally-driven transport of water molecules (in vapor phase) through porous and hydrophobic membranes. One side of the porous membrane is a hot feed with high salinity and the other side is a cold permeate. The temperature gradient between the two sides creates a vapor pressure difference that drives the vapor to pass through the membrane and collected or condensed to pure water in the other side. MD has reduced sensitivity to concentration polarization, allowing it to operate even at high NaCl concentrations at the feed side [7]. MD has several advantages such as: (a) theoretically 100% salt rejection, (b) lower operating temperature than conventional distillation processes, (c) low energy consumption when waste heat or alternative energy source is used, (d) less requirements of membrane mechanical properties, (e) and lower operating pressure compared to conventional pressure-driven membrane processes such as RO [8-12]. MD can be employed for water desalination, removal of organic matters in drinking water production, treatment of water and wastewater, recovery of valuable components, and treatment of radioactive wastes [13-18]. However to date, MD has not found large-scale industrial application yet although a number of pilot systems have been carried out in recent years [19-28].

Like all other membrane processes, a major inefficiency of MD is fouling, which causes a decline in the membrane permeability due to the accumulation of deposits on the membrane surface and inside the membrane pores. Theoretically, MD has 100% salt rejection and only water vapor is allowed to pass through the pores of the membranes; however, several factors such as poor long term hydrophobicity of the material, membrane damage and degradation, very thin thickness of the membrane, and the presence of inorganic, colloidal and particulate matters, organic macromolecules and microorganisms in the feed water could lead to fouling deposition and pore wetting, which can lower the salt rejection and deter the MD performance [29]. For MD, the issue on fouling is still not well understood, but is believed to have lesser degree of propensity compared to those in pressure-driven membrane processes such as RO and NF. However, the fouling phenomenon is a time-

dependent process, wherein its long-term effect cannot be easily predicted [30]. Several studies have indicated the negative effect of membrane fouling on the MD process.

A number of studies have investigated the effect of fouling on the overall MD process utilizing different types of membranes such as flat-sheet and hollow fibers, as well as using different modules [30]. However, from our review of literature, we have not found any review paper dedicated mainly to fouling and scaling in MD. Though, a number of review articles have been published detailing the occurrences and control of fouling in RO, NF, and UF [31-34], the fouling mechanism and propensity are expected to be different in MD due to differences in membrane structure and operational conditions. As fouling is an important issue that should be addressed to enhance the efficiency of MD process, there is a need to understand its formation mechanism, and the different parameters that affect its propensity and possible mitigation or cleaning strategies. Thus, it is deemed necessary to provide an up-to-date review of the fouling propensity of MD membranes during the MD operation. This review includes a brief overview of MD and its fundamentals, a literature review of the different kinds of fouling mechanisms that can be found in MD processes, the possible fouling mitigation and cleaning methods to enhance the MD efficiency, and the use of advanced membrane fouling characterization methods.

2. Overview of MD

MD is mainly used to remove salts from a saline solution through the use of a hydrophobic porous membrane and thermal energy. It is also used to separate heavy metals from contaminated water or to remove trace volatile organic compounds [35, 36], and to concentrate different kinds of aqueous solutions such as orange juice, whey protein solution and acid solution [37-42]. The MD membrane acts as a barrier layer for the separation of vapor and water. Water evaporates at the feed-pore interface, then the water vapor diffuses through the membrane pores, where it is then collected or condensed at the permeate side by different methods [43]. There are four main MD configurations depending on how the permeate is processed: DCMD, AGMD, VMD, and SGMD [44, 45]. In recent years, new MD configurations have been employed such as MEMD, MGMD, LGMD, and V-MEMD [46-52]. Heat and mass transfer simultaneously occur during the MD process, wherein the heat transfer resistances across the boundary layers of the membrane surface are often the rate-limiting step at low flow rates, while the membrane resistance becomes predominant at higher flow rates [30, 53]. The design and structure of the membrane are very important factors to consider for an effective MD process. In fact, the membrane unit is reported to entail 20-25% of the total capital cost of a desalination plant [54]. It is essential to understand the factors affecting the membrane performance and lifetime, especially on the issue of fouling, which affects much of the MD efficiency.

The important characteristics of a good MD membrane include high hydrophobicity, high porosity, uniform pore size and narrow pore size distribution, low tortuosity, and thin thickness.

Though MD holds a good promise as an alternative to the present pressure-driven processes, it is still not fully commercialized in industrial setting due to the following issues: (a) compared to RO, MD has relatively lower permeate flux [30, 55]; (b) temperature and concentration polarization effects and membrane fouling leading to permeate flux decay; (c) membrane and module design for MD; and (d) it is a highly thermal energy-intensive process [30]. However, recent progress of the possibility of utilizing low-grade waste heat and solar or geothermal energy sources to save in electrical energy cost has made MD more attractive as an alternative to or in conjunction to RO. Additionally, a lot of efforts have been made in recent years in the fabrication of new and improved MD membrane design and structure including flat-sheet, hollow fiber and nanofiber membranes with high MD flux and salt rejection performance that makes MD more viable for many applications [53, 56-58].

Long-term stable flux performance and salt rejection are important aspects to consider for the industrial implementation of MD. However, flux decline is usually encountered in MD operation, which is largely caused by temperature polarization effect [30, 59], wetting, and membrane fouling. Fouling is a serious problem that when left unaddressed, the MD performance especially for long term operation will suffer and can cause major damages and costs in the MD process. It is worth noting that different opinions and results have been reported in literature about the role of fouling in MD. Some studies reported no significant effect of fouling to the MD permeate flux, while other studies showed major drop in flux performance due to fouling. With the rapid expansion of the applications of MD, including treating wastewaters, complex solution make-up and characteristics can be encountered in real-world processes, leading to not only a single component fouling mechanism, but a combination of different fouling mechanisms that would be difficult to control or clean. For example, an investigation of a fouling layer after seawater pretreatment found a combination of organic, inorganic and biological fouling matters [60].

2.1. Membrane wetting

In addition to fouling, membrane wetting is another challenge. Especially for long-term operations, progressive membrane wetting has been observed [61]. To lessen the possibility of wetting and water penetration, hydrophobic materials (i.e., with high contact angles and low surface energy) such as PVDF, PP, and PTFE with small maximum pore size and good PSD are used for membranes in MD. **Figure 1** shows the different degrees of membrane wetting [62], namely: (a) non-wetted, (b) surface wetted, (c) partial-wetted, and (d) fully-wetted membrane. Surface wetting (Fig. **1B**) usually happens due to the phenomena in the surface and also associated with long term use, but the membrane still maintains a gap for the vapor to pass through, and proceeds with the vaporization-distillation process. Partial wetting (Fig. **1C**) has some portions of the membrane open for water to pass through while other pores have decreased gap between the feed and permeate. And fully-wetted membrane (Fig. **1D**) leads to inefficient MD performance, as the feed just flow through the membrane leading to low-quality permeate.

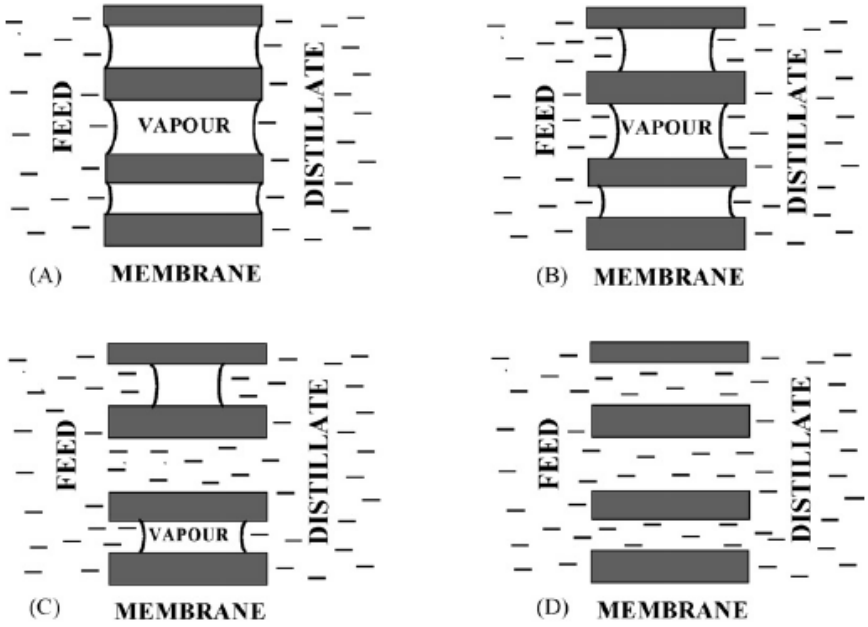

Fig. 1. Different forms of wettability of a membrane: (A) non-wetted, (B) surface-wetted, (C) partial-wetted, and (D) fully-wetted (adapted from [62]).

The surface energy of the material, surface tension of solution, and membrane pore size and geometry are factors affecting the LEP of the membranes. LEP is the pressure at which the liquid starts to penetrate the pores of the membrane, until the liquid passes through the membrane. LEP is calculated by the following Laplace-Young equation [57]:

$$LEP = (-4B_g \sigma \cos \theta)/d_{max} \quad (1)$$

where B_g is a pore geometric factor (B_g =1 for cylindrical pores), σ is the surface tension of the solution, θ is the contact angle between the solution and membrane surface, and d_{max} is the diameter of the largest pore size in the membrane. High LEP is needed for better MD efficiency. From **eq. (1)**, LEP can be increased by increasing the contact angle of the material, or using hydrophobic or superhydrophobic materials or by having smaller pore sizes. However, other factors such as the presence of surfactants in the solution can make the membrane wet, but the major contributor to membrane wetting is fouling [63].

2.2. Theoretical background

2.2.1. Mass transfer

In MD, the driving force is the gradient of partial pressure of vapor at the interface between the liquid and the hydrophobic membrane, and the transmembrane flux for mass transfer can be expressed as [64, 65]:

$$J = C_m (p_{fm} - p_{pm}) \quad (2)$$

where J is the mass transfer flux, C_m is the overall mass transfer coefficient, and p_{fm} and p_{pm} refer to the partial vapor pressures at the feed and permeate vapor-liquid interfaces [64]. The vapor pressure is related exponentially to the temperature of the solution (Antoine equation, $p=e^{(A-(B/(C+T))}$) [45], thus at higher temperature difference, a higher driving force is expected leading to increased permeate flux. Expounding **eq. (2)** based on the Knudsen-molecular diffusion model would lead to the following equation [66]:

$$J = \frac{\varepsilon}{\tau\delta} \frac{pD_{AB}}{RT_m} ln \frac{(p-p_{pm})/pD_{AB} + (3/4d)\sqrt{2\pi M_A/RT_m}}{(p-p_{fm})/pD_{AB} + (3/4d)\sqrt{2\pi M_A/RT_m}} \quad (3)$$

In this equation, all factors affecting the DCMD flux are included such as membrane characteristics (d, ε, δ, τ), temperatures of the feed and permeate fluids (p_{fm}, p_{pm}), diffusivity (D_{AB}) and molecular weight (M_A) of transported component, fluid properties, and dynamics of the fluid in the membrane module [67].

2.2.1.1. Vapor pressure depression

Vapor pressure at the feed and permeate sides is affected by temperature at both surfaces of the membrane, which is determined by the resistances offered by polarization effects at both sides of the membrane, and the microporous membrane. However, when the feed solution contains foulants, a fouling layer can be formed on the membrane surface, which could provide additional flux resistance. Several theoretical models have been presented to describe heat and mass transfer in MD [43, 44, 64, 65, 67-73] including the effect of the fouling layer. The additional layer due to fouling is known to add heat transfer resistance in the MD process. This is particularly true for fouling layers that are porous such as those formed from inorganic salts and cake-forming humic materials. However, there are fouling layers that have very small pores (<50 nm) or free volume, typically due to NOM in the form of proteins, aminosugars, polysaccharides and polyhydroxyaromatics, which usually have thin thickness (<100 μm) [29, 55, 74].

Recent studies [29, 74-76] speculated that aside from heat transfer resistance, the gel-like fouling layer (MMBF) with small pores or free volume can add hydraulic resistance to water permeation. However, these studies did not attempt to incorporate the hydraulic resistance due to fouling into an MD model. It was reported that the fouling layer with small pore (typically less than

50 nm) or free volume causes vapor-pressure depression owing to the Kelvin effect leading to the reduction of driving force, and consequently reduced flux [75]. Liquid water is drawn inside the gel-like hydrophilic MMBF layer via a capillary action, forming a concave liquid/vapor interface within the MMBF layer that results to vapor depression [75]. However, the Kelvin effect was not attempted to incorporate in a model.

In a new study, Chew et al. incorporated the effect of hydraulic resistance due to fouling in their DCMD model for MDBR application [55]. Taking into account the vapor depression at the feed side due to the presence of MMBF layer with small pores (d < 50 nm), **eq. (2)** becomes [55]:

$$J_{vd} = C_m (p'_{fm} - p_{pm}) \tag{4}$$

where p'_{fm} is the reduced vapor pressure due to vapor pressure depression. The Kelvin equations [77, 78] give the relationship between the reduced vapor pressure and the normal vapour pressure at the feed side expressed as [55]:

$$ln\frac{p'_{fm}}{p_{fm}} = -\frac{4\sigma V_w}{Rt_{fm}d} \equiv -\beta \tag{5}$$

According to Chew et al. [55], depression of p'_{fm}/p_{fm} becomes significant at d < 50 nm, reaching to 46% depression at d = 4 nm. Increasing value of dimensionless β indicates decreasing pore diameter. Incorporating the Kelvin equations (**eq. (5)**) into **eq. (4)** yields the following:

$$J_{vd} = C_m (p_{fm} e^{-\beta} - p_{pm}) \tag{6}$$

By perturbation expansion in the small parameter β, which characterizes the pore diameter, and further solution truncating after the first order, the mass flux considering the effect of vapour pressure depression owing to Kelvin effect is expressed as [55]:

$$J_{vd} = J - C_m p_{fm} \beta \tag{7}$$

Eq. (7) indicates that the Kelvin effect reduces the flux by a factor of $C_m p_{fm} \beta$. Converting **eq. (7)** into a normalized equation results to:

$$\frac{J_{vd}}{J} = 1 - \frac{1}{1-\left(\frac{p_{pm}}{p_{fm}}\right)}\beta = 1 - \left[\frac{1}{1-\left(\frac{p_{pm}}{p_{fm}}\right)}\left(\frac{4\sigma V_w}{RT_{fm}d}\right)\right] \tag{8}$$

2.2.2. Heat transfer

Heat transfer in the MD process can be analysed from the resistance of transport process. The resistances to heat transfer without fouling involves three main sections: the resistances due to the hydrodynamic boundary layers at the feed and permeate sides, and the membrane resistance. When a fouling layer is present, the layer provides an additional thermal resistance to heat transfer. The four heat transfer steps have their own driving force and thermal resistances (see **Fig. 2**), and in a steady state condition, the heat transfer is equal to each other and is expressed as follows [55, 67]:

$$q = \frac{t_f - t_{fl}}{R_1} = \frac{t_{fl} - t_{fm}}{R_2} = \frac{t_{fm} - t_{pm}}{R_3} = \frac{t_{pm} - t_p}{R_4} = \frac{1}{R_t}\left(t_f - t_p\right) \quad (9)$$

where $R_1 = 1/h_1$ and $R_4 = 1/h_4$ are convective heat transfer resistances associated with the hydrodynamic boundary layers at the feed and permeate sides, respectively; $R_2 = \delta_2/k_2$ is associated with the heat conduction at the fouling layer, and $R_3 = \frac{1}{\frac{1}{R_m}+\frac{1}{R_v}} = \frac{1}{(k_m/\delta_m)+\lambda C_m\left(\frac{dp}{dT}\Big|_{T_m}\right)}$ is the equivalent resistance of the parallel resistances associated with the heat conduction at the membrane (considering the solid part and the pores) and the heat flux required to vaporize the water through the membrane [55]; and R_t is the total heat transfer resistance from the hot feed to the cold permeate. A solution of **eq. (9)** allows the determination of the individual temperatures at both sides of the membrane surfaces (t_{fm} and t_{pm}) [55]:

$$t_{fm} = t_f - \frac{(R_1+R_2)(t_f - t_p)}{R_3+(R_1+R_2+R_4)} = t_f - \frac{R_{12}(t_f - t_p)}{R_3+R_{124}} \quad (10)$$

$$t_{pm} = t_p - \frac{R_4(t_f - t_p)}{R_3+(R_{124})} \quad (11)$$

The unknown temperature difference, $t_{fm} - t_{pm}$ in relation to the known temperature difference, $t_f - t_p$ can then be expressed as [55]:

$$t_{fm} - t_{pm} = \frac{R_3(t_f - t_p)}{R_3+(R_1+R_2+R_4)} = \frac{R_3(t_f - t_p)}{R_3+(R_{124})} \quad (12)$$

2.2.3. Temperature polarization coefficient

Heat and mass transfer occur simultaneously in MD. The temperatures at the boundary layers of both the feed and permeate sides are different from those at the bulk temperatures due to temperature polarization. Changes in the driving force (i.e., difference in partial water vapor pressure brought about by temperature difference) are usually evaluated through TPC presented as follows [65, 79, 80]:

$$\text{TPC} = (t_{fm}-t_{pm})/(t_f-t_P) \quad (13)$$

TPC indicates the thermal efficiency of the MD system, wherein a value nearing unity suggests good thermal efficiency, and values nearing zero means otherwise. It must be noted though that TPC is not a direct coefficient of the reduction in MD driving force, which means that the same TPC values do not necessarily mean having the same driving force values [59].

Considering the effect of a fouling gel-like layer (MMBF) with very small pores or free volume formed on the membrane surface, TPC becomes [55]:

$$TPC = \frac{\Delta T_K}{t_f - t_p} = \left(1 - \frac{1}{1-\left(\frac{p_{pm}}{p_{fm}}\right)}\beta\right)\left(\frac{t_{fm}-t_{pm}}{t_f-t_p}\right) = \left(1 - \frac{1}{1-\left(\frac{p_{pm}}{p_{fm}}\right)}\beta\right)\left(\frac{R_3}{R_3-R_{124}}\right) \quad (14)$$

TPC was found to decrease with the decrease of the pore diameter of the MMBF layer and also with the decrease of the membrane resistance R_3 with respect to the external resistance R_4. In the analysis of Chew et al. [55], they suggested that one possible way of mitigating the effect of vapor pressure depression due to the MMBF layer with small pores is through increasing the heat transfer resistance of the membrane. This mitigating strategy is especially effective for fouling layer with larger characteristic pore diameters. Thus, a low thermal conductivity membrane would possibly help in lessening the effect of vapor pressure depression, and at the same time, it can reduce the conductive heat losses during the MD process. Further suggestion was to utilize a dual-layer membrane wherein a hydrophilic layer with reasonably larger pores (d > 50 nm) is facing the side with MMBF layer [55].

3. MD fouling

Fouling in general is the accumulation of unwanted deposits on the surface of the membrane or inside the pores of the membrane that degrade its permeation flux and salt rejection performances [62, 81]. This is one of the major problems in membrane-based processes. Particularly in pressure-driven technologies (i.e., RO, NF, UF), fouling could pose a very detrimental effect to the desalination and purification process. Generally, the foulants are colloidal in nature that interact with each other, and/or interact with the membrane surface to form deposits. Fouling formation mechanism can be understood by examining the forces of interaction between the particles (foulants) and the membrane surface, and is best described by the classical DLVO theory [82, 83]. The DLVO theory states that the net particle-surface interaction (or particle-particle) is a summation of the van der Waals and the electrical double layer forces. If the particle and surface have different charges, they will have attractive interaction, while if the particle and surface have similar charges, they will be repulsive of

each other. In order to minimize fouling, the surface and the particle should be kept repulsive of each other or reduce the interaction between them. Moreover, particles in a solution can agglomerate and form particulates and deposit on the membrane surface. The agglomeration rate is a function of particle collision and attachment coefficient, wherein higher frequency of collision and large attachment coefficient could lead to more aggregation [84]. The electric double layer interaction is weak at high ionic strength such as in seawater and the particle-particle interaction is dominated by acid-base interaction [85, 86], while the van der Waals interaction has low sensitivity to changes in pH and concentration of electrolytes.

All known kinds of fouling found in other membrane-separation processes also exist in MD. A fouling layer gives additional thermal and hydraulic resistances, which depend on the characteristics of the fouling layer such as porosity and thickness [7, 87]. As can be seen in **Fig. 2a**, the formation of fouling layer reduces the temperature difference across the membrane or an increase in temperature polarization [88], which translates to lesser driving force. If the fouling layer is non-porous, it is likely to contribute to both thermal and hydraulic resistances, while a porous fouling layer may only result to thermal resistance [29]. Gryta [29] investigated the fouling mechanisms of different foulants from wastewater with proteins, bilge water, brines and from the production of demineralized water in a DCMD set-up using polypropylene capillary membranes. Varying fouling tendencies and intensities were observed for the different feed waters. Two types of fouling layers were observed both of which decreased the permeate flux: the porous (**Fig. 2b**) and non-porous **(Fig. 2c**) deposit layers. The porous deposit layer provides additional heat resistance, thus decreasing the permeate flux. On the other hand, the non-porous deposit lessens the transport of water vapor across the membrane or more mass transfer resistance.

Due to membrane pore size, properties, and operational parameter differences, the role of fouling in MD may be different compared to pressure-driven membrane processes, and much more different compared to those encountered in heat exchangers [30, 89]. Previous studies [29, 81, 90] reported a more severe fouling due to deposition of protein and $CaCO_3$ scaling as the feed water temperature increased. **Figures 2b-d** show the microscopic images of virgin (unfouled) (**Fig. 2d**) and fouled membranes covered with $CaCO_3$ (**Fig. 2b**) and protein (**Fig. 2c**) deposits. The flow velocity was observed to affect the growth rate of the fouling layer as well as the morphology and size of the deposits. Higher velocity led to smaller crystal formation and porous deposit layer, while lower velocity produced thicker deposits in the form of “mountain-like” structures [29].

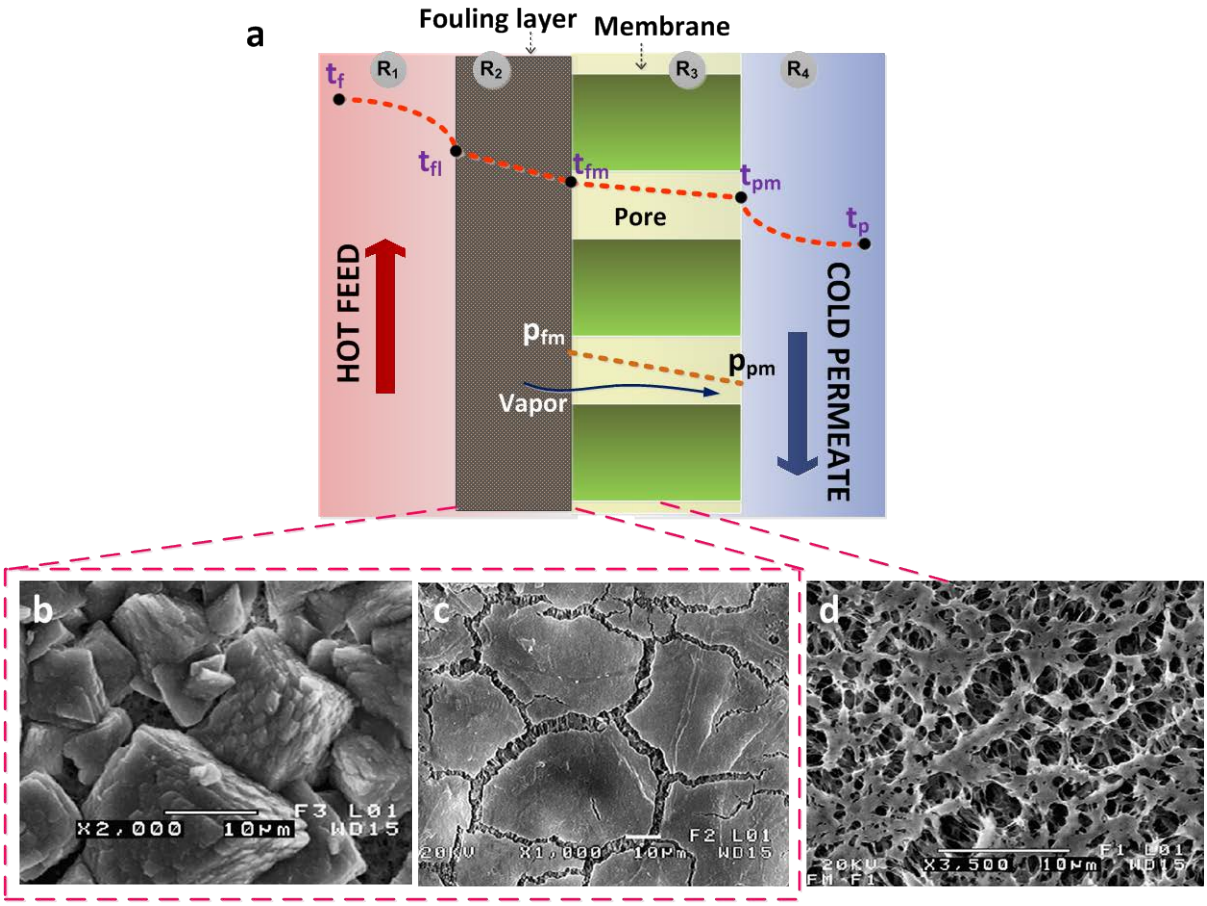

Fig. 2. (a) The effect of fouling on the temperature distribution of DCMD membrane, and; microscopic images of membranes fouled by (b) $CaCO_3$ and (c) protein, and (c) a virgin (unfouled) membrane (Figures b-d are adapted from [29]).

Fouling is a complex phenomenon, which is affected by different factors in its formation on/in the MD membrane surface. Understanding the fouling phenomena is a requisite to have a better approach in minimizing, mitigating, and cleaning the fouling formation. Generally, the following factors affect the fouling formation process: (a) foulant characteristics, (b) feed water characteristics, (c) membrane properties, and (d) operational conditions [31]. **Figure 3** shows the different factors affecting fouling grouped into four: (a) foulant characteristics (concentration, molecular size, solubility, diffusivity, hydrophobicity, charge, etc.); (b) membrane properties (hydrophobicity, surface roughness, pore size and PSD, surface charge, surface functional groups); (c) operational conditions (flux, solution temperature, flow velocity), and; (d) feed water characteristics (solution chemistry, pH, ionic strength, presence of organic/inorganic matters). The type of fouling that will occur on the membrane surface is mainly affected by the kind, concentration and properties of foulants present in the feed water, and the solution chemistry of the feed water. On the other hand, interaction between the foulants and the membrane surface could enhance the fouling propensity, thus membrane

properties can significantly affect fouling. The operational conditions such as feed temperature and flow velocity can also affect the extent of fouling.

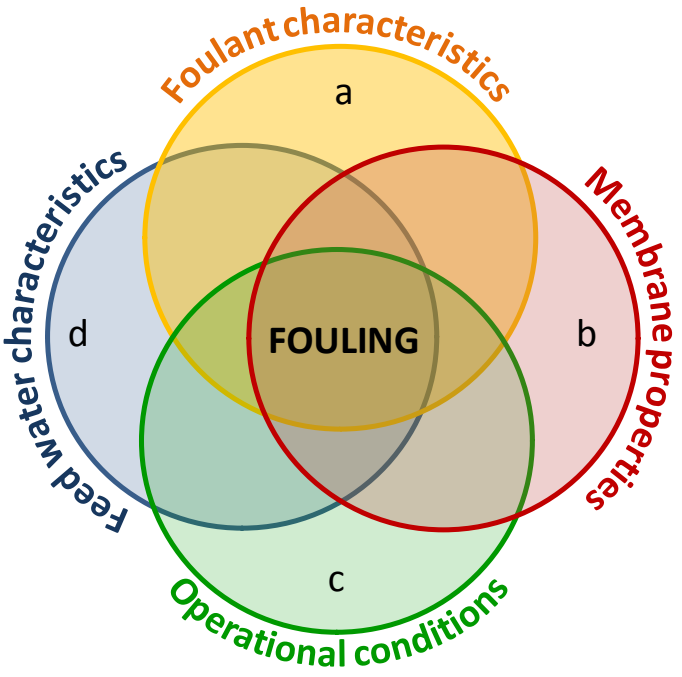

Fig. 3. Factors affecting membrane fouling: (a) foulant characteristics (concentration, molecular size, solubility, diffusivity, hydrophobicity, charge, etc.); (b) membrane properties (hydrophobicity, surface roughness, pore size and PSD, surface charge, surface functional groups); (c) operational conditions (flux, solution temperature, flow velocity), and; (d) feed water characteristics (solution chemistry, pH, ionic strength, presence of organic/inorganic matters).

The sites where fouling occurs can be divided into external surface fouling or pore blocking fouling (see **Fig. 4**) [91]. As the name implies, external surface fouling refers to the build-up or formation of deposits or cake/gel-like layers on the outer surface of the feed-side of the membrane. Pore blocking happens when scales or foulants are formed inside the pores of the membrane by partial blocking or gradual narrowing of the pore, or by complete pore blocking, wherein the full diameter and depth of the pores are covered with deposits [92]. External surface fouling is usually reversible and can be cleaned by chemical cleaning, while internal fouling or pore blocking is in most cases, irreversible, due to compaction of foulants, and membrane degradation [93]. In a previous DCMD study [29], closer inspection of the fouled membrane showed that scales were not only observed on the membrane surface, but also inside the pores of the membranes. The study observed that scale formation inside the pores could lead to damage of the membrane.

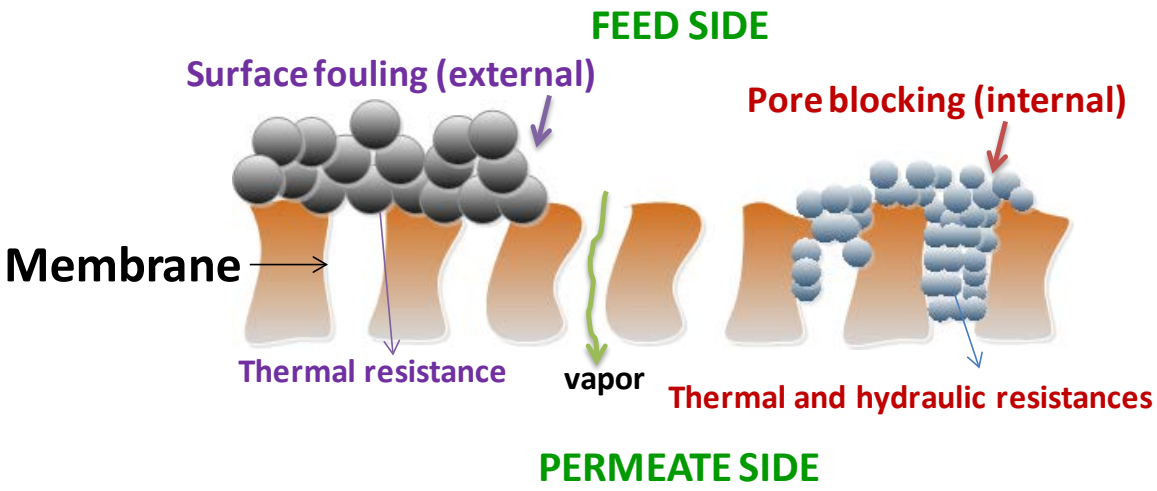

Fig. 4. The fouling sites on a membrane can be divided into surface fouling (external) or pore blocking (internal).

The foulants found in membrane technology including MD can be divided into three broad groups according to the fouling material [94]: (a) inorganic fouling, (b) organic fouling and (c) biological fouling (see **Fig. 5**). Inorganic fouling is caused by the deposition of inorganic colloidal particles and particulates and/or crystallization or precipitation of hard mineral salts from the feed such as calcium carbonate, calcium sulphate, silicate, NaCl, calcium phosphate, $BaSO_4$, $SrSO_4$, ferric oxide, iron oxide, aluminum oxide, etc. Organic fouling is due to the deposition of organic matters such as HA, fulvic acid, protein, polysaccharides, and polyacrylic polymers. And biological fouling is caused mainly by microorganisms such as bacteria and fungi, sludge, algae, yeast, etc. However, in most cases, a single fouling mechanism does not occur in real MD processes, but a combination of different fouling materials and mechanisms that make it more complicated to deal with as depicted in **Fig. 5**.

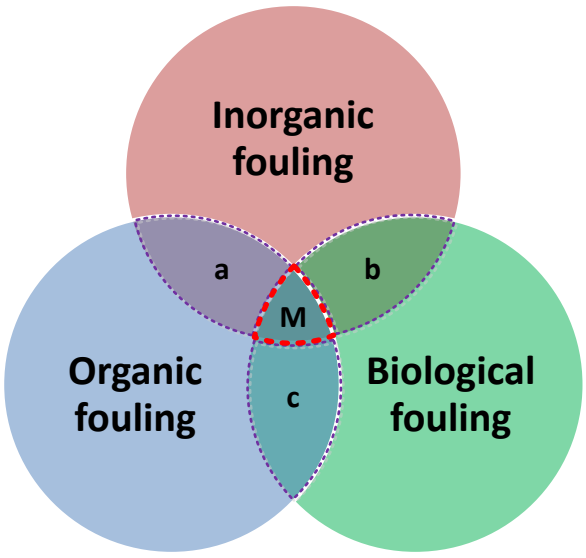

Fig. 5. Schematic representation of the different fouling mechanisms according to the fouling material found in MD. In the real world processes, fouling usually occurs as mixed fouling, i.e., the combination of different of fouling mechanisms happening simultaneously. The dotted lines in the diagram with areas a, b, c and M show the different instances of mixed fouling between two or more fouling mechanisms.

3.1. Inorganic fouling

Inorganic fouling generally refers to scaling, being the deposition of precipitated hard minerals from the feed solution that involves both crystallization and transport mechanisms. Additionally, inorganic colloidal particles and precipitates such as silica, silt, clays, corrosion products, etc. also largely contribute to inorganic fouling. Scales are formed when the ionic product of sparingly soluble salt exceeds the equilibrium solubility product [81]. Scaling is one of the major challenges that hinder the full-scale operation of MD for desalination [90]. In MD processes, a supersaturated condition is mainly caused by water evaporation and temperature changes leading to nucleation and growth of crystals in the feed solution and to the membrane surface [79]. The supersaturation condition and precipitation kinetics should be considered in determining the severity of fouling [32].

Deposits in MD usually start forming at the biggest pores of the membrane, as they are prone to accelerated wettability compared to smaller pore sizes [95]. The nucleation of crystals directly on the membrane surface (surface crystallization) is called heterogeneous crystallization, while those that nucleate in the bulk (bulk crystallization) are termed as homogeneous crystallization [96] (see **Fig. 6**). The scaling in MD usually involves these two mechanisms making it more complex. .

At supersaturated condition, there is more tendency for ions, precipitated particles and foreign matters to collide with each other thus forming secondary crystallization in the bulk phase, and go to the surface as particulates via gravitational settling or particle transport [97, 98]. Deposit layers formed on the membrane surface provide additional thermal resistance and increase the temperature polarization, thus leading to reduced driving force across the membrane, and consequently lower the permeate flux [99]. The most common scales in MD are $CaCO_3$, $CaSO_4$, calcium phosphate, and silicate [100]. Other potential scale foulants include $BaSO_4$, $SrSO_4$, $MgCl_2$, $MgSO_4$, ferric oxide, iron oxide [101], and aluminum oxide.

Several factors affect the rate of scaling such as the degree of supersaturation, flow conditions, membrane surface and solution temperature, water properties, the surface properties such as roughness and morphology, the kind of substrate material, and any nucleation site available such as particulates or impurities in water [102, 103]. **Table 1** shows a list of fouling studies on inorganic fouling in MD.

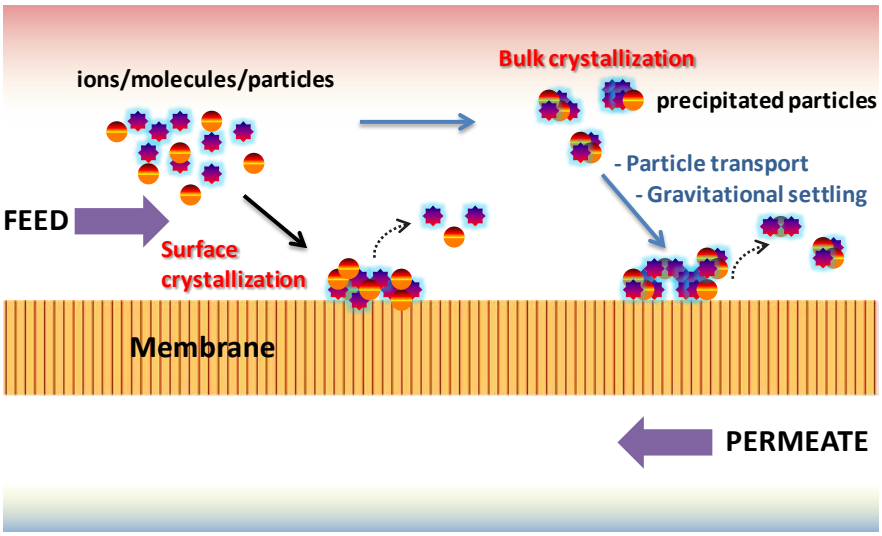

Fig. 6. Schematic representation of the surface (heterogeneous) and bulk (homogeneous) crystallization mechanisms during inorganic fouling of membrane distillation.

Calcium carbonate scales (alkaline scale) have three anhydrous crystalline polymorphs, namely: calcite, aragonite and vaterite. The most thermodynamically stable is calcite and the least one is aragonite [104, 105]. Calcite usually has a round shape, an average particle size of 10 µm, and is formed at ambient temperatures (i.e., < 30°C) [106]. Aragonite exists in needle-like structure and is usually formed above 30°C [106], while vaterite has spherical structure with diameters from 0.05 to 5 µm. $CaCO_3$ is one of the most common foulants found in cooling water systems [107-109]. For MD process, the increase of feed water temperature was found to increase the scaling formation of $CaCO_3$. This is so because $CaCO_3$ has an inverse solubility property, and increasing the water temperature decomposes the HCO_3^- ions present in water, thus forming more $CaCO_3$ deposits on the membrane surface. The reactions leading to calcium carbonate precipitation are as follows [110]:

$$HCO_{3\,(aq)}^{-} \leftrightarrow OH_{(aq)}^{-} + CO_{2\,(aq)} \quad (3)$$

$$OH_{(aq)}^{-} + HCO_3^{-} \leftrightarrow CO_{3\,(aq)}^{2-} + H_2O \quad (4)$$

$$Ca_{(aq)}^{2+} + CO_{3\,(aq)}^{2-} \leftrightarrow CaCO_{3\,(s)} \quad (5)$$

The $CaCO_3$ scaling potential of a solution can be predicted by the use of LSI, which indicates the degree of saturation of water, as shown in the following equation:

$$LSI = pH - pHs \quad (6)$$

where pH is the real measured pH of water and pHs is the saturation pH of calcite or $CaCO_3$. A positive LSI indicates higher potential for precipitation while negative LSI indicates less potential for scaling.

Table 1. Published reports in literature about inorganic fouling in membrane distillation.

Foulant	MD set-up	Membrane type	Pore size (μm)	Porosity (%)	Feed composition	Inlet temperature (Feed/permeate) (°C)	Flow rate (Feed/permeate)	Flux (kg/m^{2}h)	Salt rejection (%)	Observation	Ref
$CaCO_3$	DCMD	Capillary PP	0.22	73	Na: 29, Cl : 70, Ca: 60, Mg: 15, K: 7 (mg/l) and HCO_3^- : 2.2 – 2.4 (mol/L).	(80 ~ 90) / 20	0.3~1.4 / 0.26 ~ 0.29 (m/s)	17.1 ~ 25.3	-	Feed flow rate has a significant influence on the morphology of the formed $CaCO_3$ deposit.	[111]
$CaCO_3$	DCMD	Hollow fiber PVDF	0.18	82	Recirculating cooling water	50 / 20	0.5 / 0.2 (m/s)	-	-	NOM, antiscalant additives and Mg^{2+} in RCW act as an inhibitor to $CaCO_3$ crystal growth in aqueous phase.	[112]
$CaCO_3$	DCMD	Capillary PP	0.22	73	Na : 29.9, Ca : 63.2, Mg : 16.4, Cl : 0.2 (mg/l) and HCO_3^- : 2.2 – 2.4 (mol/L).	(50 ~ 90) / 20	0.35 ~ 1.2 / 0.12 (m/s)	6.5 ~ 23.3	-	Deposits were formed not only on the membrane surface, but also inside the pores.	[29]
$CaCO_3$	DCMD	Capillary PP	0.22	73	Tap water with the addition of $NaHCO_3$ and $CaCl_2$ (mole ratio 2:1)	80 / 20	Feed : 0.11 ~ 1.3 (m/s)	29.3 ~ 32.3	-	The formed deposit was systematically removed from pre-filter by 3 wt. % HCl solution.	[113]
$CaCO_3$	DCMD	Hollow fiber PP	0.2	-	NaCl : 23.27, Na_2SO_4 : 3.99, $NaHCO_3$: 0.193, Na_2CO_3 : 0.0072, $CaCl_2{\cdot}2H_2O$: 1.47 (mg/ml)	40 / 20	7 / 7 (l/min)	1.4 ~ 2.1	-	Two-step cleaning with citric acid aqueous solution (20 min) / NaOH aqueous solution (20 min) allowed to completely restore the transmembrane flux and the hydrophobicity of the membrane.	[7]
$CaCO_3$	DCMD	Capillary PP	0.22	73	Tap water with the addition of $NaHCO_3$ and $CaCl_2$ (mole ratio 2:1)	85 / 20	0.58 / 0.116 (m/s)	-	-	The application of magnetizer for the feed treatment during MD process also reduced negative effects of the scaling.	[114]
$CaCO_3$	DCMD	Capillary PP	0.22	73	Tap water with the addition of $NaHCO_3$ and $CaCl_2$ (mole ratio 2:1)	(80 ~ 90) / 20	0.15 ~ 0.63 / 0.12 (m/s)	25 ~ 38.5	-	An increase in the feed temperature accelerates the hydrolysis of polyphosphates.	[115]
$CaCO_3$	DCMD	Flat-sheet PTFE, PVDF	PVDF-1 : 0.2 PVDF-2 : 0.45 PTFE-1 : 0.2 PTFE-2 : 0.2	PVDF-1 : 80 PVDF-2 : 60 PTFE-1 : 65 PTFE-2 : 66	Na : 10,000, HCO_3^- : 142, SiO_3^{2-} : 1.5 (mg/l)	(30 ~ 50) / 24	0.25 / 0.25 (l/s)	~ 118	-	PVDF and PTFE showed different fouling patterns.	[116]
$CaCO_3$	DCMD	Capillary (Polypropylene)	0.2, 0.43, 0.45 and 1.0	-	0.5 M NaCl, sugar	30 ~ 50 / 20	-	1.7 ~ 5.8	95.00~99.98	A non-linear relationship has been observed between water flux and increasing temperature gradient at higher ΔT.	[117]
$CaCO_3$	VMD	Hollow fiber PVDF	0.25	79	Na : 10, Ca : 30 (mg/l) of bulk solution	Feed : 52, 60 Permeate : -90 ~ -96 kPa	Feed : 0.10 ~ 0.55 (m/s)	9.0 ~ 17.2	-	Microwave irradiation had no significant effect on the mechanical properties and hydrophobicity of the membrane materials. However, microwave irradiation could strengthen the mass transfer process of VMD.	[118]
$CaCO_3$, $CaSO_4$	DCMD	Hollow fiber PP	-	-	$CaCl_2$ and $NaHCO_3$ Or $CaCl_2$ and Na_2SO_4	(72.0 ~ 75.7) / (21.5 ~ 23.5)	465 / 138 (ml/min)	-	-	Antiscalant K752 is more effective in inhibiting $CaSO_4$ scaling compared with other antiscalants tested.	[119]
$CaCO_3$, $CaSO_4$	DCMD	Hollow fiber PP	0.1, 0.2, 0.6 (maximum)	50, 60 ~ 80	Tap water with the addition of Ca^{2+} and HO^{3-}	(70 ~ 80) / 20	80 ~ 1438 / 138 (ml/min)	4.8 ~ 14.3	-	The concentration polarization effect is stronger than the temperature polarization effect during DCMD	[120]
$CaSO_4$	DCMD	Capillary PP	0.22	73	Saline wastewater from ion exchanger regeneration	80 / 20	0.11 / 0.046 (m/s)	14.6 ~ 18.8	-	The permeate flux decline was limited by removing the $CaCO_3$ deposit from the membrane surface by rinsing it with 2 ~ 5 mass % HCl solutions.	[96]
$CaCO_3$, $CaSO_4$, silicate	DCMD	Flat-sheet PTFE	0.22	70	10 mM : $CaCO_3$ or $CaCl_2$ and $KHCO_3$ or Na_2SiO_3 20 mM : $CaSO_4$	40 / 20	1 / 1 (l/min)	1.0 ~ 35.0	-	Scaling caused by $CaSO_4$ on MD membrane was much more severe than scaling caused by $CaCO_3$ or silicate. A decrease in the induction period, and the size of the $CaSO_4$ crystals increased as the feed temperature increased.	[121]
$CaCO_3$, $CaSO_4$, silica	DCMD	Flat-sheet PP	0.1	65 ~ 70	$NaHCO_3$: 213.4, Na_2SO_4 : 3462.7, $CaCl_2$: 623.8, $Na_2SiO_3{\cdot}9H_2O$: 454.4	60.3 / 18.9	600 / 550 (ml/min)	30	99.95	Acid and alkaline washing was employed for the clean-in-place (CIP) procedure of module.	[122]
$CaSO_4$	DCMD	Hollow fiber PVDF	0.16	90.8	36.2 g/L NaCl solution, 46.5 g/L RO brine	55 ~ 77 / 35	0.205 / 0.011 (m/s)	2.5 ~ 5.8	-	Membrane fouling was more significant at the higher temperature investigated for long-time DCMD operation.	[123]
$CaSO_4$ Na_2SO_4	DCMD	Hollow fiber	0.6	60 ~ 80	NaCl : 0.06, $CaCl_2$: 18, $NaSO_4$: 40 (mol/l)	60 ~ 90 / 20	465, 889 / 138, 228 (ml/min)	7.5 ~ 22	-	Modeling shows that the highest scaling potential is to be found at high temperature.	[124]
Ca^{2+}	DCMD	Hollow fiber PP	0.2	-	Pig slurry with 5 M NaOH and 0.5 M H_2SO_4	40 / 40	4 / 3 (l/min)	3 ~ 42	-	MD process fouling is mainly caused by O, S, Fe, Na, Mg, K and microorganisms.	[125]
NaCl	DCMD	Hollow fiber	0.082	82 ~ 85	3.5 % NaCl solution	60 / 25	0.6 / 0.15	~ 16	-	A bubbling assisted DCMD module, the permeate flux	[126]

		PVDF					(Gas bubbling : 0.2) (l/min)			enhancement ratio could reach up to 1.72 at an optimized gas flow rate.	
NaCl	DCMD	Flat-sheet PTFE	0.2, 0.5	0.70, 0.85	3% and 5% NaCl solution, real seawater	(45-55)/(4-45)	3.3 (L/min)	~2-43	-	Pretreatment process is essential for DCMD if real seawater is used as the feed solution.	[88]
NaCl	DCMD	Capillary PP	0.22	72	Tap water and 10 ~ 30 wt.% NaCl solutions	(70 ~ 85) / 20	7 / 7 (cm^3/s)	~ 27.5	-	The membranes soaked in NaCl solutions were wetted faster than those soaked in distilled water.	[63]
NaCl	VMD	Hollow fiber PP	0.2	55 ~ 65	Na : 0.0344, 0.3957, Cl : 0.0166, 0.3581, 0.4299, 0.4497 (mol/l)	Feed :85 Vaccum : 0.07 (MPa)	0.02 (m/s)	4.1 ~ 42.7	-	The morphology of the deposits formed on/in membrane pores elicited a different effect on membrane scaling.	[69]
Na_2SO_4	DCMD	Flat-sheet PVDF	0.22	70	2M Na_2SO_4 and 4.5 M NaCl	(50 ~ 60) / 20 ~ 30	29 ~ 53 / 29 ~ 53 (m/s)	20	-	The critical condition occurs at a slightly lower degree of feed supersaturation for salts with a positive solubility-temperature coefficient.	[127]
NaCl	DCMD	Flat-sheet PVDF	0.2 0.22	75 80	17.8 ~ 24.7 % NaCl	(35 ~ 80) / 20	0.145 (m/s)	2.1 ~ 4.8	-	After the concentration of NaCl solution was saturated, water fluxes began to decrease sharply.	[128]
NaCl, real seawater	DCMD	Hollow fiber PP	0.60	60-80	City water; 3.5, 6, 10% NaCl solution; real seawater	(64-93)/(20-54)	34-63 (L/min)	Max 55	-	High percent recovery of water was achieved and relatively stable water vapor flux was obtained up to 19.5% salt concentration from seawater, with no sign of distillate contamination by salt.	[24]
NaCl	DCMD AGMD	Flat-sheet PTFE	0.18	64.05	10 g/l NaCl 35 g/l NaCl	30 ~ 60 / 24 60 ~ 80 / 15 ~ 37	12 / 12 (l/min) 10 / 20 (l/min)	5 – 35	67.5 ~ 87.5	This manuscript focused on cleaning strategies for removal of fouling layer.	[129]
NaCl	DCMD	Hollow fiber	-	60	1 % NaCl or RO brine	50 ~ 85 / 20	0.25~0.5	2.7 ~ 12.6		The water recovery from different produced waters was 80% by process.	[130]
Tap water	DCMD	Capillary PP	0.22	73	Tap water	60 – 85 /20	0.42 – 0.96 / 0.29 m/s	-	-	The presence of large pores on the membrane surface enables the deposition of $CaCO_3$ crystallites into their interior	[62]
Na_2SO_4 NaCl	DCMD	Flat-sheet PVDF	0.22	70	2 M Na_2SO_4 , 4.5 M NaCl	50 – 60 / 20 -30	0.53 / 0.53 m/s	< 22	-	A drastic decline in flux beyond the critical supersaturation is due to rapid growth of crystal deposition on the membrane and loss of membrane permeability.	[131]
NaCl $CaSO_4$	DCMD	Hollow fiber PP	0.2 – 0.6	60 – 80	0.06 M NaCl with calcium sulfate	60 – 90 / 20	889 / 228 ml/min	8 – 22	-	For gypsum scaling at the membrane surface, concentration polarization effects are more important than temperature polarization effects.	[81]
Synthetic seawater	VMD	Flat-sheet PVDF Flat-sheet Acrylic Flat-sheet PTFE	0.1, 0.2, 0.22	-	35 g/l synthetic seawater, 300 g/l synthetic seawater and real seawater	Feed : 25 – 75 Vacuum : 100 – 1000 Pa	0.4 ~ 2.0 m/s	< 66	-	Scaling and organic fouling are highly dependent of the feed water composition and concentration	[132]
Seawater RO brine	VMD	Flat-sheet PTFE	0.22	40	Seawater 95, 150, 300	Feed :20 – 70 Vacuum : 100 – 10000 Pa	0.4 ~ 2.0 m/s	4.5 – 10.1	-	For high salt concentrations, scaling occurs in vacuum membrane distillation but its impact on the permeate flux is very limited.	[133]
Silica	DCMD	Flat-sheet PVDF, Hollow fiber PP	0.6 (maximum)	60 ~ 80	BWRO concentrate	75 / 50	30 ~ 55 / 15 ~ 30 (L/h)	6 ~ 9	-	The intrusion of brine into the pore is accompanied by an increase in flux because of the shorter diffusion path length through the part of the pore that remains un-wetted.	[134]
Silica	DCMD	Hollow fiber PP	0.22	72	Tap water	(60-85) / 22	30-350 / 30-350 (L/h)	6.25-33	-	-Acidification to pH 4 eliminated scaling tendency. -MD performance improved when subjected to NF softening.	[135]
NaCl, $CaSO_4$, $MgCl_2$, $MgSO_4$, BSA	DCMD	Flat-sheet PVDF Flat-sheet PTFE	0.3 0.2	72	4.5 g/l or 10 g/l NaCl + either $CaSO_4$ or $MgCl_2$ or $MgSO_4$ or BSA or their combination	(40-50) / 20	0.61-0.91 / 0.61 (l/min)	2.16-9	-	- Addition of $CaSO_4$ or BSA to 4.5 or 10 g/l NaCl did not cause severe fouling on PTFE membrane - Addition of $MgCl_2$ or $MgSO_4$ to 4.5 or 10 g/l NaCl has more fouling tendency on PTFE membrane than on PVDF membrane	[136]
Iron oxide	DCMD	Capillary PP	0.22	73	1wt % NaCl solution, 0.1 wt % NaOH or Na : 615, 846, 3380 and Cl : 3380, 23100, 58100 (ppm)	(60 ~ 82) / 20	0.6 ~ 1.1 (m/s)	19.4 ~ 32.9	-	The precipitates formed on the membrane surface are characterized as highly porous.	[101]

DCMD: direct contact membrane distillation; VMD: vacuum membrane distillation; PVDF: polyvinylidene fluoride; PTFE: polytetrafluoroethylene; PP: polypropylene

The precipitation of $CaCO_3$ can be limited by lowering the feed temperature and by increasing the feed flow rate [137]. Pretreatments such as chemical water softening (acidification to pH 4) and pressure-drive membrane filtration can reduce the propensity of $CaCO_3$ scaling [7, 138]. Gryta [139] observed a sudden decline in membrane flux due to the deposition of $CaCO_3$ scales in a DCMD configuration. The deposit provided additional thermal resistance and decreased the temperature polarization coefficient, leading to lower flux. However, it was also observed that simple rinsing with 3 wt% HCl solution can remove the scales and maintain a constant flux. Other studies have also reported the elimination of $CaCO_3$ scaling during the production of demineralized water by acidification to pH 4 [79, 135].

In another study, Gryta [62] reported that rinsing the DCMD module with 2-5 wt% HCl solution has removed $CaCO_3$ scaling, however, the frequent cleaning with HCl solution was observed to gradually decrease the maximum flux attainable for the membrane. The presence of large pores in the membrane resulted to filling of the pores with scales causing wetting, which happens during the cleaning of the membrane with HCl solution. Smaller pore size was found to lessen the propensity of scaling of the membrane, however, the flux performance was also affected. He et al. [120] studied the scaling of membranes by $CaCO_3$ and mixed $CaCO_3/CaSO_4$ in desalination by DCMD. The analysis of scaling potential was presented by means of SI profiles in a cross-flow porous fluorosilicone-coated hollow fiber membrane module. It was found that $CaCO_3$ scaling did not affect the DCMD permeate flux. However, there was a drop in permeate flux for mixed $CaCO_3/CaSO_4$ scaling. The modeling results signified that the effects of concentration polarization were more important than the effects of temperature polarization.

Several reports indicated that the presence of impurities, and other ions (e.g., Mg^{2+}, $Ba^{2+,}$ and SO_4^{2-}) or inhibitors in the feed affects the growth rate and type of $CaCO_3$ scale formed. For example, the presence of Mg ions could lead to aragonite formation and hinder the formation of vaterite [140]. Magnesium is abundant in natural waters and has been reported to prolong the induction period of scale formation and also inhibit the precipitation of $CaCO_3$ [141-143]. Previous studies have indicated that $CaCO_3$ scaling can be minimized by utilizing feed water temperature below 70^oC and a feed flow velocity of at least 0.5 m/s [30, 111]. Pretreatment of the feed water could help in the reduction of fouling formation in MD.

Another common scale in MD is calcium sulphate (non-alkaline scale). Calcium sulphate is known to be a very adherent scale and it exists in three crystallographic forms, namely: dehydrate (gypsum – $CaSO_4 \cdot 2H_2O$), hemi-hydrate (bassanite – $CaSO_4 \cdot 0.5H_2O$), and anhydrite ($CaSO_4$) [102]. From among these, gypsum has the lowest solubility and is the most thermodynamically stable phase. Studies have shown that gypsum exists in the form of needles and platelets, with moclinic and prismatic structures [144, 145] (see **Fig. 7**). These structures depend on the supersaturating ratio and

crystallization kinetics. At low supersaturation ratio (<2.27), wherein surface crystallization dominates, needle-like gypsum structures were observed. On the other hand, at high supersaturation ratio (around 10.86) dominated by bulk precipitation, the platelet gypsum structures were observed [146].

Gryta [96] investigated the calcium sulphate scaling of capillary polypropylene membranes under DCMD. It was found that the composition of the feed and the operating parameters affect the nature and shape of the formed deposits. It was suggested that the concentration of SO_4^{2-} in the solution should not exceed 600 mgL^{-1} concentration to avoid any deterioration of the distillate quality. The simultaneous precipitation of $CaSO_4$ and $CaCO_3$ has yielded weak deposits on the membrane surface, which could be easily removed by HCl washing. He et al. [81] investigated the $CaSO_4$ fouling of hollow fiber membranes in cross flow DCMD. They found decreasing induction period of the scaling formation at increasing feed brine temperature and increasing degree of supersaturation. The scaling of a DCMD process utilizing high concentration of NaCl and Na_2SO_4 was investigated on its effect in MD permeate flux [131]. A gradual decrease in permeate flux was observed, and when the feed water became supersaturated, there was a sharp decrease in flux. Upon careful inspection, scales were observed to fully cover the membrane surface. As saturation of the membrane surface concentration is reached, there will be a difference in the boundary layer and bulk solution properties [128]. For VMD experiments, the fouling of high concentration solution was found to be reversible, and only water washing is needed. Flux measurements before and after washing was found to be within 5% difference only [132], however, less reversible fouling is expected at longer experiments. Mericq et al. [133] investigated the desalination of seawater reverse osmosis brine by VMD.

The behavior of gypsum formation can be described by the well-accepted kinetic model as follows [147, 148]:

$$\frac{dm}{dt} = k(C_m - C_S)^n \qquad (7)$$

where k is the crystal growth rate constant, C_m is the gypsum concentration, C_S is the $CaSO_4$ solubility, and n is a kinetic order (diffusion-controlled crystallization, $n = 1$, and surface reaction process, $n = 2$).

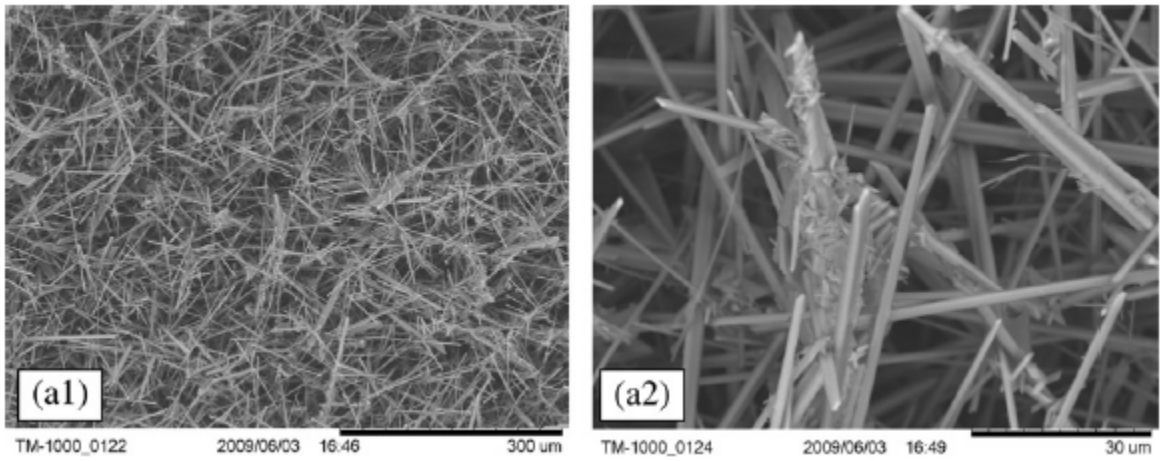

Fig. 7. Gypsum scales showing needle-like strucutures (adapted from [121]).

Silica is one of the minerals found in desalination brines and from petroleum production. Natural feed waters normally contain amorphous or crystalline silica. It possesses normal solubility, thus it precipitates out of solution at lower temperature. Silica formation depends on the pH of the silica concentration in the solution. The formation of silica is associated with aluminium, and it could form even below its saturation level due to its reaction with iron and aluminum ions [149]. Its tendency for fouling can be calculated based from silica concentration, temperature, pH and total alkalinity. Dissolved silica in the form of low molecular weight meta silicic acid can polymerize on the membrane when supersaturation is reached forming colloidal deposits or in gel-like form [32]. Other forms of silica associated with aluminum, which are related to particulate and colloidal fouling sources are silt, clay, mullite, feldspar, and andalucite [150].

In DCMD operation, the temperature polarization at the brine feed side could lead to silica deposit formation at the membrane surface, where silica supersaturation would be at the highest [134]. Gilron et al. [134] investigated the silica fouling in DCMD set-up. Two different MD membranes were utilized: hollow fiber made from fluorosilicone coated polypropylene and a flat-sheet membrane made of PVDF with 0.8 μm nominal pore size. Different concentrations of silica were tested at SI between 1.5 to 2.2. It was observed that silica caused a large decrease in permeate flux, reaching up to 70% decline using hollow fiber modules with an effective induction time of 2-7 h. Decrease in permeate flux was also observed for the flat-sheet membranes using synthetic silica solution. SEM studies not only found silica colloids on the mouths of the pores of the membrane but also inside the membrane pores as deep as 50 μm from the membrane surface. This suggests that the flux decline was due to the following mechanism: silica deposition on the membrane surface, wetting out of the pores and formation of silica deposits inside the pores. Minimizing silica fouling can be done by limiting the aluminium and iron levels, use of pretreatment techniques, and by acid cleaning. In contrast to the above study, Singh et al. [130] did not observe any formation and blinding of the membrane by silica when they utilized DCMD in the treatment of deoiled produced water. In another study, Karakulski

and Gryta [135] observed precipitation of predominantly silica solids on the entrance of the capillary membrane inlets of a DCMD module. This happened even with the use of NF as prefilter to DCMD. The application of a filtration net prior to the module inlet was found to inhibit the blocking of the capillary module from silica deposition.

Several studies using NaCl solutions have reported reduction in permeate fluxes. NaCl is the principal component of feed waters in MD experiments. It is a normal solubility salt, wherein its solubility increases at higher temperature. The pore wetting in intermittent solar MD experiments are mainly attributed to the deposition of NaCl salt crystals during membrane dry-out [151]. Drioli and Wu [117] observed a 72% reduction in permeate flux in the first 3 days of MD operation using a 0.58 wt% NaCl feed solution. In another study, treatment of groundwater from RO plant with TDS of 19000 mg/L was carried out using DCMD. At high temperature operation, the membrane was found to be covered with tenacious fouling layers leading to abrupt reduction of permeate flux, while at lower temperature operation, larger size and loosely-bound deposits were formed, enabling 67% recovery from treatment of RO secondary reject water [152]. The variances in feed temperature and flow rate are reported to have more sensitive effect on fouling rate when utilizing NaCl concentration greater than 25 wt% [128].

No report yet can be found on scaling by calcium phosphate (non-alkaline scale) in MD studies, but calcium phosphate scaling is a common problem in wastewater treatment including those involving RO [32, 153]. Its potential to scale in MD could be possibly related to the use of phosphate antiscalants, wherein improper dosage of antiscalants at their hydrolysis condition could make them as foulants themselves [32, 154]. Iron oxides are also potential foulants, which are usually in particulate form in MD systems. The corrosion of metal parts in the MD system is the main contributor to iron oxide scaling. For example, a long-term solar MD plant study in Spain has found iron oxide scales on the tested membrane, which they attributed to the internal rusting suffered by a storage tank connected to the MD system [25]. In another study, membrane autopsy was carried out after test for iron oxide fouling in DCMD using capillary polypropylene membrane [101]. It was found that considerable amount of corrosion products in reddish-brown color was introduced into the membrane modules, covering the surface of the membranes. The iron oxide deposits had good adherence to the feed membrane surface and the permeate side of the membrane was also found to have some deposits.

3.1.1. Effect of membrane dry-out on fouling

Intermittent operation of MD can result to dry-out of the membrane. This particularly happens when using solar-powered MD where operation is shut-down overnight, thus allowing the drying out of the membranes and the settling of particulates on their surfaces. A previous study [155] has indicated that there is no deterring effect on the membrane if it becomes dry or if it is operated intermittently. However, a recent study proved otherwise. A systematic investigation was carried out

on the effect of dry-out on the fouling of PVDF and PTFE membranes in a DCMD set-up for intermittent seawater desalination [151]. A series of wet/dry cycles were carried out using seawater at feed side temperature from 30-50^{o}C. It was shown that the intermittent operation has resulted to the deposition of salt crystals on the membrane surface, leading to progressive loss of surface hydrophobicity with time. The presence of salt crystals was also observed in the internal structure of the membrane, showing evidence of the wetting of the pores. This has negatively affected the permeate flux and salt rejection of MD. The crystallization of salts in the inside of the membrane has led to surface cracking and membrane damage, and eventually a decrease in membrane mechanical strength. The study has showed more fouling propensity when there is dry-out during MD operation.

3.2. Organic fouling

Organic fouling is the adsorption/deposition of dissolved and colloidal organic matters on the membrane surface such as HA, protein and polysaccharides, carboxylic acid, EPS and many others. This can be adsorption at the molecular level or a physical formation of gel on the surface. The formed organic deposits are usually not easy to clean without the use of chemicals [156]. A previous research identified the following organic materials as the most potential foulants in the order: hydrophilic neutrals > hydrophobic acids >transphillic acids [157]. **Table 2** shows a list of fouling studies on organic fouling in MD.

The most common organic fouling is due to the deposition of NOM. NOM are mainly composed of humic substances [29] and are especially abundant in natural waters [158]. HA are composed of heterogeneous and recalcitrant polymeric organic degradation products with low to moderate molecular weight. They contain both aromatic and aliphatic components with carboxylic and phenolic functional groups [159]. NOM can adsorb on the surface of the membrane through different mechanisms such as specific chemical affinity, and electrostatic and hydrophobic interactions [160]. NOM deposition can: (a) adsorb or deposit inside the pores of the membrane, either partial or complete blocking, so that water passageways are reduced; (b) form a separate gel-like layer on the surface of the membrane, thus blocking the pores, and; (c) bind particles and NOM together forming a low permeability particle/NOM layer on the surface of the membrane [161].

Previous studies using MF membranes, which are also mostly used in MD showed flux decline due to formation of large HA aggregates on the surface of the membrane but not so much fouling in the internal membrane surface. There was initial deposition of HA inside the pores of the membrane, and subsequent deposition followed on the blocked area [162, 163]. The fouling behavior of HAs is affected by the pH and ionic strength of the solution, concentration of monovalent and divalent ions, membrane surface properties and structure, and the operating conditions. The pH of a solution has significant effect on HA fouling. HA has a negative charge for a wide range of pH and its charge density increases at higher pH [164]. Humic macromolecules are reported to favorably adsorb

on hydrophobic membranes especially at low solution pH. A study showed an increasing negative charge of the membrane surface at pH 4, which was attributed to the adsorption of HA, but the membrane became less negative when the concentration of calcium in the solution was increased [165].

Table 2. Published reports in literature about organic fouling in membrane distillation.

Foulant	MD set-up	Membrane type	Pore size (μm)	Porosity (%)	Feed composition	Inlet temperature (Feed/permeate) (^{o}C)	Flow rate (feed/permeate)	Flux (kg/m^{2}h)	Salt rejection (%)	Observation	Ref
NaCl/NOM	DCMD	Capillary PP	0.2[a]	73	Na : 15300 Cl : 25400 (ppm)	80 / 20	14 / 14 (cm^3/s)	3.6 ~ 12.5	-	Membrane rinsing with 2 wt.% solution of citric acid for membrane cleaning.	[166]
Humic acid + NaCl and $CaCl_2$	DCMD	Flat-sheet PTFE and PVDF	PVDF : 0.22 PTFE : 0.2	PVDF : 75 PTFE : 80	10^{-1} M, 10^{-2} M, 10^{-3} M NaCl	30 / 20	Stirring rate : 500 (rpm)	PVDF : 0.6 PTFE : 1.8	99.5	The ionic concentration of NaCl and $CaCl_2$ has no significant effect on membrane fouling in DCMD.	[167]
Humic acid	DCMD	Flat-sheet PTFE and PVDF	PVDF : 0.22 PTFE : 0.2	PVDF : 75 PTFE : 80	10 to 50 mg/l humic acid	30 / 20	Stirring rate : 500 (rpm)	PVDF : 0.6 PTFE : 1.8	> 95 % (humic acid rejection ratio)	DCMD permeate flux is higher for the PTFE membrane than that of the PVDF membrane.	[168]
Humic acid	DCMD	Flat-sheet PVDF	0.22	75	20 ~ 100 mg/l humic acid with 20, 200 mM NaCl or $CaCl_2$	(50 ~ 70) / 20	0.23 / 0.23 (m/s)	30.6 ~ 35.1	-	The increase in ionic strength and the decrease in pH did not affect flux characteristics.	[87]
Protein	DCMD	Capillary PP	0.22	73	Na : 29.9 Cl : 0.2 (mg/l)	(50 ~ 90) / 20	(0.35 ~ 1.2) / 0.12 (m/s)	6.5 ~ 23.3	-	Deposits were formed not only on the membrane surface, but also inside the pores.	[29]
Protein	DCMD	Capillary PP			11 ~ 12 g/l proteins 2 ~ 3 g/l Cl	(50, 60 and 70) / 20	350 / 430 (ml/min)	1.5 ~ 11.3	-	The concentration of proteins and lactose in the feed increased faster at lower temperature.	[169]
Carbohydrates, proteins	MDBR	Flat-sheet PVDF	0.22	75	COD : 0.67, TN : 0.04 (g/l)	55.5 / 19.5	-	4.0 ~ 8.5	99.1 ~ 99.9 (TOC removal)	The faster flux decline in the MDBR is likely due to the increased thermal and hydraulic resistance of the fouling layer	[74]
Ethylene glycol	DCMD	Flat-sheet PTFE	0.2, 0.45, 1.0	80	37 % glycol	65 / (25 ~ 45)	-		-	The flux behavior in this concentration process is highly non-linear, because the increase of glycol concentration causes a decrease in the vapor pressure gradient.	[170]
Dye	VMD	Capillary PP	0.2	75	Dye solution	Feed : 40, 50, 60	Feed : 0.78 ~ 1.67 (m/s) Vacuum : 10 (mbar)	16.0 ~ 57.0	-	Membrane swelling has been observed, which led to an increase of transmembrane fluxes.	[171]
Traditional Chinese medicine (TCM)	DCMD	Flat-sheet PTFE	0.2	-	TCM extract	60 / 25	0.07 ~ 0.13 / 0.07 ~ 0.13 (m/s)	10 ~ 32.8	-	The membrane fouling in these studies were mainly caused by the deposition of suspended solid particles in TCM extract.	[67], [172]
Ginseng extract	VMD	Flat-sheet PTFE	0.2	-	5 % (w/w) ginseng crude extract	Feed : 55, 60	Feed : 0.56, 0.65, 0.74 (m/s) Vacuum : 87.4 (kPa)	7.6 ~ 24.7	-	It is important to prevent the membrane from fouling in VMD process.	[173]
Human urine	VMD	Flat-sheet PTFE	0.2	-	Human urine	Feed : 50, 60, 70	Feed : 30 (l/h) Vacuum : 74 ~ 92 (kPa)	5.0 ~ 13.5	96.3 ~ 98.2 % (ion rejection)	Human urine can be high effectively removed by VMD.	[174]
Skim milk, whey	DCMD	Flat-sheet PTFE	0.5	-	Skim milk and whey	54 / 5	200 / 200 (ml/min)	22	-	The skim milk fouling starts with the deposition of proteins and salts with lactose joining at later fouling stages.	[175, 176]
Fat globules	AGMD	PTFE	0.2 ~ 3	75	3.8 % NaCl	(30 ~ 70) /(2 ~ 20)	-	9.5 ~ 13.0	-	The separation of non-volatile and volatile	[177]

(milk)										solutes was investigated.	
Humic acid + NaCl and $CaCl_2$	DCMD	Flat-sheet modified PVDF	0.45	-	100 g/L NaCl, 10 mg/L humic acid with 1.26 g/L or 0.42 g/L $CaCl_2$	60 / 25	0.2 / 0.4 (m/s)	12 ~ 15	95.5 ~ 99.1 % (humic acid rejection)	Organic foulants were found to penetrate both virgin and superhydrophobic membranes via an adsorption-desorption mechanism.	[178]
Sodium alginate, humic acid, bovine serum albumin	DCMD	Flat-sheet PTFE	0.2	70 ~ 80	10 ~ 20 mg C/L the stock solution	70 / 24	1.1 / 0.3 ~ 2.2 (m/s)	12 ~ 35	99.7 % (humic acid rejection)	HA feed showed thermal disaggregation to low molecular weight HA organics with increased feed temperature (50 and 70°C).	[179]
Synthetic wastewater	DCMD	Flat-sheet PTFE	0.22	70	100 mg/L glucose, 100 mg/L peptone, 17.5 mg/L KH_2PO_4 17.5 mg/L $MgSO_4$, 10 mg/L $FeSO_4$, 225 mg/L CH_3COONa, 35 mg/L urea	40 / 20	11.7 / 11.7 (cm/s)		> 95 % removal of all TrOCs	Results reported here suggest that rejection and fate and transport of TrOC during MD would be mainly governed by the volatility and partially governed by the hydrophobicity of the compound.	[180]
RO concentrated wastewater	VMD	PVDF hollow fiber	0.16	82 ~ 85	RO concentrated wastewater	Feed : 70	Feed : 1.0 m/s Permeate vacuum : 0.085 MPa	-	-	The results show that the contaminant on the membrane surface mainly contained $CaSO_4$, $CaCO_3$, and trace organic matter in the substeady state.	[181]
Protein	DCMD	Flat-sheet PTFE	0.2 0.45	80 80	BSA solution with NaCl	30.5 ~ 56.7 / 20.7 ~ 50.7	5.9, 8.9 cm/s	0.702 ~ 2.063 L/m^2s	-	Membrane fouling is absent in MD of protein solution	[169]
Tomato puree	DCMD	Flat-sheet PTFE, Acrylic fluorourethane copolymer	0.2 0.2	78 -	Tomato puree with 28 % NaCl	20 ~ 24 / 20 ~ 24	500 / 500 ml/min	0.61 ~ 1.25	-	Fouled membranes were characterized by the adhesion of fatty substances, including pigments, to the membrane surface	[182]
Dye concentration	VMD	Shell and tube PP	0.2	-	Dye concentration with 0 ~ 1.2 M NaCl	Feed : 40 - 70	Feed : 14, 17, 30, 42 and 57 mL/s Vacuum : 5 mm Hg	4.5 ~ 8.2		The dye was concentrated in the feed reservoir and was not detected in the permeate.	[16]

DCMD: direct contact membrane distillation; VMD: vacuum membrane distillation; AGMD: air-gap membrane distillation; MDBR: Membrane distillation bio-reactor; PVDF: polyvinylidene fluoride; PTFE: polytetrafluoroethylene; PP: polypropylene

[a] The unit in the paper was given in mm but we believe this should be in µm

The influence of different parameters such as pH, ionic strength and divalent ion concentration on HA fouling was investigated [87]. In a DCMD set-up, the presence of divalent ions caused a higher reduction in water flux. The Ca^{2+} acted as a binding agent, which complexes with the negatively-charged carboxyl groups of HA, leading to the formation of bigger aggregates [165]. By changing the pH of the solution, it was found that bigger HA aggregates were formed at low pH, which is attributed to the reduction of intra- and intermolecular electrostatic repulsions brought about by the protonation of the carboxylic groups of HA. But flux performance between pH 3 and 7 without any divalent ions showed not much difference. This was because no pore blocking was observed and the fouling layers were loosely packed. When divalent ions were added, lower reduction in flux was observed at lower pH (i.e., pH 3 compared to pH 7), mainly because at low pH, there is lower instance of dissociation of HA, which translates to lower availability of carboxyl groups for the divalent ions to complex with, thus lower amount of coagulate was produced [87, 165]. The HA coagulate fouling layer was found to be easily cleaned by rinsing with clean water and 0.1 M NaOH solution [87].

In a different study, Khayet et al. [168] investigated the treatment of HA solutions. Microporous PTFE and PVDF membranes were used in a DCMD set-up. The extent of HA fouling was found to be affected by the pH, the concentration of HA, and the driving force. However, in their subsequent study [167], they reported that there was no significant effect on MD membrane fouling by the addition of different concentrations of NaCl and $CaCl_2$ in the solution. The DCMD treatment of HA was found to have lower fouling formation and higher salt rejection compared to the same HA solution treatment using nanofiltration. The hydrophobic components of NOM are the main culprit for the fouling formation, whereas the hydrophilic component has relatively little effect.

Two recent studies [178, 179] showed some penetration of HA organics through the membrane and explained the underlying causes of penetration. Meng et al. [178] investigated the DCMD performance of a superhydrophibic PVDF membrane coated with TiO_2 and fluoro-silane compounds. They found that organic foulants penetrated into both virgin and superhydrophobic membranes even without the occurrence of partial pore wetting. This was attributed to their proposed adsorption-desorption foulant migration mechanism through the membrane, which was dependent on the adsorption strength of the foulant to the membrane. The adsorption-desorption mechanism works through the following steps: 1) HA is adsorbed on the membrane surface by bonding of phenolic and carboxylic functional groups; 2) HA then migrates due to hydrogen bonding of the unattached carboxylic and phenolic groups with water vapor, leading to desorption of HA from the membrane surface; 3) with the movement of water vapor inside the pores, HA is again adsorbed further inside the membrane pores, and 4) this cycle repeats itself until HA reaches and dissolves in the permeate side. In a different study, Naidu et al. [179] investigated the organic fouling development in DCMD using synthetic model solutions of HA, alginate acid and BSA. They found significant fouling due to

BSA and HA, however, only minimal fouling was observed for alginate acid, which was attributed to its hydrophilic property and to negative electrostatic repulsion. BY LC-OCD and SEM-EDS line depth analyses of the foulant and the membrane, it was found that HA compound in the feed tends to disaggregate more at higher temperature, i.e., from 50 to 70^{o}C, forming low molecular weight HA that can penetrate through the membrane and dissolve in the permeate.

Gryta et al. [166] performed the concentration of NaCl solution containing NOM by MD using polypropylene capillary membranes. It was found that the presence of NOMs in the feed has caused the fouling formation of MD membranes leading to rapid flux decline. Their results showed that the major component of the fouling layer was composed mainly of protein and sodium chloride. It was also found out that heating the salt solution to its boiling point followed by filtration as a pretreatment method has decreased the occurrence of fouling. Furthermore, rinsing the MD module with 2 wt% citric acid solution has enabled reduction of fouling deposition and restored the module performance close to the initial efficiency. Studies found that HA fouling has fewer occurrences in MD compared to other membrane processes [87, 168]. Polysacchardies are larger molecules compared to HAs with a molecular weight ranging from a few hundreds to a few thousands kDa. They possess weak negative charges and have typically rigid fibrillar- or rod-like structures [158]. Reports indicated severe fouling by protein at higher feed water temperatures [90].

MD was utilized for the concentration of bovine serum albumin (BSA) aqueous solution [183]. It was found that no fouling was formed for a BSA concentration up to 1 % w/w and for MD operation at low temperature (i.e., 20-38^{o}C) and solution pH of 7.4. However, in a separate study [182], fouling formation occurred even at low temperature operation when MD was used for the concentration of tomato puree, which contained 0.5-1 % protein and 0.1-0.3 % fat. The results indicated the adhesion of fatty substances and tomato pigments onto the surface of the membrane, which consequently block the pores and reduce the permeate flux. Kimura et al. [177] reported a fouling formation by fat globules on a PTFE membrane in AGMD set-up during the concentration of milk.

MD can also be used effectively for the separation of dyes from water. Banat et al. [16] studied the feasibility of VMD for treating water containing MB dye at a fixed concentration of 18.5 ppm. Their results showed the applicability of VMD to treat MD solution, resulting to pure water at the permeate side, however, flux decline was observed due to the formation of fouling layer. Criscuoli et al. [171] investigated the use of VMD to treat five different kinds of dyes with concentrations from 25-500 ppm and checked the effect of fouling on the performance of the VMD. The results indicated that the permeate flux has close relation with the chemical properties of the dyes. Flux decay especially in the first 30 min of operation was observed for all tests, which was attributed to the fouling phenomenon. Prolonged cleaning with distilled water was found adequate to restore the flux close to the initial flux.

Ding et al. [67] investigated the effect of fouling layer formation on the DCMD permeate flux during the concentration of TCM extract. The suspended solid particles from the TCM extract was found to mainly cause the fouling deposition and to a little extent, due to the presence of protein in the TCM extract. The membrane surface was covered with porous fouling layer. Interestingly, no considerable wetting of the membrane was observed due to the formed deposits. A faster flux decline and fouling rate were obtained at increasing feed temperature and flow velocity. However, the results also revealed that the fouling deposition on the membrane surface can be effectively minimized by an increase in feed temperature and flow velocity.

3.3. Biological fouling

Biological fouling or biofouling is the accumulation and growth of biological species on the membrane surface that affects the permeability of the membrane, leading to loss of productivity and other operational problems. Microorganisms are the main culprit of biofouling. However, its occurrence in MD processes is limited due to the high salinity of the feed, which limits microorganism growth, and also due to the higher operating temperature, which are higher than the growth temperature of most bacteria [184]. Thus, when compared with other membrane processes such as RO, NF, UF and MF, one can expect lower biofouling formation in MD. As an example, a higher number of bacteria of 2.1 x 10^8 CFU/cm^2 was found at the feed side of the membrane for an RO process [185]. However, there are bacterial species that can survive and grow at extreme surroundings, thus biofouling can still occur in MD. Additionally, in a full-scale MD module, the temperature of the feed changes from the entrance to the exit of the module. It was reported that a typical feed inlet temperature of 70-80^{o}C could drop to 30-40^{o}C at the outlet of the module. Thus, the different temperatures along the length of the module could present growth environments for microorganisms especially at temperatures below 60^{o}C. Temperatures higher than 60^{o}C are not suitable for most mesophilic microorganisms [186]. Biofouling can occur occasionally even in the extremely oligotrophic environment in which microorganisms can live with very low levels of nutrients.

Table 3 gives a list of biofouling studies in MD process. Gryta [184] evaluated the growth of microorganisms including fungi (*Penicillium* and *Aspergillus*) and bacteria (*Pseudomonas* and *Streptococcus faecalis*) on the MD membrane surface in a DCMD set-up. Different microorganisms reacted differently to the fouling of membrane, where some bacteria and fungi where found on the feed membrane surface side, while another bacterial species was found at the distillate side. Krivorot et al. [186] studied the factors affecting the biofilm formation in a DCMD set-up under cross-flow and parallel flow conditions using PP hollow fibers. Biofilm formation was observed for all membranes especially after 28 h of operation. The entrance of the membrane module was found to have less

biofouling formation compared to the exit of the module, which is attributed to the differences in temperature, i.e., higher temperature at the inlet, and lower temperature at the outlet.

Biofilm formation is found to commence with the adsorption of a conditioning film on the membrane surface. The conditioning film usually consists of proteins, lipids, polysaccharides, HAs, nucleic acids and aromatic amino acids. Bacteria present in water then adhere on the conditioning film and bind themselves together and start to grow [187, 188]. Bacteria are more resistant when they are embedded in a biofilm as compared to those in a dispersed state [189]. Biofilm formation on the membrane surface induces wetting of the membrane due to the secretion of EPS with amphiphilic properties from microorganisms. Thus, the hydrophobicity of the membrane is decreased leading to leaking of salts from the feed side to the distillate side. Furthermore, biofilm formation could partially or completely block the pores of the membrane, so that the diffusive transport is largely reduced. There could also be an increase in temperature polarization due to the generation of hydrodynamically stagnant biofilm layer [29].

Table 3. Published reports in literature about biological fouling in membrane distillation.

Foulant	MD set-up	Membrane type	Pore size (μm)	Porosity (%)	Feed composition	Inlet temperature (Feed/permeate) (°C)	Flow rate (Feed/permeate)	Flux (kg/m^2h)	Observation	Ref
Bacteria, fungi	DCMD	Capillary PP	0.22	73 %	50 ~ 150 sugar, 5 ~ 20 yeast, 55, 160, 300 NaCl (g/l)	(60 ~ 90) / 20	(0.12 ~ 0.417) / (0.0128 ~ 0.3) (m/s)	-	Growth of fungi and anaerobic bacteria was observed on the membrane surface.	[184]
Bacteria	DCMD	Hollow fiber PP	0.6 (maximum pore size)	70 %	Real seawater	40 / 20	0.03 / 0.22 (m/s)	< 3.9	In parallel flow experiments biofilm formation did not result in flux loss. In crossflow experiment slight flow decline was observed after 180 h.	[186]
Bacteria	DCMD	Capillary PP	0.2	73 %	Na : 18500, Cl : 29000 (mg/l)	Feed : 80, 90	(0.367, 0.417) / 0.0129, 0.235 (m/s)	< 22.9	During the concentration of the prepared feed, fouling phenomenon was not observed.	[190]
Bacteria	DCMD	Capillary PP	0.22	73 %	Glycerol 1% (v/v), extract 5 g/l, peptone K 20g/l and lag phase 10% (v/v)	36 / (20 ~ 24)	Permeate : 0.78 ~ 0.85 (m/s)	< 1.3	The conditions for microorganisms' growth in the MDBR were improved and an increase in the bioreactor productivity was observed.	[191]
Sludge	MDBR	Flat-sheet PVDF	0.22	-	$K_2HPO_4 \cdot 2H_2O$: 22.2, KH_2PO_4 : 7.26, urea : 18, $MgSO_4 \cdot 7H_2O$ and 0.1 M NaOH	55 / 19.5	Permeate : 7.4	3.4 ~ 8.4	The presence of a biofilm layer in the cross-flow MD experiments resulted in a 60 % reduction in the flux.	[75]
Bacteria	MDBR	Flat-sheet and tubular PVDF and PTFE	PVDF : 0.22 PVDF: 0.2 PTFE : 0.45	PVDF : 80 PVDF : 70 PTFE : 70	Glucose : 12.5 (g/l)	56 / 25	Permeate : 700 ml/min	5	The submerged MDBR process can provide acceptable permeate flow rate with high permeate quality.	[76]
Sludge	MDBR	Tubular PVDF	0.22	-	Glucose : 3.8, Peptone : 1.8 (g/l)	(46 ~ 56) / (15 ~ 25)	3 / 3 (l/min)	2 ~ 5	The MDBR process can be operated with only modest primary energy demand, provided the latent heat comes from low grade waste heat and water cooling is available.	[192]
Petrochemical wastewater	MDBR	Flat-sheet PTFE	0.45	-	Oil, fatty acids, emulsifiers, corrosion inhibitors, bactericides, etc.	58/30	-	5.5	The decline in permeate flux was mainly due to inorganic fouling.	[193]
Macromolecular and biofouling	Modeling study		-	-	-	-	(50 ~ 90) / 20	-	The temperature polarization coefficient is a useful metric for assessing the effect of a macro-molecular- or bio-fouling layer.	[55]
Protein	DCMD	Capillary PP	0.22	73	Na : 29.9 Cl : 0.2 (mg/l)	(50 ~ 90) / 20	(0.35 ~ 1.2) / 0.12 (m/s)	6.5 ~ 23.3	Deposits were formed not only on the membrane surface, but also inside the pores.	[29]
Synthetic wastewater	MDBR	Flat-sheet PVDF	0.22	-	4.27 g/l Glucose, 0.85 g/l meat extract, 1.07 g/l peptone, 0.19 g/l KH_2PO_4, 0.19 g/l $MgSO_4$, 0.16 g/L $FeCl_3$, 3.2 g/l CH_3COONa	55.5 / 19.5	Permeate : 350 ml/min	4.1 ~ 8.3	Mass transfer resistance in the fouling layer is likely to be more significant than heat transfer resistance.	[74]
Synthetic wastewater	DCMD	Hollow fiber PP	0.2	-	NaCl : 23.27, Na_2SO_4 : 3.99, $NaHCO_3$: 0.193, Na_2CO_3 : 0.0072 (mg/ml)	40 / 20	7 / 7 (l/min)	1.4 ~ 2.1	Two-step cleaning with citric acid aqueous solution (20 min) / NaOH aqueous solution (20 min) allowed to completely restore the transmembrane flux and the hydrophobicity of the membrane.	[7]

DCMD: direct contact membrane distillation; VMD: vacuum membrane distillation; AGMD: air-gap membrane distillation; MDBR: Membrane distillation bio-reactor; PVDF: polyvinylidene fluoride; PTFE: polytetrafluoroethylene; PP: polypropylene

Krivorot et al. [29] investigated the factors affecting biofilm formation and biofouling in seawater desalination by DCMD. In contrast to the previous studies on biofouling, this study considered feed water with high salinity and low COD/TOC content. In particular, the study focused on the effects of hydrodynamics and temperature regimes on the biofouling formation on hydrophobic hollow fiber membranes made of polypropylene coated with fluorosilicone. Cross-flow and parallel flow experiments were conducted at two different feed temperatures (40^{o}C, and initially 70^{o}C then running at 40^{o}C). Conditioning film was observed as early as 4 h of operation, however, biofilm formation was only discerned after 28 h. Interestingly, the biofilm formation did not result to decline in permeate flux for the parallel flow configuration, but a slight flux loss was observed for the cross-flow experiment only after 180 h. Biofilm and conditioning film were formed more at the outlet side of the module in cross-flow experiment compared to that at the inlet side, primarily because of the differences in temperature. The outlet side has lower temperature, thus it is less detrimental to the microorganisms, leading to more growth. **Figure 8** shows a biofouling layer containing microorganisms and some salt crystals.

The extent of biofouling formation in a DCMD set-up can be lessened by utilizing constant or cycling feed temperature of 70^{o}C or higher. Gryta [184] also observed the dependence of microbial growth to the feed temperature and its composition for wastewater treatment. In recent years, MD/MD hybrid systems have been employed for the reclamation of hot industrial wastewaters or those with access to waste heat, and containing solutes with low volatility or those containing recalcitrant organics (e.g., textiles) [74, 192-195]. A recent study [74] showed significant flux decline due to biofouling formation in an MDBR process. However, the fouling was controlled through periodic cleaning and process optimization. Reducing the organic and nutrient concentration of the retentate resulted to delayed membrane wetting, which consequently lowered the number of cleaning times. In another study, the formation of a biofouling layer was found to result to large vapor pressure depression of 20-36% in diffusional and vacuum-enhanced evaporation experiments [75]. A 60% flux reduction was also observed during cross-flow experiments primarily due to the effect of biofouling formation.

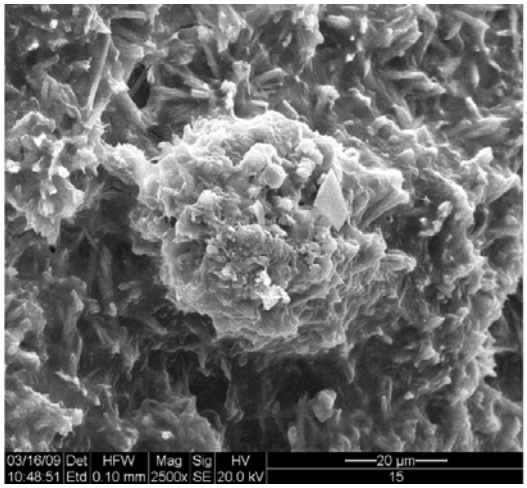

Fig. 8. Biofouling layer on hollow fiber membranes made of polypropylene coated with flurosilicone (adapted from [29]).

In real MD processes, the feed water usually contains a combination of different components such as mineral salts, colloidal matters and precipitates, organics, and microorganisms, thus, not only a single fouling mechanism can be observed. A mixed fouling mechanism is most likely to occur, which oftentimes have synergistic effect with each other. Particulates can first be transported to the membrane surface, which could act as a site for bacteria to grow. When biofilm is formed, it can adhere different particles and impurities that make fouling more severe. Curcio et al. [7] investigated the kinetics of calcium carbonate scaling on a microporous polypropylene membrane when treating seawater with high concentration factors by DCMD. In a semi-pilot plant, DCMD test showed a 33% decrease in transmembrane permeate flux. The presence of HA in the solution, even at a low concentration, was found to help retard the nucleation and growth of vaterite crystals at low supersaturation.

Several factors can affect the kind of fouling mechanism that happens on the surface such as the feed water properties (e.g., hardness, pH, ionic strength, etc.), membrane surface properties, geometry, and morphology, and the physico-chemical properties of the foulants [156]. When deposits are accumulated at the surface, it can lead to pore wetting, and at a severe case, pore flooding which drastically degrades the MD membrane performance. Additionally, minerals from the feed can also intrude inside the pores and could possibly pollute the distillate; or the scales can form inside the pores, thus clogging them, drastically lowering the mass transfer rate. The formed foulants and scales can easily be wetted, in which case, could result to progressive wettability of the membrane (lowers the contact angle), most especially if deposits are formed inside the pores of the membranes [29, 30, 116]. Fouling and cleaning of membranes entail large amount of costs that include increased energy consumption, system downtime for replacement, cleaning, maintenance, membrane replacement, and additional personnel costs [99, 196].

4. MD fouling control and cleaning

Several efforts have been undertaken to address the issue of fouling, especially on cleaning. However, effective fouling control techniques for MD are still lacking. The current techniques for the control of fouling are feed pretreatment and membrane cleaning [57]. Some other approaches to mitigate fouling include making of novel membranes with new design and materials, changing the flow regimes, development of anti-fouling membranes including membrane surface modification, design of new membrane modules, and use of physical and chemical techniques [29, 197].

4.1. Pretreatment

Pretreatment of feed is an effective way of minimizing the extent of fouling on membrane-separation processes, thus resulting to increased quality of the permeate [198]. In fact, pretreatment is a requirement for seawater RO desalination to combat fouling [199]. Ineffective or unreliable pretreatment can lead high rates of membrane fouling, high frequency of membrane cleanings, lower recovery rates, high operating pressure, poor product quality and reduced membrane life [200]. Pretreatment can alter the physico-chemical and/or biological properties of the feed water resulting to lesser fouling formation and improved desalination performance. Pretreating seawater in a biofilter was found to reduce the nutrient concentration, thus significantly declining the biofilm formation in RO systems [189]. Several methods such as coagulation/precipitation, media filtration, sonication, boiling (thermal water softening), membrane filtration, pH changes, chlorination, etc. are used as pretreatment methods for desalination and water purification processes [201]. The efficiency of pretreatment depends on many parameters such as the agents used, temperature, dosing point, solution and foulant properties, and the characteristics of the membrane [33].

MD is anticipated to require less intensive pretreatment compared to pressure-driven membrane processes due to the absence of high pressure that lead to the compaction of fouling layers [30, 202]. However, the importance of pretreatment in MD cannot be underestimated because it acts as the first line of defense for membrane fouling especially in industrial desalination setting. Different real feed source waters contain mixed constituents (i.e., inorganic, organic, colloids and particulates, and microorganisms) and may be exposed to variable feed water qualities, hence pretreatment is a necessary first step for practical MD application, but is not as intensive compared to pretreatment in pressure-driven desalination technologies. In general, pretreatment in MD must be applied to the feed to initially remove macroparticles and microorganisms. The removal of turbidity and fine particulates (TSS) is necessary for seawater RO but not required for MD [88]. However, when real seawater is used as feed, pretreatment is an essential process for MD to reduce fouling formation [88].

Many pilot scale MD plant studies employ different pretreatment methods in their experiments. For example, Jansen et al. [51] operated an MD pilot plant based on liquid gap MD and

employed filtration and degassing to pretreat the feed seawater. High quality permeate could be obtained with simple pretreatment (such as sieving at ~40 μm). One notable small DCMD pilot plant study was carried out by Song et al. [24] and successfully operated on a daily basis for three months. The hot brine used was either city water at different salt concentrations (3.5, 6, and 10 %) or trucked-in seawater. The results indicated high water recovery and relatively stable water vapor flux, with no salt contamination in the distillate side. Concentrating the seawater up to 19% did not result to fouling of the modules, even though scaling salt precipitates were floating around. This pilot study applied prefiltration using 1 μm PP prefilter as pretreatment to the DCMD pilot plant, which could explain its less fouling propensity as the prefilter prevented macroparticles, biological and other slimy materials in seawater from coming and fouling the membrane modules. In contrast, direct use of coastal seawater as feed without pretreatment from the Mediterranean Sea taken during the summer and autumn seasons [186] showed biofilm formation on the membrane surfaces after sufficient operating time.

Coagulation is recognized as one of the effective and low-cost pretreatment methods for membrane separation processes. The coagulants can change the stability of the particles present in the feed by neutralizing the charge and allows the small suspended particles to collide and agglomerate into bigger and heavier particles. Wang et al. [112] investigated the effect of PACl coagulant as a pretreatment for the desalination by MD of RCW. Distorted rhombic magnesium-calcite scales were formed when coagulation pretreatment was used compared to loosely-packed deposits with small-size particles when no coagulation was employed. Coagulation was found to remove substantial parts of NOM including total organic carbon and total phosphorus, and also removed some antiscalant additives, which lead to the formation of large crystals on the membrane surface. The formation of bigger crystals due to coagulation reduces the tendency of membrane partial wetting, because the bigger crystals find it difficult to enter the membrane pores, and just deposit on the surface. The results revealed that coagulation pretreatment has improved the MD flux by 23% compared to that without pretreatment [112]. In another study, pretreatment by precipitation of foulants by $Ca(OH)_2$ was found to significantly limit the occurrence of membrane fouling during the MD treatment of generated effluents from the regeneration of ion exchangers [203].

Membrane-based filtration pretreatments such as the use of MF, UF and even NF are gaining increasing attention due to their efficient removal of particulate materials and large macromolecules in the feed. El-Abbassi et al. [204] investigated the effect of two pretreatment methods (coagulation/flocculation and MF) in the treatment of OMW by DCMD. They found that between the two pretreatment methods, MF showed the better results when integrated with DCMD. A reduction of 30% in total solids was observed when using MF as pretreatment compared to a reduction of 23% total solids using coagulation/flocculation method. Pretreatment by MF prior to MD process was found to increase the permeate flux by 25%, thus rendering pretreatment as an effective technique to enhance the flux performance [79]. Zhiqing et al. [181] investigated the effect of UF with coagulation

as pretreatment on membrane fouling and VMD performance of RO concentrated wastewater. PACl, $FeCl_3$, and PAM were selected as coagulants. After coagulation with optimized dosages, the feed solution was further treated with UF hydrophilic membrane by dead-end filtration process. The feed solution flowed through the hollow fiber membranes and the vacuum system was connected to the module. The results showed that the flux of VMD process was increased after pretreatment by coagulation and UF, and when the concentration factor reached 8, the flux of VMD process using properly pretreated solution was 30 % higher than that using unpretreated solution. The COD_{cr} removal also reached 40%. Among the coagulants used, PACl showed the best results compared with PAM and $FeCl_3$. Pretreated feed water by PACl and UF showed higher normalized flux and low fouling tendency than those of unpretreated feed and the feed treated with PACl only. In another study, NF was used as pretreatment, which significantly improved the performance of a DCMD module using tap water as feed [135]. However, some silica precipitation after NF pretreatment was found that blocked the DCMD module inlet. This blocking problem was resolved by just adding a filtration net after NF and prior to the module inlet, and the process was run without flux decline for 1100 h. The use of cartridge filters/screens is reported to be enough in effectively removing particulates from the feed water.

Thermal pretreatment or boiling of water to remove most bicarbonates from water was also reported to minimize the scaling of the membrane in MD [205]. This treatment would be more beneficial when utilizing groundwater that usually contains high hardness by intentionally breaking down bicarbonates at high temperature. In another study, boiling and filtration of saline wastewater was found to reduce the occurrence of protein fouling [29]. The wastewater was boiled for 30 min and then after cooling to room temperature, was filtered out using a filter paper. As a result, the TOC and turbidity of the wastewater decreased by 60 and 79%, respectively after boiling. This lead to the prevention of rapid flux decline in DCMD, confirming that the thermal (boiling pretreatment) has removed protein foulants from the feed.

Conventional precipitation as water softening method is often used to induce $CaCO_3$ precipitation by chemical dosing using lime, caustic and soda ash [206]. However, this method requires longer time for settling and has low solid production (2-30% solid content) [206]. To aid in this deficiency, seeded precipitation process was developed. In a previous work, APS method was used as pretreatment for the high-recovery desalination of RO concentrate by DCMD. Qu et al. [138] employed APS method by pH adjustment with sodium hydroxide together with calcite seeding, and followed by MF. The APS pretreatment removed 92% of calcium, leading to the reduction of scaling potential from $CaCO_3$ and $CaSO_4$. The permeate flux was found to only decline by 20% after 300 h of operation. Controlling the pH of the feed solution is a good pretreatment strategy to alleviate the effect of scaling in MD. Many researchers add acid such as HCl to bring feed water to pH 4 or 5 [112, 120] and found effective mitigation of $CaCO_3$ scaling , but not much success for silica [135]. One

issue of this is the cost associated with the use of acid, which could be costly depending on the usage volume and the desired pH.

Table 4 shows some MD studies reported in literature using pretreatment to control the effect of fouling. These studies show that pretreatment can positively affect the performance of MD through an improved permeate flux and lower occurrence of membrane fouling. The availability of renewable energy such as solar and geothermal, and the possibility of coupling MD with waste heat, can provide a more energy efficient MD process together with pretreatment. It is ought to be emphasized that pretreatment in MD is a necessary step toward practical industrial and pilot-scale desalination, water treatment and purification processes, that would lead to lesser fouling formation, and more efficient MD operation.

Table 4. Some pretreatment strategies for MD application reported in literature.

MD configuration (membrane material)	**Feed type**	**Pretreatment**	**Observation/remarks**	**Ref**
DCMD (PVDF hollow fiber)	Recirculating cooling water	PACl coagulation, precision filtration, acidification and degasification	- MD flux improved by 23% after employing coagulation pretreatment in 30 days operation.	[112]
DCMD (PP hollow fiber)	Tap water	NF and filtration net	- NF pretreatment and filtration net prior to module inlet has improved the long-term DCMD performance up to 1100 h.	[135]
DCMD (PP hollow fiber)	Groundwater, tap water, lake water	Thermal softening or boiling and filtration by filter paper	- Bicarbonate ions were found to lower by 2–3 times after boiling water for 15 min. - Boiling only benefits underground waters with high hardness.	[205]
DCMD (PVDF hollow fiber)	RO concentrate	Accelerated precipitation softening (i.e., pH adjustment + calcite seeding + MF)	- APS treatment resulted to high removal of calcium and total hardness. - Flux was improved dramatically after APS treatment, with only 20% flux decline in 300 h.	[138]
DCMD (PP hollow fiber)	Bilge water, saline wastewater	- (1) Sedimentation + UF - (2) thermal pretreatment + filtration	-Significant flux decline was observed for pretreatment (1) - Rapid flux decline was prevented for pretreatment (2) due to removal of protein from boiling	[29]
DCMD pilot plant	City water (3.5, 6,	1 μm PP filter	- Very limited flux reduction was	[24]

(fluorosilicone-coated PP hollow fiber)	and 10 %), real seawater		observed even at seawater feed concentrated up to 19.5%	
MD pilot plant (PVDF, PP, UHM-PE)	Seawater	Filtration + degassing	- Production of excellent product water quality with little need of pretreatment	[51]
DCMD (PP hollow fiber)	$CaCO_3$ and $CaSO_4$ solutions, Mixed $CaCO_3$/$CaSO_4$ solution	Acidification with HCl to pH 4	- Induction period was extended for at least 7 h - Stable flux was obtained from beginning to end	[120]

4.2. Membrane flushing

Nghiem and Cath [121] investigated a scaling mitigation approach by regular membrane flushing during DCMD. Scaling tests were performed on a PTFE membrane at different feed inlet temperatures (40-60^{o}C) using $CaSO_4$, $CaCO_3$ and silicate as foulants. The initial results found that $CaSO_4$ scaling has more severe occurrence than the other two foulants, thus additional tests were only carried out with $CaSO_4$. The induction period of $CaSO_4$ scaling was found to decrease with the increase in feed temperature [121] as was also previously observed by another study [81]. The precipitated $CaSO_4$ crystal sizes showed increasing sizes with the increase of feed temperature, which is consistent with the $CaSO_4$ precipitation kinetics and thermodynamics [81, 119]. The effect of $CaSO_4$ feed concentration showed varying duration of induction period. The results suggest that membrane scaling is not only due to the attainment of supersaturation, but also it can occur after a sufficient induction time. A long induction period was observed, which provides an opportunity for mitigation strategies if one can reset the induction period. If the nucleation sites at the membrane surface are constantly removed before rapid crystallization, membrane scaling can be effectively controlled. **Figure 9** shows the flux results after regular flushing of Milli-Q water for every 20 h interval of DCMD test with 2000 mg/L $CaSO_4$ solution. The flux was held constant for the whole duration of DCMD test after regular flushing, showing the effectiveness of simple flushing of Milli-Q water in removing nucleation sites during the induction period even at a supersaturated condition (i.e., at 2000 mg/L $CaSO_4$).

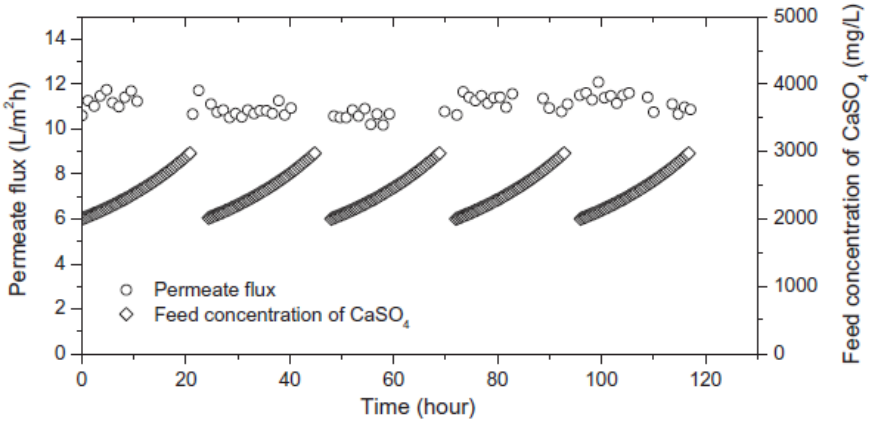

Fig. 9. Permeate flux and feed concentration of $CaSO_4$ versus time during five repetitive DCMD tests with membrane flushing after each test. A fresh 2000 mg/L $CaSO_4$ was used after each test (adapted from [121]).

4.3. Gas bubbling

The formation of mineral deposits on the membrane surface decreases the permeate flux and deters the life of a membrane. The formation of deposits on the membrane surface can be minimized by increasing the shear rate at the surface to constantly remove fouling layers [207, 208]. One way of doing this is through gas bubbling method, which forms a gas-liquid two phase flow that induces secondary flows increasing the maximum shear stress at the membrane surface [209, 210]. The following are identified as the mechanisms of gas bubbling in controlling fouling [211]: (a) bubble induced secondary flow, (b) physical displacement of the concentration polarization layer, (c) pressure pulsing caused by passing bubbles, and (d) increase in superficial cross-flow velocity. The effect of gas bubbling on the scaling of a PVDF hollow fiber membrane in a high salt concentration DCMD set-up was investigated by Chen et al. [212]. A nozzle connected to an air pump was placed at the inlet side of the feed (**Fig. 10**) to disperse air and bubbles inside the MD module. The utilization of gas bubbling was found to increase the permeate flux enhancement ratio by about 1.72 at an optimized gas flow rate. It was found that gas bubbling could reduce temperature polarization and could enhance the surface shear rate, leading to delay of crystallization of scales at the surface. This means that scaling of membrane was reduced due to the introduction of gas bubbling. It was suggested that together with gas bubbling, a higher enhancement in flux could be realized by operating at higher feed temperature, or at lower feed and permeate velocities, or by using an inclined module, shorter fiber length or lower fiber density. However, one must also take note that the effectiveness of gas bubbling is greatly affected by the size of induced bubbles, wherein uniformly distributed fine bubbles showed better result than coarse bubbles [213]. Utilizing direct observation and statistical analysis, their succeeding study [214] confirmed that it is preferential to employ bubbles with narrow size distribution and small mean bubble size to create even flow distribution, intensity mixing, and enhance the shear rate.

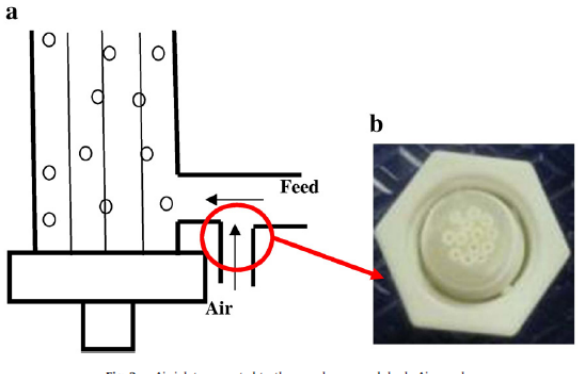

Fig. 10. Schematic of the (a) air inlet position in the feed side of the MD module and the (b) photographic image of the air nozzle (adapted from [212]).

In another study, Ding et al. [172] used intermitted gas bubbling to mitigate fouling during the concentration of TCM extract via DCMD. Gas bubbling was introduced into the DCMD module with PTFE membrane by a fan connected at the entrance side of the feed. The influence of gas flow rate, bubbling duration and MD duration in each cycle on the fouling mitigation were investigated. In the initial test, it was observed that the permeate flux started to decline at the start of bubbling, and the flux remained at low level at continuous introduction of bubbles in the module. This could be due to the tendency of the bubbles to occupy part of the membrane surface, which reduces the contact area of the feed liquid to the membrane. Additionally, it could also be that some bubbles would stay inside the membrane pores, which affect the partial vapor pressure at the membrane pore leading to reduced flux. Thus, to address this tendency, intermittent gas bubbling was carried out for a duration of 1-3 min. Effective reduction of fouling was realized with the use of intermittent bubbling, wherein its mitigating or cleaning efficiency is improved with the increase of gas flow rate and gas bubbling duration, and the decrease of MD duration. Due to its mechanism of increasing the shear rate at the membrane surface, gas bubbling is mainly effective in addressing external membrane fouling.

4.4. Temperature and flow reversal

A recent study [215] reported on the use of temperature and flow reversal techniques as new methods for the effective mitigation of fouling of MD, so as to restore flux and salt rejection performances. In flow reversal method, the feed side and the permeate side channels were reversed, i.e., the feed side became the permeate side, and the permeate side became the feed side. On the other hand, the temperature reversal method was carried out by circulating a colder feed stream (15^{o}C of Great Salt Lake water in this case) while maintaining the same water and at the same temperature at the permeate side, which was warmer (at 30^{o}C). For both methods, prior to the reversal of either flow or temperature, the DCMD tests were first terminated before the occurrence of scaling or after recovering 35-40% of the feed water. The results showed good effectiveness in maintaining the water

flux and salt rejection using both methods, however the temperature reversal method showed better overall performance. Similar with membrane flushing and gas bubbling, the working mechanisms of these new techniques were inhibiting the homogeneous precipitation of salts and disrupting the nucleation of salt crystals on the membrane surface. However, no in-depth explanation on the nucleation kinetics and scale formation was provided in this study [215].

4.5. Surface modification for anti-fouling membrane

In recent years, a number of research studies have been geared on membrane surface modification to enhance hydrophobicity and anti-fouling properties of MD membranes. Different superhydrophobic coatings were applied on various substrates, and results showed less biofouling formation on these coated substrates than the uncoated ones [216, 217]. A previous study has reported the control of organic fouling by hydrophilization of the membrane surface. By coating a PTFE membrane with sodium alginate hydrogel, the adsorption of citrus oil on the membrane surface was significantly lessened [218].

Increasing the hydrophobicity of a membrane usually leads to higher LEP, and consequently more resistance to pore wetting. Razmjou et al. [8] fabricated a superhydrophobic PVDF membrane by incorporating TiO_2 nanoparticles via a low temperature hydrothermal process. DCMD tests were carried out including the effect of fouling formation using HA and calcium chloride as foulants. The deposition of TiO_2 forming hierarchical structure with multilevel roughness on the surface has increased the hydrophobicity up to 166^o, and consequently increasing the LEP to 195 kPa. Fouling tests revealed similar fouling behavior for both virgin and modified membranes, but the modified membrane showed much higher flux recovery, indicating a better anti-fouling property. A different study has suggested that a good technique of inhibiting surface nucleation and particle attachment of $CaSO_4$ scales on membrane surfaces is to utilize polypropylene membranes coated with fluorosilicone layer [81].

In another study, Zhang et al. [219] fabricated a superhydrophobic PVDF flat-sheet membrane by casting and spraying a mixture of polydimethylsiloxane (PDMS) and hydrophobic SiO_2 nanoparticles onto the membrane surface. The modified membrane showed a contact angle (CA) of 156^o, which was much higher than that of the original membrane (CA = 107^o). The DCMD flux performance of the modified membrane however showed lower than that of the original membrane, but is compensated with a high salt rejection efficiency. Fouling tests were carried out at very high concentration of 25wt% NaCl solution. The results showed in the first 40 h, the flux profile was similar for both membranes, however after 40 h, there was a steep flux decline for the original membrane, indicating membrane wetting and fouling. The modified membrane showed more stable flux. By examining the membranes after the test, NaCl deposits were found on the original membrane surface, with some are blocking the pores, while on the modified membrane surface, almost no

deposits were found. This study indicated the potential of surface modification by SiO_2 nanoparticles as a good method in fabricating anti-fouling MD membranes.

4.6. Effect of magnetic field and microwave irradiation

The effect of magnetic water treatment on the scaling of DCMD was investigated. The use of magnetic field for the mitigation of scaling has a long history in heat exchanger and cooling water fouling application. The magnetic effect is claimed to reduce the nucleation rate and accelerate the crystal growth [220, 221]. Several reports have indicated the good mitigating efficiency of the use of magnetic fields for cooling-water and heat exchanger fouling [106, 222]. Due to similarities in operation between MD and heat exchanger process except that porous membrane is used in MD, Gryta [114] investigated whether the MWT could help mitigate the scaling formation in MD. The source of the magnetic field was two S-S permanent magnets with strength of 0.1 T each. The magnetic treatment of the feed has resulted to formation of bigger crystallites (mainly calcite), and thinner and more porous deposits on the membrane surface compared to the untreated feed. The permeation test showed smaller reduction in permeate flux when MWT was used compared to that without the use of MWT. However, using MWT did not help in reducing membrane wetting, wherein all membranes tested (with and without MWT) showed partial wetting up to a depth of 40-50 μm inside the pore walls.

In two complementary studies [223, 224], a non-chemical water treatment method utilizing microwave irradiation was investigated on its scaling mitigation effect in MD. There are four mechanisms involved during microwave irradiation: (a) the microwave energy can help destroy the water molecule clusters, thus it can help in accelerating the escape of molecules from the bulk solution; (b) microwave can also increase the polar structure activity of the membrane material, which lead to faster penetration of molecules; (c) polar molecules such as in water can move faster upon absorption of microwave energy; and (d) microwave irradiation can induce thermal effect, which can help reduce temperature polarization in MD. In a VMD study, the use of microwave irradiation could induce uniform heating in the radial direction and has led to the improvement of the mass transfer during MD process, but its effect on scaling was still ambiguous [224]. Microwave irradiation had somehow aggravated the deposition of calcium carbonate on the membrane surface. In a subsequent study [223], the effect of the same microwave irradiation technique on the crystallization of inorganic salts was further investigated. The results showed no significant difference in flux for the test with microwave irradiation compared to no microwave irradiation. It has been concluded that the ionic conduction was the main factor affecting the absorption of microwave energy in the solution. Differing effect of microwave irradiation to NaCl crystallization compared to $CaCO_3$ crystallization was observed. Crystal growth and higher deposition was observed for $CaCO_3$ (more aragonite), while fewer number of crystals but with more uniform size distribution was observed for NaCl crystals. The

use of microwave irradiation could be useful if adjustment of crystal phase is needed during inorganic scaling process.

4.7. Use of antiscalants

Antiscalants are chemical additives that interfere with the precipitation reaction of scales and weaken the adherence of scales to the membrane surface. The use of antiscalants has been proven to be effective in inhibiting scaling in RO, in conventional thermal processes such as MSF desalination, MED, and in heat exchanger and cooling-water applications [225-228]. Among the commonly used antiscalants are condensed polyphosphates, organophosphonates, and polyelectrolytes [229]. Dose of trace amounts of antiscalants is found to effectively suppress scaling by physical mechanism rather than chemical mechanism [230]. The antiscalant adsorbs on the crystal surface blocking the active growth sites, which leads to: (a) retardation of crystal growth rate, (b) changes in crystal surfaces properties and agglomeration tendency, and (c) changes in crystal morphology leading to deformed or friable scales that are weakly adhered to the membrane surface [231, 232].

In MD application, it is important to retain the hydrophobicity of the membrane and avoid wetting so as to maintain high MD performance efficiency. As the mechanism of antiscalant in inhibiting scaling involves some modification of the surface energy of crystals, there could be a tendency that antiscalants, which have water-like hydrophilic property [119], could affect the membrane surface energy if used in MD, and may lead to membrane wetting. Thus, He et al. [119] conducted a study investigating the effect of 5 different antiscalants namely K797, K752, GHR, GLF, and GSI on the membrane wetting and scaling by calcite $CaCO_3$ and gypsum in DCMD set-up. **Table 5** lists the composition and properties of the antiscalants used. Hydrophobic polypropylene hollow fibers coated with fluorosilicone coating were used as membranes. The concentration of antiscalants varied from 0.6 to 70 mg/L. Surface tension measurements of the solution with antiscalant showed similar surface tension value to that of tap water, which means that the 5 tested antiscalants had negligible surfactant effects. Breakthrough pressure test indicated no wetting of the membrane, supporting the surface tension measurement results. The addition of antiscalants was found to affect the induction period of both $CaCO_3$ and $CaSO_4$, i.e., they slowed down the precipitation of crystals even at a very low dosage of 0.6 mg/L. Different antiscalants showed varying degree of inhibiting scaling, where antiscalant K752, showed the most effective in inhibiting $CaSO_4$ scaling.

In a recent study, Gryta [115] investigated the effect of polyphosphates on $CaCO_3$ scaling of MD using a capillary tube module. The results showed that polyphosphates have affected the morphology of the precipitated scales. Without the use of antiscalants (i.e., polyphosphate), large amounts of scales in cubic-like structures (average size = 10 μm) were formed on the membrane surface. Checking by XRD revealed that these were mainly calcite scales. However, when polyphosphates were added in the solution (2-20 ppm), the scales formed were amorphous in a low-porous layer. The non-porous layer has resulted to decrease in permeate flux, lower than that without

the use of antiscalant. However, a simple periodic rinsing of HCl solution was found to easily remove the low-porous layer and restore the initial flux efficiency. This is because the amorphous, low-porous scale was only observed to deposit on the membrane surface, and not inside the membrane pores, thereby reducing the tendency of the membrane to be wetted after acid rinsing.

The use of antiscalants can generally aid in minimizing scaling of inorganic salts. However, care must also be taken with the use of antiscalants due to the following limitations [32]: (a) overly high dosage of antiscalants could make them as foulants themselves, thus optmimum dosage is important; (b) some antiscalants are reported to increase the biological growth of some microorganisms, leading to more biofouling formation; (c) some antiscalants can react with chemicals used during pretreatment, which can form fouling formation or can degrade the efficiency of antiscalants; (d) some metal ions such as iron can react with antiscalants to form a foulant layer, and; (d) the use of antiscalants is complicated and not easy to monitor in the system.

Table 5. The antiscalants used in the study (adapted from [119]).

Antiscalants	**Chemical name**	**Weight % less than**	**pH**	**Recommendation conditions**		
				Dosage (mg/L)	$CaCO_3$	$CaSO_4$
K797[b]	Water Acrylic terpolymer/Solids	50 50	2.4-3.0	N/A	N/A	N/A
K752[b]	Polacrylic acid Water Sodium polyacrylate	47 37 16	2.2-3.0	N/A	N/A	N/A
GHR[c]	Aqueous solution of nitrogen containing organo-phosphorus compound	N/A	1.8-2.0	0.4-0.8	Best choice	Effective
GLF[c]	Aqueous solution of an organo-phosphorus compound	N/A	9.8-10.2	2-4	Best choice	Effective
GSI[c]	Synergistic blend of antiscalants based on neutralised carboxylic and phosphoric acids	N/A	9.8-10.2	2-5	Effective	Effective

[a] Provided by manufacturers.

[b] From Noveon Inc. (Cleveland, OH).

[c] From Genesys International LTD. (Minneapolis, MN).

4.8. Chemical cleaning

Chemical cleaning agents are abundant commercially, which include acids, alkalis, metal chelating agents, surfactants, enzymes and oxidizing agents [34, 233]. In MD processes, strong or weak acids are usually used for cleaning especially those dealing with $CaCO_3$ fouling [62]. Generally, rinsing with acid (commonly using HCl) is particularly effective in removing inorganic scales, while rinsing with basic/alkali solution is relatively effective in the reduction of organic fouling [87, 135]. For biofouling, the main prevention method is the continuous dosage of biocides.

Depending on the location of the scales, rinsing can usually recover the initial flux if the scales are only deposited on the surface. However, formation of crystals inside the pores of the membrane could be harder to remove, and could lead to pore wetting if rinsed repeatedly, thus full

recovery is impossible in this case.A study has shown that rinsing the module with 3 wt% HCl solution can effectively remove scaling and obtain permeate flux close to the initial flux. Microscopic images of acid-cleaned surface showed similar characteristics as those of a new membrane [139]. Wang et al. [112] utilized 2 wt% HCl or 2 wt% NaOH solutions to remove the $CaCO_3$ scales from fouled hollow fiber membranes. The rinsing using both acid and base solutions resulted to the removal of the majority of the deposits, recovering the hydrophobic property of the membrane. In a recent study, membrane fouling and cleaning were investigated by lab-scale experiments and through intermittent long-term (2010-2013) solar MD pilot plant operation in Spain [25]. From among the cleaning agents tested initially in the laboratory (i.e., 5 wt% citric acid, 5 wt% formic acid, 5 wt% sulphuric acid, 0.1 wt% oxalic acid + 0.8 wt% citric acid, and 0.1 wt% $Na_5P_3O_{10}$ (detergent agent) + 0.2 wt% EDTA), the 0.1 wt% oxalic acid + 0.8 wt% citric acid solution showed the best cleaning performance of scaling mainly composed of NaCl and Fe, Mg, and Al oxides. However, membrane structural damage was observed which was attributed to fouling as well as due to chemical treatment that lead to the enhanced wetting of the membrane. When the identified cleaning agent was used for the MD pilot plant, greater than 85% salt rejection was obtained only after second cleaning procedure that eventually reduced the wetting tendency. However, the dry-out periods (inactive periods) were found to favor membrane wetting again.

5. Fouling monitoring and characterization techniques

To better understand and minimize the fouling formation and propensity, it is important to assess and characterize the foulant by several diagnostic and measurement techniques. These techniques including physical, chemical and biological characterization can provide information on the fundamental processes governing membrane fouling [234]. **Table 6** lists the different characterization and measurement methods used in membrane fouling study.

Table 6. Characterization and measurement techniques used for membrane fouling study.

	Physical characterization							Chemical characterization								Biological characterization		
Parameter	**Direct visualization**	**SEM**	**AFM**	**Optical laser**	**UTDR**	**Contact Angle**	**Zeta Potential**	**Tensile Strength**	**ICP-MS**	**EDX**	**FTIR**	**XRD**	**TOC**	**HPSEC**	**FlFFF**	**Isolation & Identification**	**CLSM**	**FlFFF**
Structure	◙	◙	◙														◙	
Roughness			◙															
Thickness		◙		◙	◙													
Hydrophobicity						◙												
Charge effect							◙											
Strength								◙										
Calcium, magnesium									◙	◙								
Aluminium, iron									◙	◙								
Sillicate									◙	◙								
Particle	◙	◙	◙												◙			
Functional group											◙							
Biopolymer											◙		◙	◙	◙			
Humic acid											◙		◙	◙	◙			
Polysaccharides											◙		◙	◙	◙			
Crystal composition												◙						
Biofilm structure																	◙	
Microorganism																◙		
Foulant interaction															◙			◙

SEM = scanning electron microscopy; AFM = atomic force microscopy; ICP-MS = inductively coupled plasma mass spectroscopy; UTDR = ultrasonic time-domain reflectometry; EDS = energy-dispersive x-ray spectroscopy; FTIR = Fourier transform infrared spectroscopy; XRD = X-ray diffraction; TOC = total organic carbon; HPSEC = high pressure size exclusion chromatography; FIFFF = flow field-flow fractionation; CLSM = confocal laser scanning microscopy.

The lifetime of a membrane is affected by several factors including the operational conditions, and the physical and chemical control or cleaning techniques associated in combating fouling. Membrane autopsy is a reliable method in understanding the various questions about the decline in performance and lifetime of a membrane [235]. It involves the dissection of the membrane, inspection of the surface and fouling deposits, and other components to check for any damage. Autopsy can determine the real identity of the foulants, and through characterization and analysis, future pretreatment, control and cleaning strategies can be prepared with confidence [100].

5.1. Physical characterization

Direct visualization by optical microscope of the particle deposition on a membrane is a simple and straightforward technique that provides a non-invasive, in situ visualization and quantification of fouling [236]. The set-up is usually composed of a microscope, a video camera, and a membrane module and can visualize particles larger than 1 μm. This is termed as direct observation through membrane [237] when the camera lens is focused on the permeate side and direct visual observation [238] when the camera is focused on the feed side of the membrane. These techniques have been successfully carried out for flat-sheet membranes for the visualization of particle deposition in real time, but not so much on the observation of deposit thickness. Attempts to quantify the thickness of fouling deposits by in-situ visualization on hollow fibers were carried out by Marselina et al. [236, 239]. A similar technique for real-time crystal monitoring of membranes is through the use of EXSOD [240, 241]. It consists of on-line image analysis and control capability as an actuator for EXSOD that can be integrated in the desalination system.

SEM is one of the most commonly used techniques to view the morphology and structure of surfaces and cross-sections of samples at the microscopic level. A focused high-energy electron beam is generated and travels through a series of magnetic lenses towards the target area and an image is generated on a screen. Usually, a very thin coating of gold, carbon, or platinum layer is sputter-coated onto the sample to increase its conductivity, and improve the resolution of the image. SEM analysis can provide quantitative and qualitative assessment of the the foulants and membrane surface, giving details on thickness, morphology, and structure. However, one drawback of SEM is the need for partially or completely dried samples, which could be an issue for some foulants because of the tendency to change in structure during drying [196]. **Figure 11** gives example of SEM images from unfouled and fouled membranes.

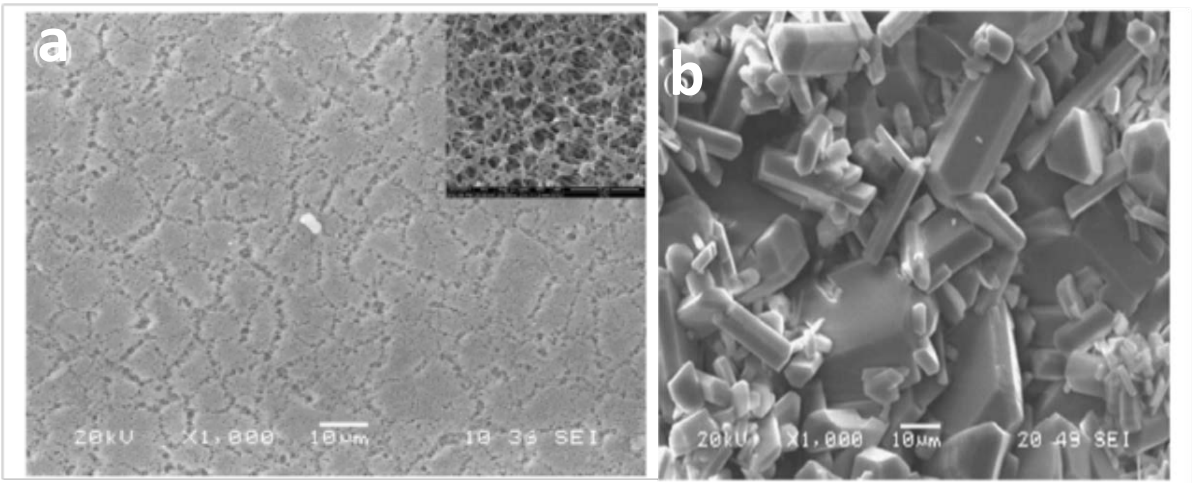

Fig. 11. Microscopic SEM images of (a) virgin (unfouled) and (b) scaled PP membrane (adapted from [122]).

To provide a more realistic three-dimensional (3D) image of the surface down to the nanoscale level, AFM will be very useful for this. AFM provides details of the topology, morphology and roughness of the surface, giving a 3D surface profile without the need of pretreatment of samples. AFM can be carried out by contact or non-contact mode using a cantilever that deflects according to Hooke's law. For example, dimension of pores and roughness measurements showing the hills and valleys where deposits could form were directly measured by AFM imaging and proved useful for analysis [242, 243]. By comparing virgin and fouled membranes, significant differences in morphologies were observed using AFM.

The optical laser sensor method is used to investigate the deposit thickness on a membrane [244]. The technique uses laser light to traverse through the deposit layer, and differences in the detected signal intensity is converted into the deposit thickness. This was successfully presented in the investigation of fouling in microfiltration of bentonite suspensions [244].

UTDR uses ultrasonic waves to provide real-time measurement of the location of an interface (stationary or moving). UTDR also provides the physical characteristics of the media where the waves travel [245]. The velocity of the propagated sound waves are dictated by the medium they travel , and if there is an interface between two media, there will be partitioning of energy leading to reflection of waves. The reflected waves are detected by an ultrasonic transducer, and when the velocity of the medium is known, the propagation path or thickness can be calculated. Mairal et al. [245] first used UTDR to characterize the fouling layers on a flat-sheet membrane, while others [246, 247] used it to investigate fouling of hollow fibers.

The wettability of a surface is determined by the geometrical structure of the surface and material composition. To quantify wettability, the CA is measured, which is the angle between the liquid drop and the horizontal surface. The three interfacial forces that are thermodynamically in balance when

putting a drop of water on a surface include liquid-vapor surface tension, solid-vapor interfacial tension, and solid-liquid interfacial tension [248, 249]. These forces determine whether the droplet becomes a thin film or forms into a cylindrical shape. When the angle is below 90^{o}, it exhibits a hydrophilic behaviour, while angles above 90^{o} exhibit hydrophobicity [99]. When the angle reaches above 150^{o}, then it is considered as a superhydrophic surface. For MD, maintaining the hydrophobic behaviour of the membrane is important so as to prevent pore wetting. However, formation of fouling layers on the surface can drastically reduce the surface hydrophobicity because the foulants are usually hydrophilic, thus promoting pore wetting phenomenon leading to flux decline and low salt rejection efficiency.

5.2. Chemical characterization

Zeta potential, defined as the potential at the surface of shear is an important parameter in determining the electrokinetic phenomena of membranes. The value of zeta potential is determined by indirectly measuring the potential difference between the dispersion medium and the charged surface. The determination of zeta potential is used to evaluate the surface charge of a membrane, which dictates the possible interaction between the particles (foulants) and the membrane surface.

The mechanical integrity of a membrane is an important factor for its long-term performance. Tensile strength is an important indicator of how well the membrane could withstand the stress associated with the MD operation before suffering permanent deformation or fracture. The tensile strength has been used as a parameter for membrane autopsy studies [250]. Investigating the tensile strength of the membrane is particularly important when comparing the effect of fouling to that of unfouled or virgin membranes. It is known that fouling can degrade or affect some changes in the membrane structure and properties, and when left unaddressed, could severely damage the membrane. Moreover, doing extensive cleaning and fouling control strategies on membranes could also affect the mechanical integrity in the long term. Thus, checking the tensile strength of the unfouled and fouled membrane, and also in consideration of the duration of use (in years), could give a general indication of the “tiredness” of the membrane. Tensile testing is a destructive method, and can be done using a universal testing machine, following standard procedures such as ASTM D368-10 (Standard test method for tensile properties of plastics).

The concentration (in parts per billion (ppb) or parts per million (ppm)) of metal and non-metal elements in a fouling layer can be selectively determined using ICP-MS. Individual ions such as calcium and magnesium ions can be individually detected at high accuracy. To prepare the samples, deposits attached on the membrane surface should first be dissolved in acidic or alkaline solutions. Inorganic and organic deposits are better extracted by acidic and alkaline solutions, respectively.

EDS is an analytical technique to analyse the elemental composition of a fouled surface and the device is usually attached to SEM or TEM. As each element has a unique atomic structure, the peaks generated from the interaction of electromagnetic radiation and the foulant in EDS represent different

atomic elements, thus the surface elemental composition can be identified. **Figure 12b** shows the EDS spectra of the deposits shown in **Fig. 12a**. Using tap water, fouling deposits were formed on a polypropylene membrane. EDS investigation showed the deposit was composed mainly of calcium, and some traces of Mg, Al, S and Cl. This indicates that the deposit mainly consists of $CaCO_3$ scales.

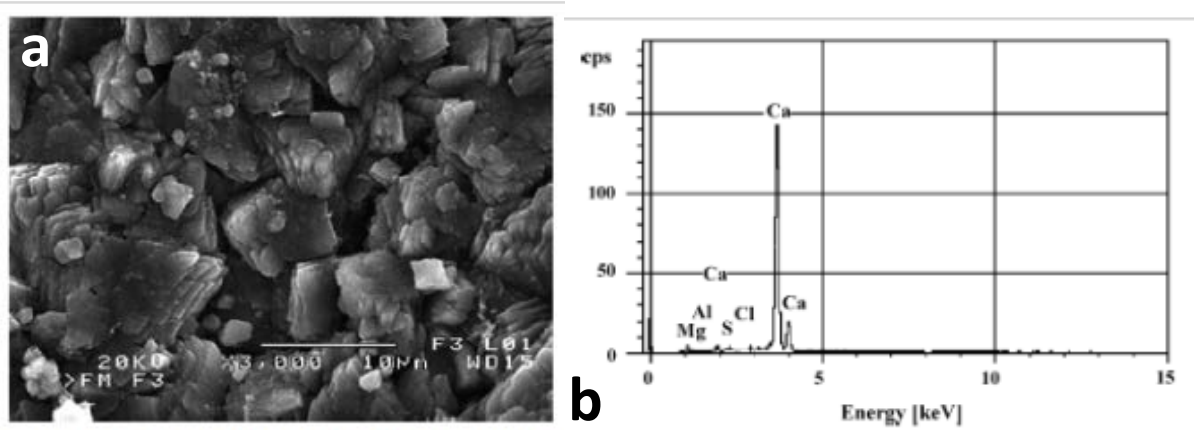

Fig. 12. (a) SEM image and its corresponding EDS spectra of $CaCO_3$ formed on the membrane surface with tap water as feed (adapted from [62]).

FTIR can be used to characterize and identify the chemical bonds and molecular structure of organic molecules by obtaining the IR spectra of the sample. Advances in FTIR have led to analysis of organic and inorganic functional groups on the surface. Functional groups are assigned with absorption bands, and shifting of the bands indicates changes in the chemical structure or in the environment around the polymer membrane.

XRD is a versatile analytical technique to investigate and quantify the crystalline nature of materials may they be inorganic, organic, polymers, metals or composites. XRD measures the diffraction of X-rays from the planes of atoms within the material. Every substance has a unique XRD spectrum that serves as like its fingerprint [251]. XRD can find the crystal structure of the material, determine the orientation of a single crystal or grain, measure the average spacings between layers or rows of atoms, and measure the size, shape and internal stress of small crystalline regions. XRD has practical applications in a broad range of scientific field. Gryta [115] checked the components of a scale on a polypropylene membrane with and without antiscalant by XRD analysis (see **Fig. 13).** Based from the figure, calcite crystals were observed for the scale without the use of antiscalant, and this calcite peak disappeared after using antiscalant.

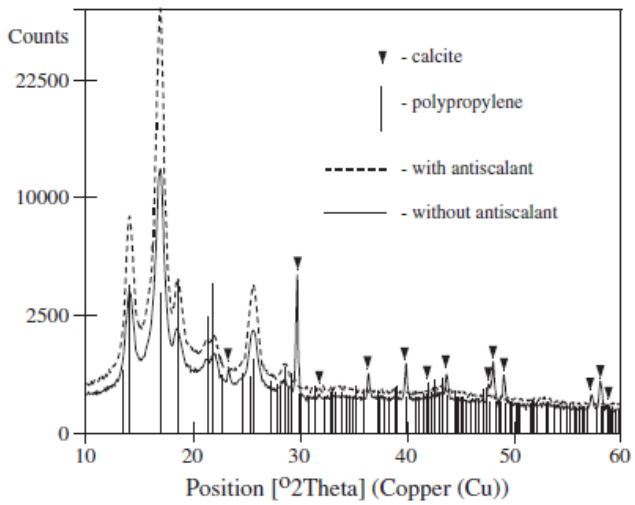

Fig. 13. XRD analysis of the formed deposit on the membrane surface showing the presence calcite crystals (adapted from [115]).

For organic foulants, the TOC can be extracted from the fouling layer using NaOH solution, which can desorb or dissolve fractions of organics. The samples are then injected into a high-temperature furnace or chemically-oxidizing environment, wherein with the help of a catalyst, the organic matter is oxidized to carbon dioxide, and quantitative measurement is carried out by an infrared analyser.

The hydrophobic property of MD membranes are prone to enhanced organic fouling if used in wastewater treatment especially to protein because of the high affinity of protein to adhere on membranes [90, 218]. A more detailed analysis of organic constituents of a fouling layer by specific groups of organic compounds can provide helpful information to the problem of fouling [252]. Organic size or molecular weight distribution can be determined by HPSEC (other names are gel permeation chromatography or gel filtration chromatography) or by FlFFF. In HPSEC, which is an elution technique, the degree at which the organic foulant constituents can diffuse through the pores of the stationary phase controls the differences in retention. This depends on the dimension of the molecules and the distribution of the pore size. The driving force for the retention is the differences in entropy of the solute inside the pore volume compared with that in the mobile phase. FlFFF is also an elution technique, wherein the hydronamics involved are quite similar as with the hydrodynamics of a crossflow membrane filtration system. FIFFF uses the average residence time of the solute as the basic measurement parameter and separation of components is based on the differences in solute diffusion coefficients and Stokes radii [253]. Measurements of retention times can yield these properties for each fractionated component. FlFFF has also been used to measure the sizes of bacteria during biofouling test [254, 255].

5.3. Biological characterization

The characterization associated with biofouling is complicated due to the presence of living microorganisms. One of the simplest ways to characterize biofouling is through determining the number of microorganisms present. This is done by a streak-plate method, wherein a bacterial colony is inoculated in an agar plate, and incubated for about 12-24 h. The bacterial colonies grow in number, and the colonies can clearly be counted by the naked eye or by a colony counter. However, some microorganisms do not grow in agar plate, making it a limitation of this method.

CLSM is a non-destructive technique which obtains high-resolution optical images with depth selectivity. In combination with a fluorescent probe, in-situ visualization and quantification of biofilms are possible through CLSM [256]. The CLSM works by focusing a laser beam onto a small focal volume on the target surface, and the reflected light is collected back and detected by a photodetection device, and the light signal is converted into images that can be observed through a computer monitor.

6. Future perspectives and concluding remarks

Fouling is a persistent problem in areas where water is utilized including desalination, water and wastewater treatment, heat exchangers, and cooling water systems. In membrane-based separation processes including MD, unwanted deposits on the surface of the membrane, or inside the membrane pores are formed due to the precipitation of mineral salts (scaling) or deposition of colloidal matters and precipitates (inorganic fouling), accumulation of organic compounds such as HA and protein (organic fouling), and deposition and growth of microorganisms (biofouling).

Due to the promising potential of membrane distillation for many applications, increasing number of studies has been carried out in recent years. However, fouling studies are still lacking. Most of the MD papers published in literature focused on the flux performance, and some on the fouling phenomena, but very little can be found on the in-depth study of the actual mechanism behind fouling in MD. The research on the fouling mechanism should be carried out in accordance to the working principles of MD. In order to understand fouling and how to deal with it effectively, more in-depth research and analysis have to be done, especially in differentiating the fouling problem specific for MD operational parameters and mechanisms compared to other membrane-separation processes. As MD utilizes bigger pore sizes compared to pressure-driven membrane processes, the pore sizes and pore size distribution must be accounted for in the study of fouling. Additional exploration on the differences in MD fouling formation and mechanism happening on different types of membrane such as flat-sheet, hollow fiber, and most recently, nanofiber membrane should be carried out.

Most of the previous studies were focused on the scaling problem. However, extension of MD application to wastewater treatment needs to address more of organic and biological fouling, in conjunction with inorganic scaling. This makes the fouling study more complex, thus

more insight of the mechanisms of mixed fouling should be given importance in the future. The more stringent laws on conservation of the environment and protection of human health should lead to fouling control procedures that lessen or eliminate the use of chemicals. New non-chemical methods such as process optimization, membrane surface modification, or even physical water treatment techniques need to be given more attention in future studies as anti-fouling strategies. The mitigation or prevention method should be simple and inexpensive to give more viability for the commercialization of MD.

It could be noticed that most of the MD studies in literature utilized a DCMD set-up, thus fouling problems reported may not be representative of the fouling potential in other MD set-ups such as vacuum-assisted MD, air-gap MD, and sweep gas MD. There is a need to provide more detailed information on fouling formation in various types of MD set-ups, as well as on the use of different membrane types including flat-sheet, hollow fiber and nanofiber membranes. As new works have been reported on the use of MD for groundwater purification and removal of toxic inorganic constituents, the fouling formation on these situations should also be evaluated.

Additionally, more modelling studies incorporating the effect of fouling in conjunction with experimental studies should be carried out. A few previous modelling studies have taken into account the effect of fouling layer in MD. Gryta [29] reported experimental and modelling studies of DCMD for the concentration of saline wastewater. The model used only took into account the effect of thermal resistance, and not hydraulic resistance. It was found that the model can give good prediction of porous deposit layer only when thermal resistance is considered. However, for gel or layer with very small pore size, the hydraulic resistance must be taken into account to provide good prediction, but the effect of hydraulic resistance was not attempted for modelling in this study. Several succeeding reports [74, 75, 192] for MDBR application carried out modelling studies, however, the effect of hydraulic resistance was also left out and not incorporated in the model. These studies have speculated that the biofouling/gel layer might have contributed a hydraulic resistance to water permeation [29, 74] , or by vapor-pressure depression due to the very small pore structure of the biofouling layer [75]. In a recent study, Chew et al. [55] developed a model that incorporated the vapor-depression effect especially designed for MMBF layers with very small pores or free volume (<50 nm). The results indicated that the large flux reduction in previous reports could be explained by the vapor-depression effect associated with the very small pores (i.e., 3.9 to 8.5 nm) of the hydrophilic fouling layer. Increasing the thermal resistance by utilizing thicker, high porosity membrane, or by utilizing dual-layer membranes with hydrophilic layer with large pores at the feed side, are suggested to reduce the effect of vapor-depression and improve the MD performance for MDBR application.

Understanding the fouling phenomena and the processes involved is the first step to solving the fouling problem. This review gives an overall view of the status of fouling problem and their mechanisms in membrane distillation, and some steps taken to alleviate the fouling problem. Aside from optimizing the operational parameters as well as improving the membrane structure to enhance the MD performance, addressing the fouling problem with non-chemical or less chemical mitigation or cleaning techniques should be one of the directions for the future.

Acknowledgements

This research was supported by a grant from the Industrial Facilities & Infrastructure Research Program funded by the Ministry of Land, Infrastructure and Transport of the Korean government. The authors acknowledge the grant from the UTS Chancellor's Postdoctoral Research Fellowship 2013 and ARC Future Fellow.

References

1. Z. Zeng, J. Liu, H.H.G. Savenije, A simple approach to assess water scarcity integrating water quantity and quality, Ecological Indicators 34(0) (2013) 441-449.
2. L.A. Hoover, W.A. Phillip, A. Tiraferri, N.Y. Yip, M. Elimelech, Forward with osmosis: Emerging applications for greater sustainability, Environ Sci Technol 45(23) (2011) 9824-9830.
3. M.A. Shannon, P.W. Bohn, M. Elimelech, J.G. Georgiadis, B.J. Marinas, A.M. Mayes, Science and technology for water purification in the coming decades, Nature 452(7185) (2008) 301-310.
4. C. Charcosset, A review of membrane processes and renewable energies for desalination, Desalination 245(1–3) (2009) 214-231.
5. T.A. Dabbagh. *The role of desalination in sustaining economic growth in the Gulf*. in *Proceedings of the IDA World Congress on Desalination and Water Sciences*. 1995. United Arab Emirates, Abu Dhabi: Abu Dhabi Publishing Co.
6. A. Al-Rewiali, Performance evaluation of SWCC SWRO plants, Research Center and Development, Jubail (2000) 1-30.
7. E. Curcio, X. Ji, G. Di Profio, A.O. Sulaiman, E. Fontananova, E. Drioli, Membrane distillation operated at high seawater concentration factors: Role of the membrane on CaCO3 scaling in presence of humic acid, J Membrane Sci 346(2) (2010) 263-269.
8. A. Razmjou, E. Arifin, G. Dong, J. Mansouri, V. Chen, Superhydrophobic modification of TiO2 nanocomposite PVDF membranes for applications in membrane distillation, Journal of Membrane Science 415–416(0) (2012) 850-863.

9. S. Al-Obaidani, E. Curcio, F. Macedonio, G. Di Profio, H. Al-Hinai, E. Drioli, Potential of membrane distillation in seawater desalination: Thermal efficiency, sensitivity study and cost estimation, J Membrane Sci 323(1) (2008) 85-98.
10. M. Khayet, T. Matsuura, Preparation and Characterization of Polyvinylidene Fluoride Membranes for Membrane Distillation, Ind Eng Chem Res 40(24) (2001) 5710-5718.
11. X. Yang, R. Wang, L. Shi, A.G. Fane, M. Debowski, Performance improvement of PVDF hollow fiber-based membrane distillation process, J Membrane Sci 369(1) (2011) 437-447.
12. P. Wang, M.M. Teoh, T.-S. Chung, Morphological architecture of dual-layer hollow fiber for membrane distillation with higher desalination performance, Water Res. 45(17) (2011) 5489-5500.
13. H. Liu, J. Wang, Treatment of radioactive wastewater using direct contact membrane distillation, J. Hazard. Mater. 261(0) (2013) 307-315.
14. A. Criscuoli, J. Zhong, A. Figoli, M. Carnevale, R. Huang, E. Drioli, Treatment of dye solutions by vacuum membrane distillation, Water Res. 42(20) (2008) 5031-5037.
15. P. Zolotarev, V. Ugrozov, I. Volkina, V. Nikulin, Treatment of waste water for removing heavy metals by membrane distillation, J. Hazard. Mater. 37(1) (1994) 77-82.
16. F. Banat, S. Al-Asheh, M. Qtaishat, Treatment of waters colored with methylene blue dye by vacuum membrane distillation, Desalination 174(1) (2005) 87-96.
17. M. Gryta, K. Karakulski, The application of membrane distillation for the concentration of oil-water emulsions, Desalination 121(1) (1999) 23-29.
18. A. Alkhudhiri, N. Darwish, N. Hilal, Produced water treatment: Application of air gap membrane distillation, Desalination 309 (2013) 46-51.
19. J. Koschikowski, M. Wieghaus, M. Rommel, Solar thermal-driven desalination plants based on membrane distillation, Desalination 156(1) (2003) 295-304.
20. F. Banat, N. Jwaied, M. Rommel, J. Koschikowski, M. Wieghaus, Desalination by a “compact SMADES” autonomous solarpowered membrane distillation unit, Desalination 217(1) (2007) 29-37.
21. E. Guillén-Burrieza, J. Blanco, G. Zaragoza, D.-C. Alarcón, P. Palenzuela, M. Ibarra, et al., Experimental analysis of an air gap membrane distillation solar desalination pilot system, J Membrane Sci 379(1) (2011) 386-396.
22. R.G. Raluy, R. Schwantes, V.J. Subiela, B. Peñate, G. Melián, J.R. Betancort, Operational experience of a solar membrane distillation demonstration plant in Pozo Izquierdo-Gran Canaria Island (Spain), Desalination 290 (2012) 1-13.
23. E. Guillén-Burrieza, G. Zaragoza, S. Miralles-Cuevas, J. Blanco, Experimental evaluation of two pilot-scale membrane distillation modules used for solar desalination, J Membrane Sci 409 (2012) 264-275.

24. L. Song, Z. Ma, X. Liao, P.B. Kosaraju, J.R. Irish, K.K. Sirkar, Pilot plant studies of novel membranes and devices for direct contact membrane distillation-based desalination, J Membrane Sci 323(2) (2008) 257-270.
25. E. Guillen-Burrieza, A. Ruiz-Aguirre, G. Zaragoza, H.A. Arafat, Membrane fouling and cleaning in long term plant-scale membrane distillation operations, J Membrane Sci 468(0) (2014) 360-372.
26. S. Ben Abdallah, N. Frikha, S. Gabsi, Design of an autonomous solar desalination plant using vacuum membrane distillation, the MEDINA project, Chem. Eng. Res. Des. 91(12) (2013) 2782-2788.
27. G.W. Meindersma, C.M. Guijt, A.B. de Haan, Desalination and water recycling by air gap membrane distillation, Desalination 187(1–3) (2006) 291-301.
28. Y. Xu, B.-K. Zhu, Y.-y. Xu, Pilot test of vacuum membrane distillation for seawater desalination on a ship, Desalination 189(1) (2006) 165-169.
29. M. Gryta, Fouling in direct contact membrane distillation process, J Membrane Sci 325(1) (2008) 383-394.
30. M.S. El-Bourawi, Z. Ding, R. Ma, M. Khayet, A framework for better understanding membrane distillation separation process, Journal of Membrane Science 285(1–2) (2006) 4-29.
31. C.Y. Tang, T.H. Chong, A.G. Fane, Colloidal interactions and fouling of NF and RO membranes: A review, Adv. Colloid Interface Sci. 164(1–2) (2011) 126-143.
32. A. Antony, J.H. Low, S. Gray, A.E. Childress, P. Le-Clech, G. Leslie, Scale formation and control in high pressure membrane water treatment systems: A review, J Membrane Sci 383(1–2) (2011) 1-16.
33. W. Gao, H. Liang, J. Ma, M. Han, Z.-l. Chen, Z.-s. Han, et al., Membrane fouling control in ultrafiltration technology for drinking water production: A review, Desalination 272(1–3) (2011) 1-8.
34. A. Al-Amoudi, R.W. Lovitt, Fouling strategies and the cleaning system of NF membranes and factors affecting cleaning efficiency, J Membrane Sci 303(1–2) (2007) 4-28.
35. F.A. Banat, J. Simandl, Removal of benzene traces from contaminated water by vacuum membrane distillation, Chem. Eng. Sci. 51(8) (1996) 1257-1265.
36. C.-K. Chiam, R. Sarbatly, Vacuum membrane distillation processes for aqueous solution treatment—A review, Chemical Engineering and Processing: Process Intensification 74(0) (2013) 27-54.
37. G. Galaverna, G. Di Silvestro, A. Cassano, S. Sforza, A. Dossena, E. Drioli, et al., A new integrated membrane process for the production of concentrated blood orange juice: Effect on bioactive compounds and antioxidant activity, Food Chem. 106(3) (2008) 1021-1030.

38. V.D. Alves, I.M. Coelhoso, Orange juice concentration by osmotic evaporation and membrane distillation: A comparative study, J. Food Eng. 74(1) (2006) 125-133.
39. S. Gunko, S. Verbych, M. Bryk, N. Hilal, Concentration of apple juice using direct contact membrane distillation, Desalination 190(1–3) (2006) 117-124.
40. S. Nene, S. Kaur, K. Sumod, B. Joshi, K.S.M.S. Raghavarao, Membrane distillation for the concentration of raw cane-sugar syrup and membrane clarified sugarcane juice, Desalination 147(1–3) (2002) 157-160.
41. K. Christensen, R. Andresen, I. Tandskov, B. Norddahl, J.H. du Preez, Using direct contact membrane distillation for whey protein concentration, Desalination 200(1–3) (2006) 523-525.
42. M. Tomaszewska, M. Gryta, A.W. Morawski, The influence of salt in solutions on hydrochloric acid recovery by membrane distillation, Sep. Purif. Technol. 14(1–3) (1998) 183-188.
43. A. Alkhudhiri, N. Darwish, N. Hilal, Membrane distillation: A comprehensive review, Desalination 287 (2012) 2-18.
44. M.S. El-Bourawi, Z. Ding, R. Ma, M. Khayet, A framework for better understanding membrane distillation separation process, J Membrane Sci 285(1-2) (2006) 4-29.
45. K.W. Lawson, D.R. Lloyd, Membrane distillation, J Membrane Sci 124(1) (1997) 1-25.
46. K. Zhao, W. Heinzl, M. Wenzel, S. Büttner, F. Bollen, G. Lange, et al., Experimental study of the memsys vacuum-multi-effect-membrane-distillation (V-MEMD) module, Desalination 323 (2013) 150-160.
47. D. Winter, J. Koschikowski, M. Wieghaus, Desalination using membrane distillation: Experimental studies on full scale spiral wound modules, J Membrane Sci 375(1) (2011) 104-112.
48. L. Francis, N. Ghaffour, A.A. Alsaadi, G.L. Amy, Material gap membrane distillation: A new design for water vapor flux enhancement, J Membrane Sci 448 (2013) 240-247.
49. C. Dotremont, B. Kregersman, R. Sih, K.C. Lai, K. Koh, H. Seah, Seawater desalination with memstill technology-a sustainable solution for the industry, Water Practice & Technology 5(2) (2010).
50. M. Khayet, T. Matsuura, *Membrane distillation: principles and applications*2011: Elsevier.
51. A.E. Jansen, J.W. Assink, J.H. Hanemaaijer, J. van Medevoort, E. van Sonsbeek, Development and pilot testing of full-scale membrane distillation modules for deployment of waste heat, Desalination 323(0) (2013) 55-65.
52. M. Essalhi, M. Khayet, Application of a porous composite hydrophobic/hydrophilic membrane in desalination by air gap and liquid gap membrane distillation: A comparative study, Sep. Purif. Technol. 133(0) (2014) 176-186.
53. M. Khayet, Membranes and theoretical modeling of membrane distillation: A review, Advances in Colloid and Interface Science 164(1–2) (2011) 56-88.

54. P. Dydo, M. Turek, J. Ciba, K. Wandachowicz, J. Misztal, The nucleation kinetic aspects of gypsum nanofiltration membrane scaling, Desalination 164(1) (2004) 41-52.
55. J.W. Chew, W.B. Krantz, A.G. Fane, Effect of a macromolecular- or bio-fouling layer on membrane distillation, J Membrane Sci 456 (2014) 66-76.
56. L.D. Tijing, J.-S. Choi, S. Lee, S.-H. Kim, H.K. Shon, Recent progress of membrane distillation using electrospun nanofibrous membrane, J Membrane Sci 453(0) (2014) 435-462.
57. A. Alkhudhiri, N. Darwish, N. Hilal, Membrane distillation: A comprehensive review, Desalination 287(0) (2012) 2-18.
58. L.D. Tijing, Y.C. Woo, M.A.H. Johir, J.-S. Choi, H.K. Shon, A novel dual-layer bicomponent electrospun nanofibrous membrane for desalination by direct contact membrane distillation, Chem. Eng. J. 256 (2014) 155-159.
59. L. Martínez-DíezM.I. Vázquez-González, Temperature and concentration polarization in membrane distillation of aqueous salt solutions, J Membrane Sci 156(2) (1999) 265-273.
60. A.S. Al-Amoudi, A.M. Farooque, Performance restoration and autopsy of NF membranes used in seawater pretreatment, Desalination 178(1–3) (2005) 261-271.
61. M. Gryta, Long-term performance of membrane distillation process, J Membrane Sci 265(1–2) (2005) 153-159.
62. M. Gryta, Influence of polypropylene membrane surface porosity on the performance of membrane distillation process, J Membrane Sci 287(1) (2007) 67-78.
63. M. Gryta, J. Grzechulska-Damszel, A. Markowska, K. Karakulski, The influence of polypropylene degradation on the membrane wettability during membrane distillation, J Membrane Sci 326(2) (2009) 493-502.
64. L. Martínez, J.M. Rodríguez-Maroto, On transport resistances in direct contact membrane distillation, J Membrane Sci 295(1–2) (2007) 28-39.
65. R.W. Schofield, A.G. Fane, C.J.D. Fell, Heat and mass transfer in membrane distillation, J Membrane Sci 33(3) (1987) 299-313.
66. J. Phattaranawik, R. Jiraratananon, A.G. Fane, Effect of pore size distribution and air flux on mass transport in direct contact membrane distillation, J Membrane Sci 215(1–2) (2003) 75-85.
67. Z. Ding, L. Liu, Z. Liu, R. Ma, Fouling resistance in concentrating TCM extract by direct contact membrane distillation, J Membrane Sci 362(1–2) (2010) 317-325.
68. S. Adnan, M. Hoang, H. Wang, Z. Xie, Commercial PTFE membranes for membrane distillation application: Effect of microstructure and support material, Desalination 284(0) (2012) 297-308.
69. L. Wang, B. Li, X. Gao, Q. Wang, J. Lu, Y. Wang, et al., Study of membrane fouling in cross-flow vacuum membrane distillation, Sep. Purif. Technol. 122(0) (2014) 133-143.

70. S. Srisurichan, R. Jiraratananon, A.G. Fane, Mass transfer mechanisms and transport resistances in direct contact membrane distillation process, J Membrane Sci 277(1–2) (2006) 186-194.
71. L. Song, B. Li, K.K. Sirkar, J.L. Gilron, Direct Contact Membrane Distillation-Based Desalination: Novel Membranes, Devices, Larger-Scale Studies, and a Model, Ind Eng Chem Res 46(8) (2007) 2307-2323.
72. J. Gilron, L. Song, K.K. Sirkar, Design for Cascade of Crossflow Direct Contact Membrane Distillation, Ind Eng Chem Res 46(8) (2007) 2324-2334.
73. A.M. Alklaibi, N. Lior, Heat and mass transfer resistance analysis of membrane distillation, J Membrane Sci 282(1–2) (2006) 362-369.
74. S. Goh, J. Zhang, Y. Liu, A.G. Fane, Fouling and wetting in membrane distillation (MD) and MD-bioreactor (MDBR) for wastewater reclamation, Desalination 323(0) (2013) 39-47.
75. S. Goh, Q. Zhang, J. Zhang, D. McDougald, W.B. Krantz, Y. Liu, et al., Impact of a biofouling layer on the vapor pressure driving force and performance of a membrane distillation process, J Membrane Sci 438(0) (2013) 140-152.
76. J. Phattaranawik, A.G. Fane, A.C.S. Pasquier, W. Bing, F.S. Wong, Experimental Study and Design of a Submerged Membrane Distillation Bioreactor, Chem Eng Technol 32(1) (2009) 38-44.
77. L.R. Fisher, J.N. Israelachvili, Experimental studies on the applicability of the Kelvin equation to highly curved concave menisci, J. Colloid Interface Sci. 80(2) (1981) 528-541.
78. A.C. Mitropoulos, The Kelvin equation, J. Colloid Interface Sci. 317(2) (2008) 643-648.
79. A.M. Alklaibi, N. Lior, Membrane-distillation desalination: Status and potential, Desalination 171(2) (2005) 111-131.
80. M. Gryta, Osmotic MD and other membrane distillation variants, J Membrane Sci 246(2) (2005) 145-156.
81. F. He, J. Gilron, H. Lee, L. Song, K.K. Sirkar, Potential for scaling by sparingly soluble salts in crossflow DCMD, J Membrane Sci 311(1–2) (2008) 68-80.
82. B.V. Derjaguin, L. Landau, Theory of the stability of strongly charged lyophobic sols and of the adhesion of strongly charged particles in solutions of electrolytes, Acta Phys. Chim. URSS 14 (1941) 633-662.
83. E.J.W. Verwey, J.T.G. Overbeek, *Theory of the stability of lyphobic colloids*1948, Amsterdam: Elsevier.
84. M. Filella, *Colloidal properties of submicon particles in natural waters* in *Environmental colloids and particles: behaviour, separation and characterisation*, K.J. Wilkinson and J.R. Lead, Editors. 2007, John Wiley and Sons: England. p. 17-93.

85. W. Kühnl, A. Piry, V. Kaufmann, T. Grein, S. Ripperger, U. Kulozik, Impact of colloidal interactions on the flux in cross-flow microfiltration of milk at different pH values: A surface energy approach, J Membrane Sci 352(1–2) (2010) 107-115.
86. X. Jin, X. Huang, E.M.V. Hoek, Role of Specific Ion Interactions in Seawater RO Membrane Fouling by Alginic Acid, Environ Sci Technol 43(10) (2009) 3580-3587.
87. S. Srisurichan, R. Jiraratananon, A.G. Fane, Humic acid fouling in the membrane distillation process, Desalination 174(1) (2005) 63-72.
88. S.T. Hsu, K.T. Cheng, J.S. Chiou, Seawater desalination by direct contact membrane distillation, Desalination 143(3) (2002) 279-287.
89. T.R. Bott, *Fouling of heat exchangers*1995, Netherlands: Elsevier Science B.V.
90. M. Gryta, M. Tomaszewska, K. Karakulski, Wastewater treatment by membrane distillation, Desalination 198(1–3) (2006) 67-73.
91. T.V. Knyazkova, A.A. Maynarovich, Recognition of membrane fouling: testing of theoretical approaches with data on NF of salt solutions containing a low molecular weight surfactant as a foulant, Desalination 126(1–3) (1999) 163-169.
92. H. Zhu, M. Nyström, Cleaning results characterized by flux, streaming potential and FTIR measurements, Colloids and Surfaces A: Physicochemical and Engineering Aspects 138(2–3) (1998) 309-321.
93. E.M.V. Hoek, J. Allred, T. Knoell, B.-H. Jeong, Modeling the effects of fouling on full-scale reverse osmosis processes, Journal of Membrane Science 314(1–2) (2008) 33-49.
94. F. Meng, S.-R. Chae, A. Drews, M. Kraume, H.-S. Shin, F. Yang, Recent advances in membrane bioreactors (MBRs): Membrane fouling and membrane material, Water Res. 43(6) (2009) 1489-1512.
95. K. Schneider, W. Hölz, R. Wollbeck, S. Ripperger, Membranes and modules for transmembrane distillation, J Membrane Sci 39(1) (1988) 25-42.
96. M. Gryta, Calcium sulphate scaling in membrane distillation process, Chem Pap 63(2) (2009) 146-151.
97. G.J. Lee, L.D. Tijing, B.C. Pak, B.J. Baek, Y.I. Cho, Use of catalytic materials for the mitigation of mineral fouling, International Communications in Heat and Mass Transfer 33(1) (2006) 14-23.
98. L.D. Tijing, H.Y. Kim, D.H. Lee, C.S. Kim, Y.I. Cho, Use of an Oscillating Electric Field to Mitigate Mineral Fouling in a Heat Exchanger, Experimental Heat Transfer 22(4) (2009) 257-270.
99. B.L. Pangarkar, M.G. Sane, M. Guddad, Reverse Osmosis and Membrane Distillation for Desalination of Groundwater: A Review, ISRN Materials Science 2011 (2011) 9.
100. T. Darton, U. Annunziata, F. del Vigo Pisano, S. Gallego, Membrane autopsy helps to provide solutions to operational problems, Desalination 167(0) (2004) 239-245.

101. M. Gryta, Effect of iron oxides scaling on the MD process performance, Desalination 216(1–3) (2007) 88-102.
102. T.A. Hoang, H.M. Ang, A.L. Rohl, Effects of temperature on the scaling of calcium sulphate in pipes, Powder Technol 179(1–2) (2007) 31-37.
103. L.D. Tijing, B.C. Pak, D.H. Lee, Y.I. Cho, Heat-Treated Titanium Balls for the Mitigation of Mineral Fouling in Heat Exchangers, Experimental Heat Transfer 21(2) (2008) 115-132.
104. C. Tzotzi, T. Pahiadaki, S.G. Yiantsios, A.J. Karabelas, N. Andritsos, A study of CaCO3 scale formation and inhibition in RO and NF membrane processes, Journal of Membrane Science 296(1–2) (2007) 171-184.
105. A.G. Xyla, J. Mikroyannidis, P.G. Koutsoukos, The inhibition of calcium carbonate precipitation in aqueous media by organophosphorus compounds, Journal of Colloid and Interface Science 153(2) (1992) 537-551.
106. Y.I. Cho, A.F. Fridman, S.H. Lee, W.T. Kim, *Physical Water Treatment for Fouling Prevention in Heat Exchangers*, in *Advances in Heat Transfer*2004, Elsevier. p. 1-72.
107. L.D. Tijing, M.-H. Yu, C.-H. Kim, A. Amarjargal, Y.C. Lee, D.-H. Lee, et al., Mitigation of scaling in heat exchangers by physical water treatment using zinc and tourmaline, Applied Thermal Engineering 31(11–12) (2011) 2025-2031.
108. L.D. Tijing, H.Y. Kim, D.H. Lee, C.S. Kim, Y.I. Cho, Physical water treatment using RF electric fields for the mitigation of $CaCO_3$ fouling in cooling water, Int. J. Heat Mass Transfer 53(7-8) (2010) 1426-1437.
109. L.D. Tijing, B.C. Pak, B.J. Baek, D.H. Lee, Y.I. Cho, An experimental study on the bulk precipitation mechanism of physical water treatment for the mitigation of mineral fouling, Int Commun Heat Mass 34(6) (2007) 673-681.
110. V.I. Snoeyink, D. Jenkins, *Water chemistry*1980, USA: John Wiley and Sons.
111. M. Gryta, Alkaline scaling in the membrane distillation process, Desalination 228(1-3) (2008) 128-134.
112. J. Wang, D. Qu, M. Tie, H. Ren, X. Peng, Z. Luan, Effect of coagulation pretreatment on membrane distillation process for desalination of recirculating cooling water, Sep. Purif. Technol. 64(1) (2008) 108-115.
113. M. Gryta, *Scaling diminution by heterogeneous crystallization in a filtration element integrated with membrane distillation module*, in *Pol J Chem Technol*2009. p. 60.
114. M. Gryta, The influence of magnetic water treatment on $CaCO_3$ scale formation in membrane distillation process, Sep. Purif. Technol. 80(2) (2011) 293-299.
115. M. Gryta, Polyphosphates used for membrane scaling inhibition during water desalination by membrane distillation, Desalination 285 (2012) 170-176.

116. E. Guillen-Burrieza, R. Thomas, B. Mansoor, D. Johnson, N. Hilal, H. Arafat, Effect of dry-out on the fouling of PVDF and PTFE membranes under conditions simulating intermittent seawater membrane distillation (SWMD), J Membrane Sci 438 (2013) 126-139.
117. E. DrioliY. Wu, Membrane distillation : An experimental study, Desalination 53(1–3) (1985) 339-346.
118. Z. Ji, J. Wang, D. Hou, Z. Yin, Z. Luan, Effect of microwave irradiation on vacuum membrane distillation, J Membrane Sci 429 (2013) 473-479.
119. F. He, K.K. Sirkar, J. Gilron, Effects of antiscalants to mitigate membrane scaling by direct contact membrane distillation, J Membrane Sci 345(1-2) (2009) 53-58.
120. F. He, K.K. Sirkar, J. Gilron, Studies on scaling of membranes in desalination by direct contact membrane distillation: CaCO3 and mixed CaCO3/CaSO4 systems, Chem. Eng. Sci. 64(8) (2009) 1844-1859.
121. L.D. Nghiem, T. Cath, A scaling mitigation approach during direct contact membrane distillation, Sep. Purif. Technol. 80(2) (2011) 315-322.
122. X. Yu, H. Yang, H. Lei, A. Shapiro, Experimental evaluation on concentrating cooling tower blowdown water by direct contact membrane distillation, Desalination 323(0) (2013) 134-141.
123. J. Ge, Y. Peng, Z. Li, P. Chen, S. Wang, Membrane fouling and wetting in a DCMD process for RO brine concentration, Desalination 344(0) (2014) 97-107.
124. F. He, J. Gilron, H. Lee, L. Song, K.K. Sirkar, Potential for scaling by sparingly soluble salts in crossflow DCMD, Journal of Membrane Science 311(1-2) (2008) 68-80.
125. A. Zarebska, D.R. Nieto, K.V. Christensen, B. Norddahl, Ammonia recovery from agricultural wastes by membrane distillation: fouling characterization and mechanism, Water research 56 (2014) 1-10.
126. G. Chen, X. Yang, R. Wang, A.G. Fane, Performance enhancement and scaling control with gas bubbling in direct contact membrane distillation, Desalination 308 (2013) 47-55.
127. C.M. Tun, A.G. Fane, J.T. Matheickal, R. Sheikholeslami, Membrane distillation crystallization of concentrated salts—flux and crystal formation, J Membrane Sci 257(1-2) (2005) 144-155.
128. Y. Yun, R. Ma, W. Zhang, A.G. Fane, J. Li, Direct contact membrane distillation mechanism for high concentration NaCl solutions, Desalination 188(1–3) (2006) 251-262.
129. E. Guillen-Burrieza, A. Ruiz-Aguirre, G. Zaragoza, H.A. Arafat, Membrane fouling and cleaning in long term plant-scale membrane distillation operations, Journal of Membrane Science 468 (2014) 360-372.
130. D. Singh, P. Prakash, K.K. Sirkar, Deoiled Produced Water Treatment Using Direct-Contact Membrane Distillation, Ind Eng Chem Res 52(37) (2013) 13439-13448.

131. C.M. Tun, A.G. Fane, J.T. Matheickal, R. Sheikholeslami, Membrane distillation crystallization of concentrated salts—flux and crystal formation, J Membrane Sci 257(1–2) (2005) 144-155.
132. J.P. Mericq, S. Laborie, C. Cabassud, Vacuum membrane distillation for an integrated seawater desalination process, Desalination and Water Treatment 9(1-3) (2009) 287-296.
133. J.-P. Mericq, S. Laborie, C. Cabassud, Vacuum membrane distillation of seawater reverse osmosis brines, Water Res. 44(18) (2010) 5260-5273.
134. J. Gilron, Y. Ladizansky, E. Korin, Silica fouling in direct contact membrane distillation, Ind Eng Chem Res 52(31) (2013) 10521-10529.
135. K. KarakulskiM. Gryta, Water demineralisation by NF/MD integrated processes, Desalination 177(1–3) (2005) 109-119.
136. T.-W. Cheng, C.-J. Han, K.-J. Hwang, C.-D. Ho, W.J. Cooper, Influence of Feed Composition on Distillate Flux and Membrane Fouling in Direct Contact Membrane Distillation, Sep. Sci. Technol. 45(7) (2010) 967-974.
137. M. Gryta, Alkaline scaling in the membrane distillation process, Desalination 228(1–3) (2008) 128-134.
138. D. Qu, J. Wang, L. Wang, D. Hou, Z. Luan, B. Wang, Integration of accelerated precipitation softening with membrane distillation for high-recovery desalination of primary reverse osmosis concentrate, Sep. Purif. Technol. 67(1) (2009) 21-25.
139. M. Gryta, Application of membrane distillation process for tap water purification, Membrane Water Treatment 1(1) (2010) 1-12.
140. K. Sawada, The mechanism of crystallization and trasnformation of calcium carbonates, Pure Appl. Chem. 69 (1997) 921-928.
141. C.Y. Tai, W.-C. Chien, Effects of operating variables on the induction period of CaCl2–Na2CO3 system, Journal of Crystal Growth 237–239, Part 3(0) (2002) 2142-2147.
142. T. Chen, A. Neville, M. Yuan, Influence of on formation—bulk precipitation and surface deposition, Chemical Engineering Science 61(16) (2006) 5318-5327.
143. A. Stashans, G. Chamba, A new insight on the role of Mg in calcite, International Journal of Quantum Chemistry 111(10) (2011) 2436-2443.
144. S. Lee, C.-H. Lee, Effect of operating conditions on CaSO4 scale formation mechanism in nanofiltration for water softening, Water Research 34(15) (2000) 3854-3866.
145. M. Uchymiak, E. Lyster, J. Glater, Y. Cohen, Kinetics of gypsum crystal growth on a reverse osmosis membrane, Journal of Membrane Science 314(1–2) (2008) 163-172.
146. J.N.A. Lewis, S. Seewoo, S. Lacour. *Prevention of scaling in mine water using slurry precipitation and recycle reverse osmosis (SPARRO).* in *International Symposium on Industrial Crystallization*. 2002. Sorrento, Italy.

147. S.H. Najibi, H. Müller-Steinhagen, M. Jamialahmadi, Calcium sulphate scale formation during subcooled flow boiling, Chemical Engineering Science 52(8) (1997) 1265-1284.
148. R. Sheikholeslami, H.W.K. Ong, Kinetics and thermodynamics of calcium carbonate and calcium sulfate at salinities up to 1.5 M, Desalination 157(1–3) (2003) 217-234.
149. M. Luo, Z. Wang, Complex fouling and cleaning-in-place of a reverse osmosis desalination system, Desalination 141(1) (2001) 15-22.
150. E.G. Darton, M. Fazell. *A statistical review of 150 membrane autopsies*. in *62nd Annual International Water Conference*. 2001. Pittsburgh.
151. E. Guillen-Burrieza, R. Thomas, B. Mansoor, D. Johnson, N. Hilal, H. Arafat, Effect of dry-out on the fouling of PVDF and PTFE membranes under conditions simulating intermittent seawater membrane distillation (SWMD), J Membrane Sci 438(0) (2013) 126-139.
152. N. Dow, J. Zhang, M. SDuke, J. Li, G. S.R., E. Ostarcevic, Membrane distillation of brine wastes, Researcg Report 63, Water Quality Research Australia Ltd. (2008).
153. G. Greenberg, D. Hasson, R. Semiat, Limits of RO recovery imposed by calcium phosphate precipitation, Desalination 183(1–3) (2005) 273-288.
154. M. Gryta, Polyphosphates used for membrane scaling inhibition during water desalination by membrane distillation, Desalination 285(0) (2012) 170-176.
155. J. Koschikowski, M. Wieghaus, M. Rommel, Solar thermal-driven desalination plants based on membrane distillation, Desalination 156(1–3) (2003) 295-304.
156. L.D. Tijing, B.C. Pak, B.J. Baek, D.H. Lee, A study on heat transfer enhancement using straight and twisted internal fin inserts, Int Commun Heat Mass 33(6) (2006) 719-726.
157. L. Fan, J.L. Harris, F.A. Roddick, N.A. Booker, Influence of the characteristics of natural organic matter on the fouling of microfiltration membranes, Water Res. 35(18) (2001) 4455-4463.
158. J. Buffle, K.J. Wilkinson, S. Stoll, M. Filella, J. Zhang, A generalized description of aquatic colloidal interactions: The three-colloidal component approach, Environ Sci Technol 32(19) (1998) 2887-2899.
159. G.R. Aiken, *Humic substance in soil, sediment, and water*1985, New York: Wiley.
160. A.I. Schäfer, U. Schwicker, M.M. Fischer, A.G. Fane, T.D. Waite, Microfiltration of colloids and natural organic matter, J Membrane Sci 171(2) (2000) 151-172.
161. W.S. Guo, H.H. Ngo, J.X. Li, A mini-review on membrane fouling, Bioresour. Technol. 122 (2012) 27-34.
162. W. Yuan, A.L. Zydney, Humic acid fouling during microfiltration, J Membrane Sci 157(1) (1999) 1-12.
163. W. Yuan, A. Kocic, A.L. Zydney, Analysis of humic acid fouling during microfiltration using a pore blockage–cake filtration model, J Membrane Sci 198(1) (2002) 51-62.

164. C.Y. Tang, Y.-N. Kwon, J.O. Leckie, Fouling of reverse osmosis and nanofiltration membranes by humic acid—Effects of solution composition and hydrodynamic conditions, J Membrane Sci 290(1–2) (2007) 86-94.
165. S. Hong, M. Elimelech, Chemical and physical aspects of natural organic matter (NOM) fouling of nanofiltration membranes, J Membrane Sci 132(2) (1997) 159-181.
166. M. Gryta, M. Tomaszewska, J. Grzechulska, A.W. Morawski, Membrane distillation of NaCl solution containing natural organic matter, J Membrane Sci 181(2) (2001) 279-287.
167. M. Khayet, J.I. Mengual, Effect of salt concentration during the treatment of humic acid solutions by membrane distillation, Desalination 168(0) (2004) 373-381.
168. M. Khayet, A. Velázquez, J.I. Mengual, Direct contact membrane distillation of humic acid solutions, J Membrane Sci 240(1–2) (2004) 123-128.
169. M. Tomaszewska, L. Białończyk, Influence of proteins content in the feed on the course of membrane distillation, Desalin Water Treat 51(10-12) (2012) 2362-2367.
170. C. Rincón, J.M. Ortiz de Zárate, J.I. Mengual, Separation of water and glycols by direct contact membrane distillation, J Membrane Sci 158(1–2) (1999) 155-165.
171. A. Criscuoli, J. Zhong, A. Figoli, M.C. Carnevale, R. Huang, E. Drioli, Treatment of dye solutions by vacuum membrane distillation, Water Res. 42(20) (2008) 5031-5037.
172. Z. Ding, L. Liu, Z. Liu, R. Ma, The use of intermittent gas bubbling to control membrane fouling in concentrating TCM extract by membrane distillation, J Membrane Sci 372(1–2) (2011) 172-181.
173. Z.-P. Zhao, C.-Y. Zhu, D.-Z. Liu, W.-F. Liu, Concentration of ginseng extracts aqueous solution by vacuum membrane distillation 2. Theory analysis of critical operating conditions and experimental confirmation, Desalination 267(2–3) (2011) 147-153.
174. Z.-P. Zhao, L. Xu, X. Shang, K. Chen, Water regeneration from human urine by vacuum membrane distillation and analysis of membrane fouling characteristics, Sep. Purif. Technol. 118(0) (2013) 369-376.
175. A. Hausmann, P. Sanciolo, T. Vasiljevic, M. Weeks, K. Schroën, S. Gray, et al., Fouling mechanisms of dairy streams during membrane distillation, J Membrane Sci 441(0) (2013) 102-111.
176. A. Hausmann, P. Sanciolo, T. Vasiljevic, M. Weeks, K. Schroën, S. Gray, et al., Fouling of dairy components on hydrophobic polytetrafluoroethylene (PTFE) membranes for membrane distillation, J Membrane Sci 442(0) (2013) 149-159.
177. S. Kimura, S.-I. Nakao, S.-I. Shimatani, Transport phenomena in membrane distillation, J Membrane Sci 33(3) (1987) 285-298.
178. S. Meng, Y. Ye, J. Mansouri, V. Chen, Fouling and crystallisation behaviour of superhydrophobic nano-composite PVDF membranes in direct contact membrane distillation, J Membrane Sci 463(0) (2014) 102-112.

179. G. Naidu, S. Jeong, S.-J. Kim, I.S. Kim, S. Vigneswaran, Organic fouling behavior in direct contact membrane distillation, Desalination 347(0) (2014) 230-239.
180. K.C. Wijekoon, F.I. Hai, J. Kang, W.E. Price, T.Y. Cath, L.D. Nghiem, Rejection and fate of trace organic compounds (TrOCs) during membrane distillation, J Membrane Sci 453(0) (2014) 636-642.
181. Y. Zhiqing, L. Xiaolong, W. Chunrui, W. Xuan, Effect of pretreatment on membrane fouling and VMD performance in the treatment of RO-concentrated wastewater, Desalin Water Treat 51(37-39) (2013) 6994-7003.
182. R.J. Durham, M.H. Nguyen, Hydrophobic membrane evaluation and cleaning for osmotic distillation of tomato puree, J Membrane Sci 87(1–2) (1994) 181-189.
183. J.M. Ortiz De Zárate, C. Rincón, J.I. Mengual, Concentration of Bovine Serum Albumin Aqueous Solutions by Membrane Distillation, Sep. Sci. Technol. 33(3) (1998) 283-296.
184. M. Gryta, The assessment of microorganism growth in the membrane distillation system, Desalination 142(1) (2002) 79-88.
185. H.S. Vrouwenvelder, J.A.M. van Paassen, H.C. Folmer, J.A.M.H. Hofman, M.M. Nederlof, D. van der Kooij, Biofouling of membranes for drinking water production, Desalination 118(1–3) (1998) 157-166.
186. M. Krivorot, A. Kushmaro, Y. Oren, J. Gilron, Factors affecting biofilm formation and biofouling in membrane distillation of seawater, J Membrane Sci 376(1–2) (2011) 15-24.
187. J.S. Baker, L.Y. Dudley, Biofouling in membrane systems — A review, Desalination 118(1–3) (1998) 81-89.
188. N. Siboni, S. Martinez, A. Abelson, A. Sivan, A. Kushmaro, Conditioning film and initial biofilm formation on electrochemical $CaCO_3$ deposition on a metallic net in the marine environment, Biofouling 25(7) (2009) 675-683.
189. T. Griebe, H.-C. Flemming, Biocide-free antifouling strategy to protect RO membranes from biofouling, Desalination 118(1–3) (1998) 153-IN9.
190. M. Gryta, Concentration of saline wastewater from the production of heparin, Desalination 129(1) (2000) 35-44.
191. M. Gryta, A. Markowska-Szczupak, J. Bastrzyk, W. Tomczak, The study of membrane distillation used for separation of fermenting glycerol solutions, J Membrane Sci 431(0) (2013) 1-8.
192. J. Phattaranawik, A.G. Fane, A.C.S. Pasquier, W. Bing, A novel membrane bioreactor based on membrane distillation, Desalination 223(1–3) (2008) 386-395.
193. T.-H. Khaing, J. Li, Y. Li, N. Wai, F.-s. Wong, Feasibility study on petrochemical wastewater treatment and reuse using a novel submerged membrane distillation bioreactor, Sep. Purif. Technol. 74(1) (2010) 138-143.

194. V. Calabrò, E. Drioli, F. Matera, Membrane distillation in the textile wastewater treatment, Desalination 83(1–3) (1991) 209-224.
195. S. Mozia, A.W. Morawski, M. Toyoda, T. Tsumura, Effect of process parameters on photodegradation of Acid Yellow 36 in a hybrid photocatalysis–membrane distillation system, Chem. Eng. J. 150(1) (2009) 152-159.
196. S. Shirazi, C.-J. Lin, D. Chen, Inorganic fouling of pressure-driven membrane processes — A critical review, Desalination 250(1) (2010) 236-248.
197. M. Al-Shammiri, M. Safar, M. Al-Dawas, Evaluation of two different antiscalants in real operation at the Doha research plant, Desalination 128(1) (2000) 1-16.
198. H. Huang, K. Schwab, J.G. Jacangelo, Pretreatment for low pressure membranes in water treatment: A review, Environ Sci Technol 43(9) (2009) 3011-3019.
199. H.K. Shon, S.H. Kim, S. Vigneswaran, R. Ben Aim, S. Lee, J. Cho, Physicochemical pretreatment of seawater: fouling reduction and membrane characterization, Desalination 238(1–3) (2009) 10-21.
200. P.H. Wolf, S. Siverns, S. Monti, UF membranes for RO desalination pretreatment, Desalination 182(1–3) (2005) 293-300.
201. S. Ebrahim, M. Abdel-Jawad, S. Bou-Hamad, M. Safar, Fifteen years of R&D program in seawater desalination at KISR part I. Pretreatment technologies for RO systems, Desalination 135(1–3) (2001) 141-153.
202. F. Macedonio, E. Curcio, E. Drioli, Integrated membrane systems for seawater desalination: energetic and exergetic analysis, economic evaluation, experimental study, Desalination 203(1–3) (2007) 260-276.
203. M. Gryta, K. Karakulski, M. Tomaszewska, A. Morawski, Treatment of effluents from the regeneration of ion exchangers using the MD process, Desalination 180(1–3) (2005) 173-180.
204. A. El-Abbassi, A. Hafidi, M. Khayet, M.C. García-Payo, Integrated direct contact membrane distillation for olive mill wastewater treatment, Desalination 323(0) (2013) 31-38.
205. M. Gryta, Desalination of thermally softened water by membrane distillation process, Desalination 257(1–3) (2010) 30-35.
206. AWWA, *Water Quality and Treatment: A Handbook of CommunityWater Supplies*. 5th ed. ed1999, New York: McGraw-Hill.
207. M.M. Teoh, S. Bonyadi, T.-S. Chung, Investigation of different hollow fiber module designs for flux enhancement in the membrane distillation process, J Membrane Sci 311(1–2) (2008) 371-379.
208. X. Yang, R. Wang, A.G. Fane, Novel designs for improving the performance of hollow fiber membrane distillation modules, J Membrane Sci 384(1–2) (2011) 52-62.

209. A.P.S. Yeo, A.W.K. Law, A.G. Fane, The relationship between performance of submerged hollow fibers and bubble-induced phenomena examined by particle image velocimetry, J Membrane Sci 304(1–2) (2007) 125-137.
210. N. Ratkovich, C.C.V. Chan, P.R. Berube, I. Nopens, Experimental study and CFD modelling of a two-phase slug flow for an airlift tubular membrane, Chem. Eng. Sci. 64(16) (2009) 3576-3584.
211. Z.F. Cui, S. Chang, A.G. Fane, The use of gas bubbling to enhance membrane processes, J Membrane Sci 221(1–2) (2003) 1-35.
212. G. Chen, X. Yang, R. Wang, A.G. Fane, Performance enhancement and scaling control with gas bubbling in direct contact membrane distillation, Desalination 308(0) (2013) 47-55.
213. Y. Lu, Z. Ding, L. Liu, Z. Wang, R. Ma, The influence of bubble characteristics on the performance of submerged hollow fiber membrane module used in microfiltration, Sep. Purif. Technol. 61(1) (2008) 89-95.
214. G. Chen, X. Yang, Y. Lu, R. Wang, A.G. Fane, Heat transfer intensification and scaling mitigation in bubbling-enhanced membrane distillation for brine concentration, J Membrane Sci (2014) In press.
215. K.L. Hickenbottom, T.Y. Cath, Sustainable operation of membrane distillation for enhancement of mineral recovery from hypersaline solutions, J Membrane Sci 454(0) (2014) 426-435.
216. H. Zhang, R. Lamb, J. Lewis, Engineering nanoscale roughness on hydrophobic surface—preliminary assessment of fouling behaviour, Sci Technol Adv Mat 6(3–4) (2005) 236-239.
217. B.J. Privett, J. Youn, S.A. Hong, J. Lee, J. Han, J.H. Shin, et al., Antibacterial Fluorinated Silica Colloid Superhydrophobic Surfaces, Langmuir 27(15) (2011) 9597-9601.
218. J.B. Xu, S. Lange, J.P. Bartley, R.A. Johnson, Alginate-coated microporous PTFE membranes for use in the osmotic distillation of oily feeds, J Membrane Sci 240(1–2) (2004) 81-89.
219. J. Zhang, Z. Song, B. Li, Q. Wang, S. Wang, Fabrication and characterization of superhydrophobic poly (vinylidene fluoride) membrane for direct contact membrane distillation, Desalination 324(0) (2013) 1-9.
220. F. Alimi, M. Tlili, M. Ben Amor, C. Gabrielli, G. Maurin, Influence of magnetic field on calcium carbonate precipitation, Desalination 206(1–3) (2007) 163-168.
221. R.A. Barrett, S.A. Parsons, The influence of magnetic fields on calcium carbonate precipitation, Water Res. 32(3) (1998) 609-612.
222. W. Tae Kim, Y.I. Cho, C. Bai, Effect of electronic anti-fouling treatment on fouling mitigation with circulating cooling-tower water, Int Commun Heat Mass 28(5) (2001) 671-680.

223. Z. Ji, J. Wang, Z. Yin, D. Hou, Z. Luan, Effect of microwave irradiation on typical inorganic salts crystallization in membrane distillation process, J Membrane Sci 455(0) (2014) 24-30.
224. Z. Ji, J. Wang, D. Hou, Z. Yin, Z. Luan, Effect of microwave irradiation on vacuum membrane distillation, J Membrane Sci 429(0) (2013) 473-479.
225. S. Ghani, N.S. Al-Deffeeri, Impacts of different antiscalant dosing rates and their thermal performance in Multi Stage Flash (MSF) distiller in Kuwait, Desalination 250(1) (2010) 463-472.
226. Z. Amjad, Calcium sulfate dihydrate (gypsum) scale formation on heat exchanger surfaces: The influence of scale inhibitors, J. Colloid Interface Sci. 123(2) (1988) 523-536.
227. A.L. Kavitha, T. Vasudevan, H.G. Prabu, Evaluation of synthesized antiscalants for cooling water system application, Desalination 268(1–3) (2011) 38-45.
228. E. Lyster, M.-m. Kim, J. Au, Y. Cohen, A method for evaluating antiscalant retardation of crystal nucleation and growth on RO membranes, J Membrane Sci 364(1–2) (2010) 122-131.
229. R. Ketrane, B. Saidani, O. Gil, L. Leleyter, F. Baraud, Efficiency of five scale inhibitors on calcium carbonate precipitation from hard water: Effect of temperature and concentration, Desalination 249(3) (2009) 1397-1404.
230. L.A. Perez, *Mechanism of calcium phosphate scale formation and inhibition in cooling systems*1998, New York: Kluwer Academic Press.
231. M. GloedeT. Melin, Physical aspects of membrane scaling, Desalination 224(1–3) (2008) 71-75.
232. Y.-P. Lin, P.C. Singer, Inhibition of calcite crystal growth by polyphosphates, Water Res. 39(19) (2005) 4835-4843.
233. H. Lee, G. Amy, J. Cho, Y. Yoon, S.-H. Moon, I.S. Kim, Cleaning strategies for flux recovery of an ultrafiltration membrane fouled by natural organic matter, Water Res. 35(14) (2001) 3301-3308.
234. H. Shon, S. Phuntsho, S. Vigneswaran, J. Kandasamy, R. Aryal, V. Jegatheesan, *Physical, chemical, and biological characterization of membrane fouling*, in *Membrane Technology and Environmental Applications*. p. 457-503.
235. S. Phuntsho, A. Listowski, H.K. Shon, P. Le-Clech, S. Vigneswaran, Membrane autopsy of a 10 year old hollow fibre membrane from Sydney Olympic Park water reclamation plant, Desalination 271(1–3) (2011) 241-247.
236. Y. Marselina, Lifia, P. Le-Clech, R.M. Stuetz, V. Chen, Characterisation of membrane fouling deposition and removal by direct observation technique, J Membrane Sci 341(1–2) (2009) 163-171.
237. H. Li, A.G. Fane, H.G.L. Coster, S. Vigneswaran, Direct observation of particle deposition on the membrane surface during crossflow microfiltration, J Membrane Sci 149(1) (1998) 83-97.

238. W.D. Mores, R.H. Davis, Direct visual observation of yeast deposition and removal during microfiltration, J Membrane Sci 189(2) (2001) 217-230.
239. Y. Marselina, P. Le-Clech, R. Stuetz, V. Chen, Detailed characterisation of fouling deposition and removal on a hollow fibre membrane by direct observation technique, Desalination 231(1–3) (2008) 3-11.
240. M. Uchymiak, A. Rahardianto, E. Lyster, J. Glater, Y. Cohen, A novel RO ex situ scale observation detector (EXSOD) for mineral scale characterization and early detection, J Membrane Sci 291(1–2) (2007) 86-95.
241. M. Uchymiak, A.R. Bartman, N. Daltrophe, M. Weissman, J. Gilron, P.D. Christofides, et al., Brackish water reverse osmosis (BWRO) operation in feed flow reversal mode using an ex situ scale observation detector (EXSOD), J Membrane Sci 341(1–2) (2009) 60-66.
242. N. Hilal, W.R. Bowen, Atomic force microscope study of the rejection of colloids by membrane pores, Desalination 150(3) (2002) 289-295.
243. E.M. Vrijenhoek, S. Hong, M. Elimelech, Influence of membrane surface properties on initial rate of colloidal fouling of reverse osmosis and nanofiltration membranes, J Membrane Sci 188(1) (2001) 115-128.
244. M. Hamachi, M. Mietton-Peuchot, Experimental investigations of cake characteristics in crossflow microfiltration, Chem. Eng. Sci. 54(18) (1999) 4023-4030.
245. A.P. Mairal, A.R. Greenberg, W.B. Krantz, L.J. Bond, Real-time measurement of inorganic fouling of RO desalination membranes using ultrasonic time-domain reflectometry, J Membrane Sci 159(1–2) (1999) 185-196.
246. X. Xu, J. Li, H. Li, Y. Cai, Y. Cao, B. He, et al., Non-invasive monitoring of fouling in hollow fiber membrane via UTDR, J Membrane Sci 326(1) (2009) 103-110.
247. J. Mendret, C. Guigui, C. Cabassud, N. Doubrovine, P. Schmitz, P. Duru, et al., Development and comparison of optical and acoustic methods for in situ characterisation of particle fouling, Desalination 199(1–3) (2006) 373-375.
248. N.J. Shirtcliffe, G. McHale, S. Atherton, M.I. Newton, An introduction to superhydrophobicity, Adv. Colloid Interface Sci. 161(1–2) (2010) 124-138.
249. X. Zhang, F. Shi, J. Niu, Y. Jiang, Z. Wang, Superhydrophobic surfaces: from structural control to functional application, J. Mater. Chem. 18(6) (2008) 621-633.
250. L.D. Nghiem, A.I. Schäfer, Fouling autopsy of hollow-fibre MF membranes in wastewater reclamation, Desalination 188(1–3) (2006) 113-121.
251. W.F. Smith, *Principles of materials science and engineering*1986, Singapore: McGraw-Hill Book Co.
252. S.A. Huber, Evidence for membrane fouling by specific TOC constituents, Desalination 119(1–3) (1998) 229-234.

253. J.F. Ranville, C. Muzny, *Predicting membrane flux decline using parameters derived from field-flow fractionation measurements*, in *Desalination and water purification research and development program*2006.
254. E. Lee, H.K. Shon, J. Cho, Biofouling characteristics using flow field-flow fractionation: Effect of bacteria and membrane properties, Bioresource Technology 101(5) (2010) 1487-1493.
255. S. Lim, S. Lee, S. Choi, J. Moon, S. Hong, Evaluation of biofouling potential of microorganism using flow field-flow fractionation (Fl-FFF), Desalination 264(3) (2010) 236-242.
256. M.-A. Yun, K.-M. Yeon, J.-S. Park, C.-H. Lee, J. Chun, D.J. Lim, Characterization of biofilm structure and its effect on membrane permeability in MBR for dye wastewater treatment, Water Research 40(1) (2006) 45-52.

Figure captions

Fig. 1. Different forms of wettability of a membrane: (A) non-wetted, (B) surface-wetted, (C) partial-wetted, and (D) fully-wetted (adapted from [62]).

Fig. 2. (a) The effect of fouling on the temperature distribution of DCMD membrane, and; microscopic images of membranes fouled by (b) $CaCO_3$ and (c) protein, and (c) a virgin (unfouled) membrane (Figures b-d were adapted from [29]).

Fig. 3. Factors affecting membrane fouling: (a) foulant characteristics (concentration, molecular size, solubility, diffusivity, hydrophobicity, charge, etc.); (b) membrane properties (hydrophobicity, surface roughness, pore size and PSD, surface charge, surface functional groups); (c) operational conditions (flux, solution temperature, flow velocity), and; (d) feed water characteristics (solution chemistry, pH, ionic strength, presence of organic/inorganic matters).

Fig. 4. The fouling sites on a membrane can be divided into surface fouling (external) or pore blocking (internal).

Fig. 5. Schematic representation of the different fouling mechanisms according to the fouling material found in MD. In the real world processes, fouling usually occurs as mixed fouling, i.e., the combination of different of fouling mechanisms happening simultaneously. The dotted lines in the diagram with areas a, b, c and M show the different instances of mixed fouling between two or more fouling mechanisms.

Fig. 6. Schematic representation of the surface (heterogeneous) and bulk (homogeneous) crystallization mechanisms during inorganic fouling of membrane distillation.

Fig. 7. Gypsum scales showing needle-like strucutures (adapted from [121]).

Fig. 8. Biofouling layer on hollow fiber membranes made of polypropylene coated with flurosilicone (adapted from [29]).

Fig. 9. Permeate flux and feed concentration of $CaSO_4$ versus time during five repetitive DCMD tests with membrane flushing after each test. A fresh 2000 mg/L $CaSO_4$ was used after each test.

Fig. 10. Schematic of the (a) air inlet position in the feed side of the MD module and the (b) photographic image of the air nozzle (adapted from [212]).

Fig. 11. Microscopic images of (a) virgin (unfouled) and (b) scaled PP membrane (adapted from [122]).

Fig. 12. (a) SEM image and its corresponding EDS spectra of $CaCO_3$ formed on the membrane surface with tap water as feed (adapted from [62]).

Fig. 13. XRD analysis of the formed deposit on the membrane surface showing the presence calcite crystals (adapted from [115]).

Table captions

Table 1. Published reports in literature studying about inorganic fouling in membrane distillation.

Table 2. Published reports in literature studying about organic fouling in membrane distillation.

Table 3. Published reports in literature studying about biological fouling in membrane distillation.

Table 4. Some pretreatment strategies for MD application reported in literature.

Table 5. The antiscalants used in the study (adapted from [119]).

Table 6. Characterization and measurement techniques used for membrane fouling study.